Институт физики высоких давлений
РАН

С.М. Стишов

Современное состояние физики высоких давлений

Райвола, Март 2010

Физика высоких давлений – область физики, изучающая свойства вещества при высоких давлениях.

Почему это - важно?

~90% вещества Вселенной, сосредоточенное в громадных самогравитирующих телах, находится при давлении, превышающим 10 кбар.

Содержание:

•Определения

•История

•Давление в Природе

•Техника высоких давлений

•Шкала высоких давлений

•Фазовые диаграммы и эволюция вещества при высоких давлениях

•Уравнения состояния и фазовые переходы

•Некоторые результаты

•<u>Институт физики высоких давлений РАН</u>

Физика высоких давлениий как наука сформировалась в начале прошлого века в результате создания и развития адекватных методов исследования.

Экспериментальная физика высоких давлений оперирует с давлениями, варьирующими от одной до нескольких миллионов атмосфер (1 атмосфера = ~ 0.98 бар; 1 бар = 106 дин / cm2 = 10 Паскаль (Па)).

Диапазон изменения давлений в природе столь велик, что вряд ли сможет быть воспроизведен в лаборатории в обозримое время.

Тем не менее, необходимо отметить, что развитие экспериментальной техники позволяет уже сейчас моделировать условия, существующие в центре Земли

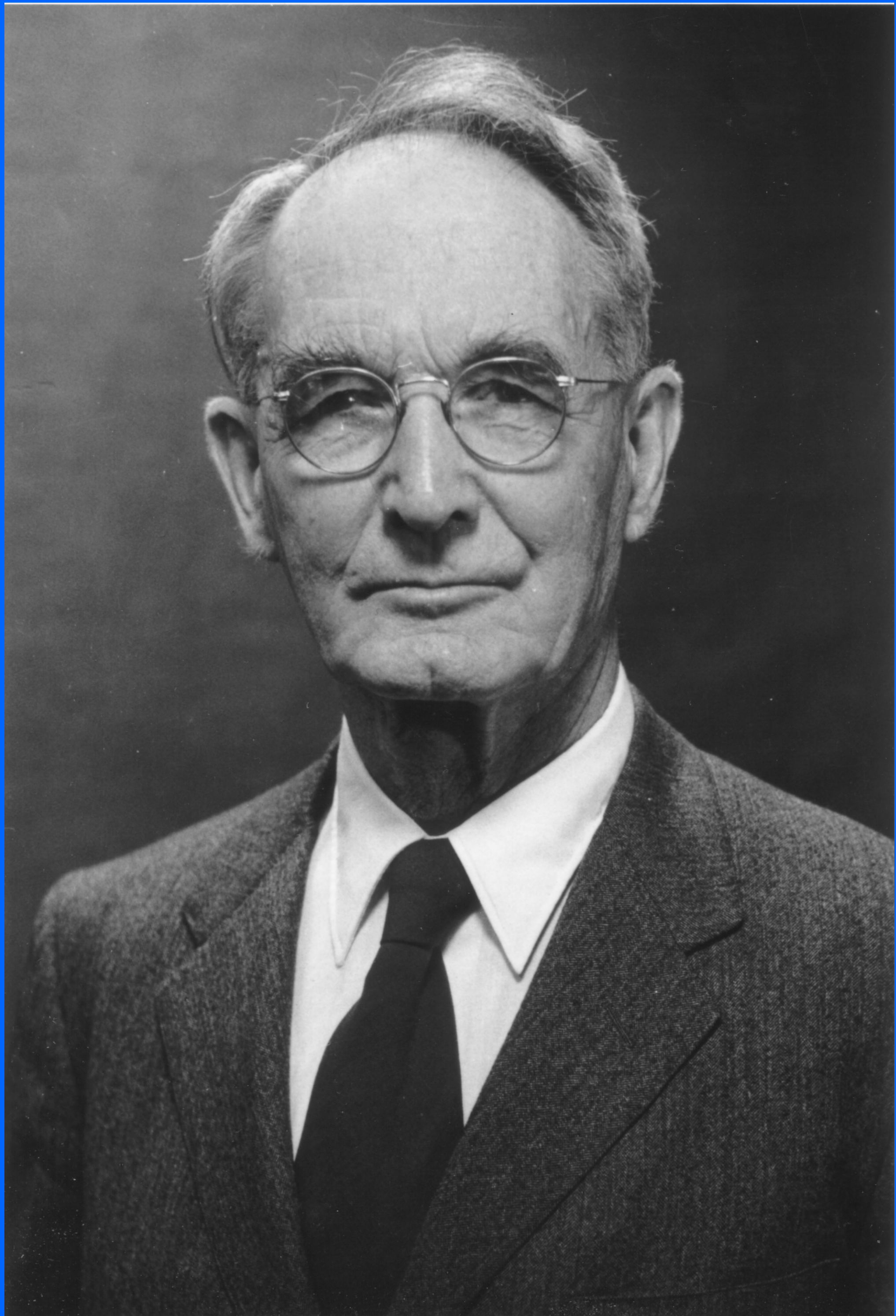

Percy Williams Bridgman

1882-1961

Перси Вильям Бриджмен , гарвардский профессор и нобелевский лауреат , сыграл главную роль в развитии экспериментальной техники высоких давлений и формиро-вании физики высоких давлений как науки.

Основные направления исследований:

- Физика конденсированного состояния вещества
- Создание новых материалов
- Строение Земли и планет

История развития физики высоких давлений не столь богата выдающимися открытиями в отличие, например, от случая физики низких температур.

Физика высоких давлений знаменита своими применениями, которые столь многочисленны и разнообразны, что делает невозможным даже их краткое упоминание. В этой связи <u>физика высоких давлений</u> может быть охарактеризована как скромная «рабочая лошадь» физики конденсированного состояния.

Формула Нобелевской премии Перси В. Бриджмена (1946): ” *for the invention of an apparatus to produce extremely high pressures and for the discoveries he made therewith in the field of high pressure physics*”

Важные даты

- 1762 – 1764 Джон Кантон (сжимаемость жидкостей)
- 1820 Якоб Перкинс (давление выше 2000 атм.)
- 1861 Томас Эндрюс (открытие критических явлений)
- 1893 – 1903 Густав Тамман (плавление, фазовые переходы)
- 1906 Первая статья П. В. Бриджмена
- 1931 публикация книги P.W. Bridgman "The Physics of High Pressure"
- 1955 Первые синтетические алмазы (Дженерал Электрик)
- 1961 Плотный кремнезем (ИФВД)
- 1968 Стабильность металлического водорода (Нил Ашкрофт)
- 1972 Изобретение рубинового манометра (НБС)
- 1977 Давление > 1.7 Мбар(Дэйв Мао и Питер Белл)

Pressure units and definitions

1Pa (1N / m²) = 10 dyn / cm² = 10⁻⁵ bar = 1.02 · 10⁻⁵ kgf / cm²

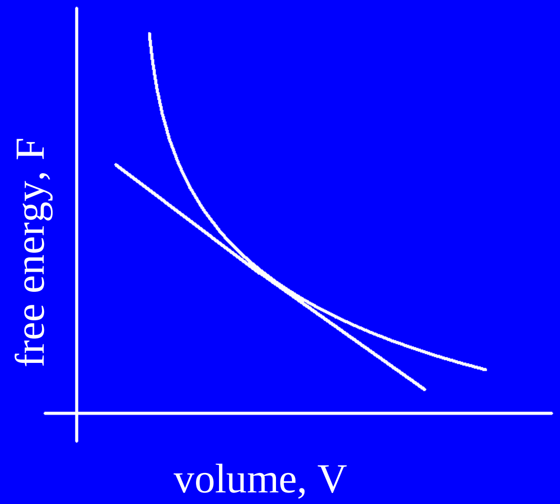

$$P = \frac{F}{S}$$

$$P = -\left(\frac{\partial F}{\partial V}\right)_T$$

$$\int p \partial V$$

$$\int p \partial V / \mathrm{F_o}$$

Natural units of pressure

Pressure = Energy / Volume

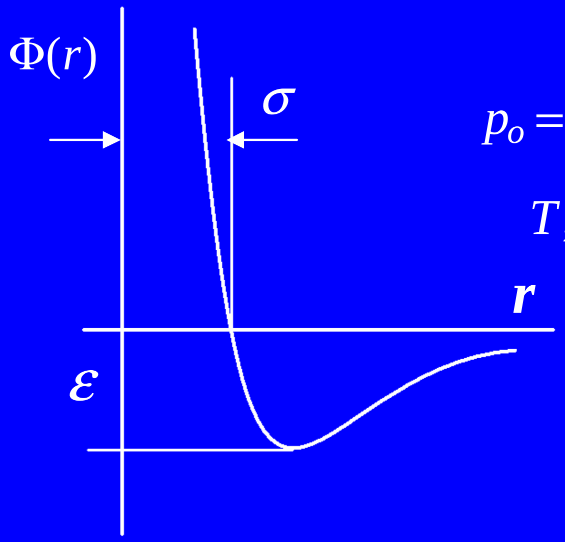

$p_o = \varepsilon / \sigma^3 -$ molecular unit of pressure

$T, l, \varepsilon, \sigma -$ characteristic quantities

$p_o(He) \approx$ 84 bar

$p_o(Xe) \approx$ 450 bar

Atomic unit:

$e^2 / a_o^4 \approx 3 \cdot 10^2$ Mbar

$e^2 / a_o = 2Ry \approx 27.2\ eV$

$a_o = \hbar^2 / me^2$ (Bohr radius)

ДАВЛЕНИЕ В ПРИРОДЕ

	Давление Мбар	Плотность г/cm^3
Земля (центр)	4	~10-20
Солнце (центр)	10^5	10^2
Белые карлики	10^{10}	10^6
Нейтронные звезды	10^{22}	10^{14}

Evolution of matter at cold compression

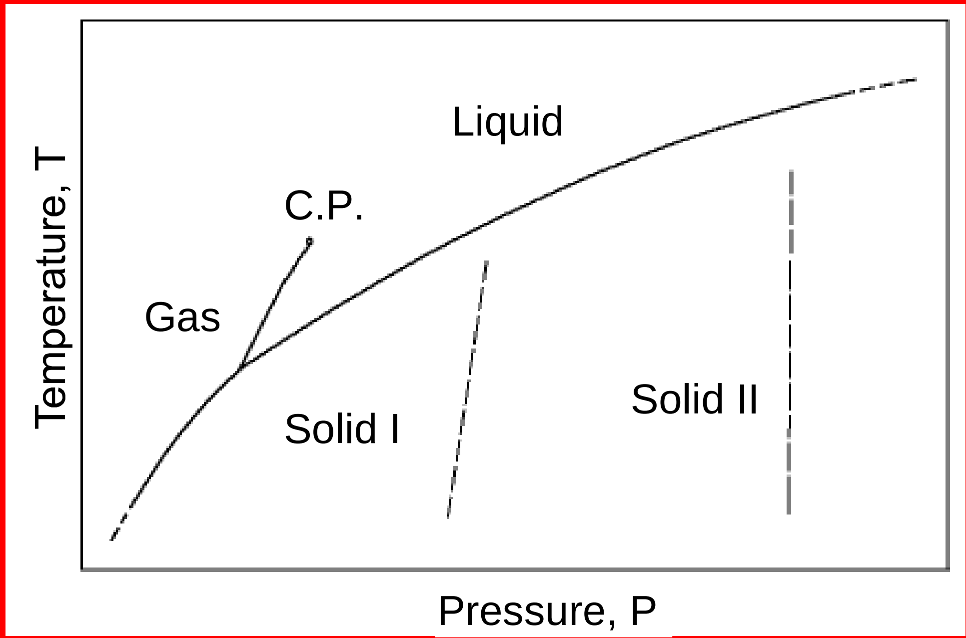

Pressure

$P \approx e^2 / a_o^4 \sim 10^2 Mbar$ $P \approx Z^5 e^2 / a_o^4 \sim Z^5 \cdot 10^2 Mbar$

Gas ⟷ Liquid ⟷ Solid … Solid ⟷ Metallic solid ⟷ Totally ionized matter (white dwarfs) ⟷ Nuclear reactions (Neutron stars) ⟷ Quark stars …

$P >> 10^{18} Mbar$

Melting at extreme conditions

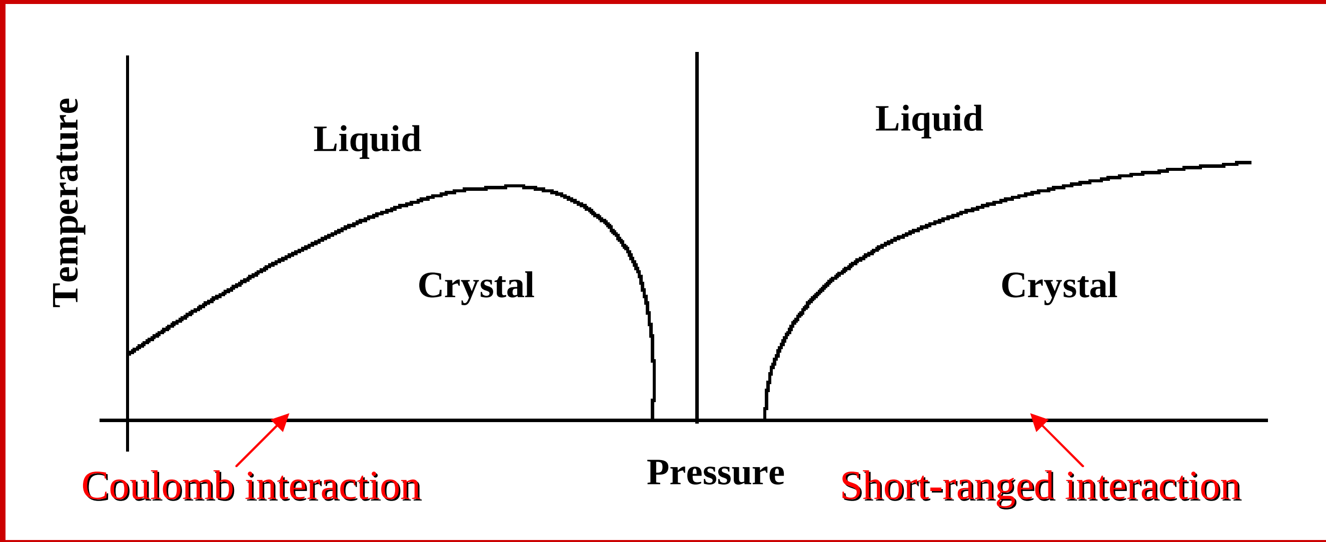

Jones, Ceperley, Phys.Rev.Lett., 76,4572, 1996 →

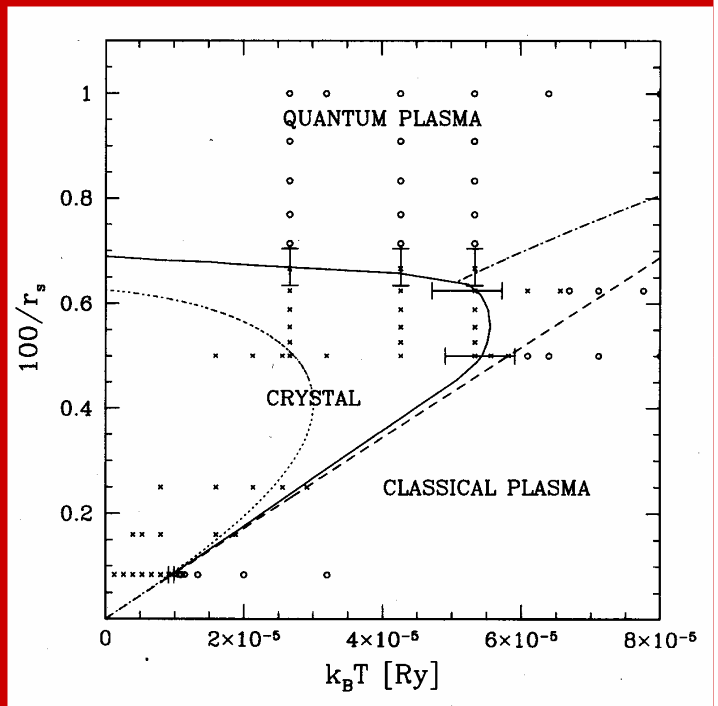

$$P \propto T^{1+3/n}$$

$$\Gamma = Z^2 e^2 / r_s kT \approx 150$$

$$\lambda_T \propto T^{(2-n)/2n}$$

$$T_m \propto V^{-n/3}$$

$$\lambda_T = \hbar/(mkT)^{1/2}$$

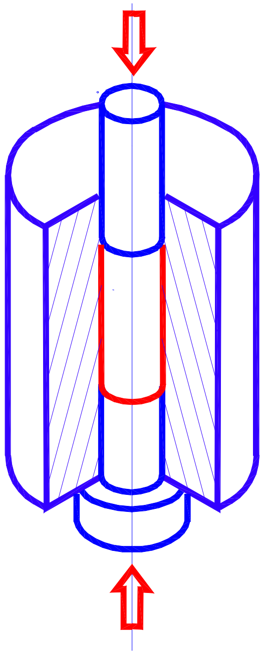

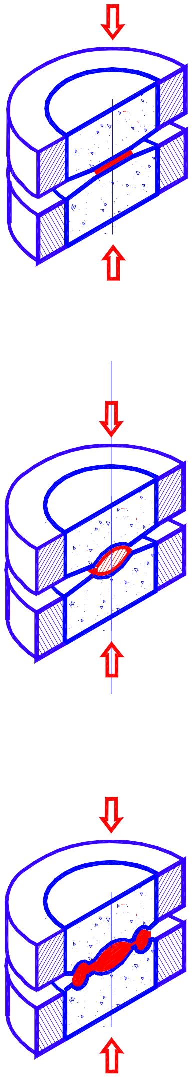

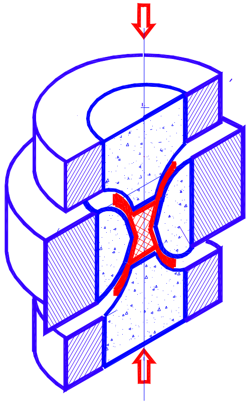

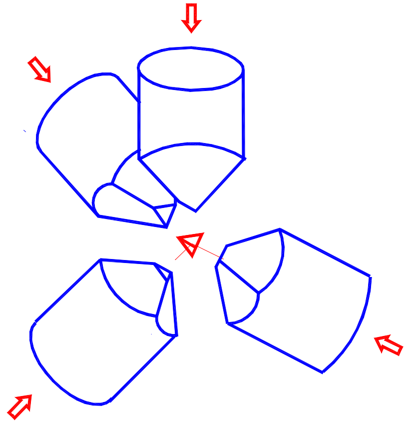

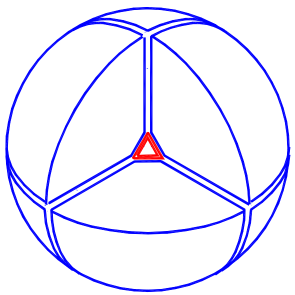

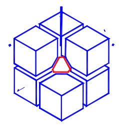

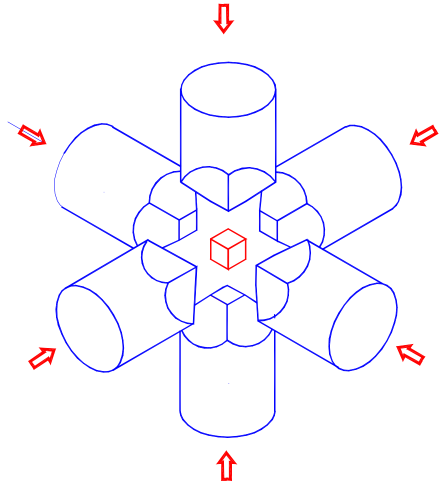

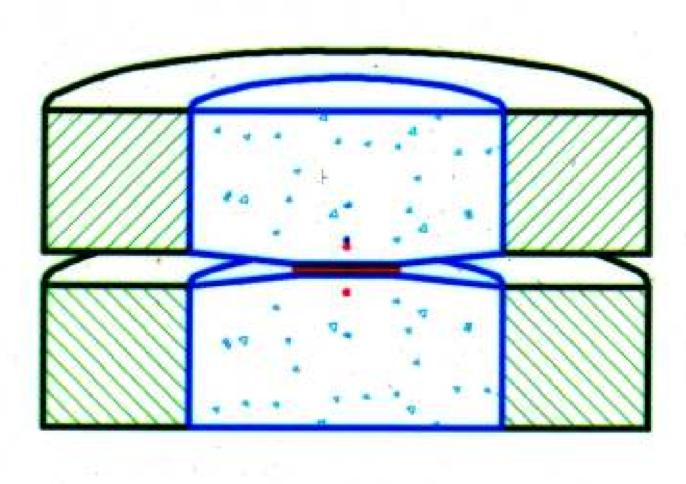

Bridgman anvils

(Bridgman, 1935)

“Lentil” or Recessed anvils

(Ivanov, Slesarev, Vereschagin, 1959)

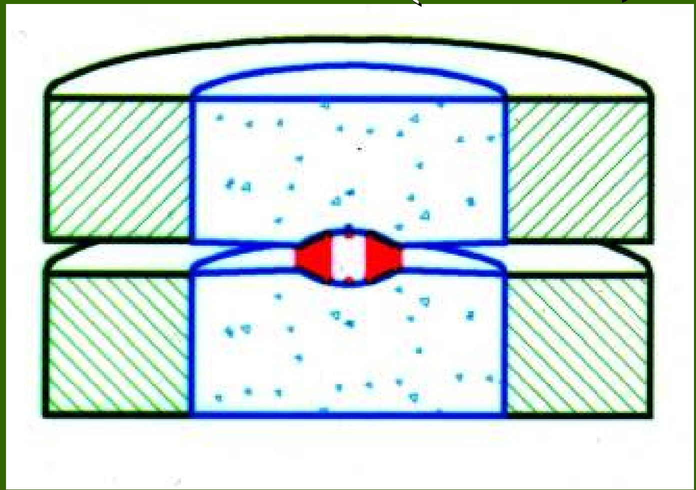

Toroid (Khvostancev, Novikov, Vereschagin, 1969)

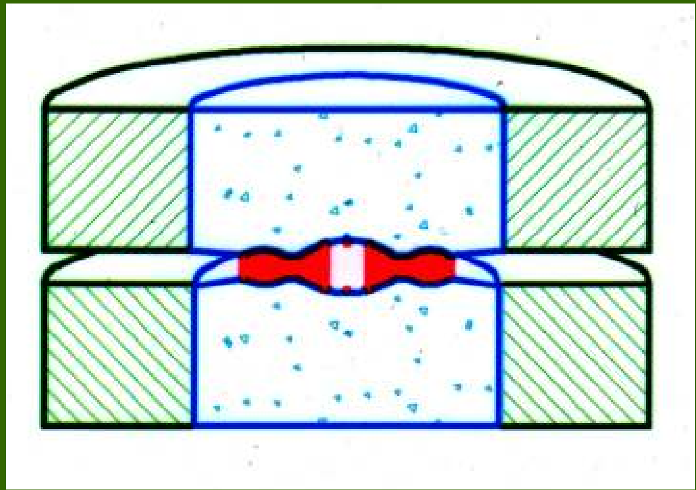

Diamond Anvils

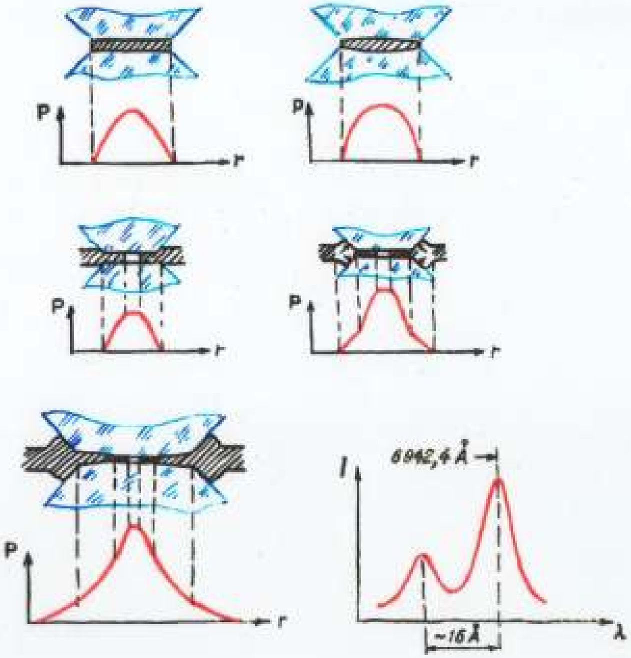

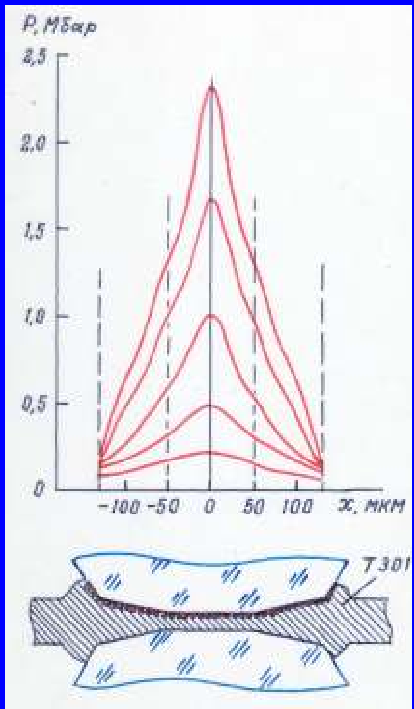

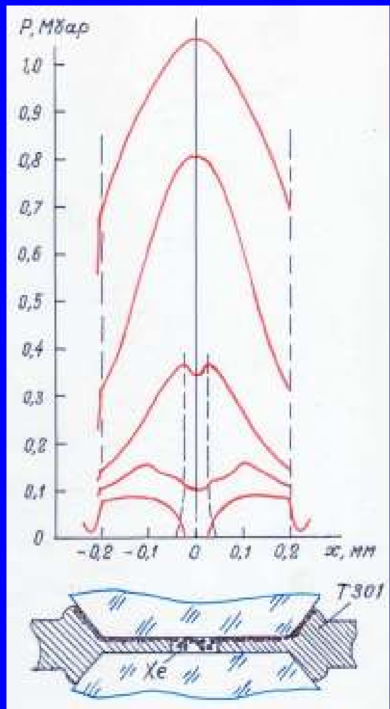

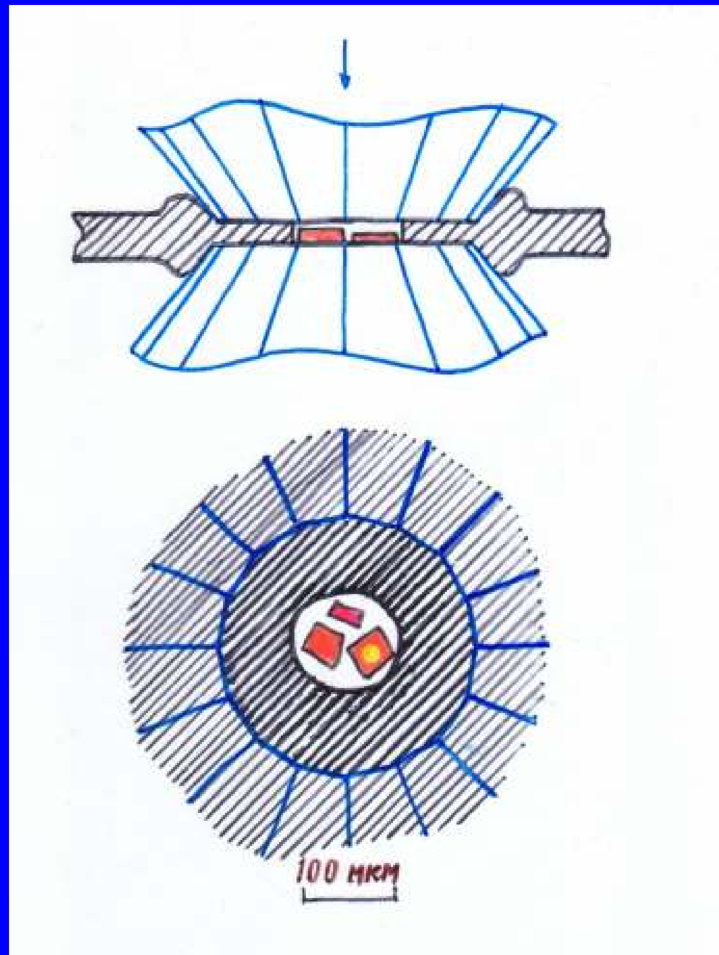

Sulfur (1), Iodine (2) and Mercury Iodide (3) in diamond anvils

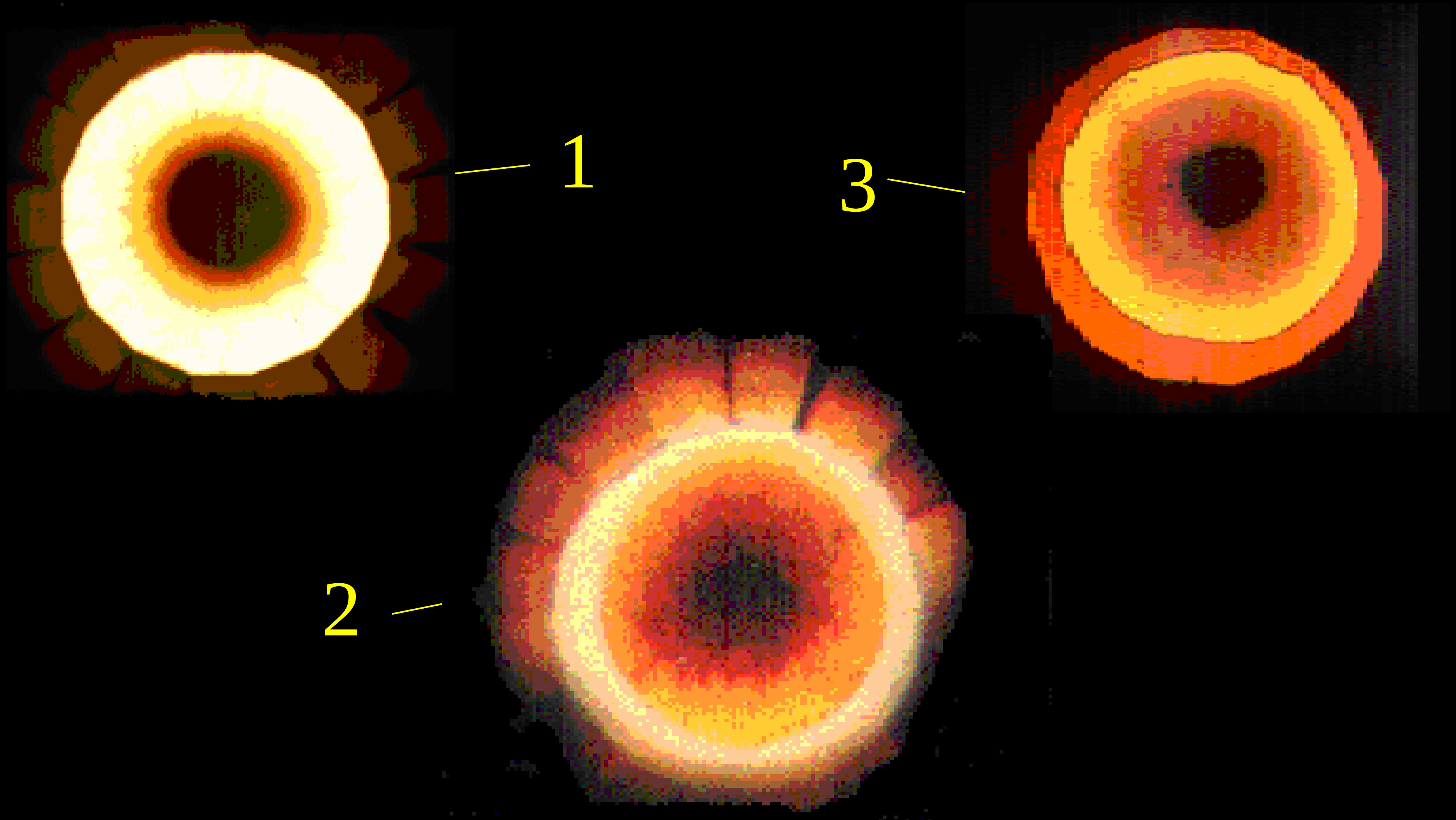

CsJ + Xe in diamond anvils

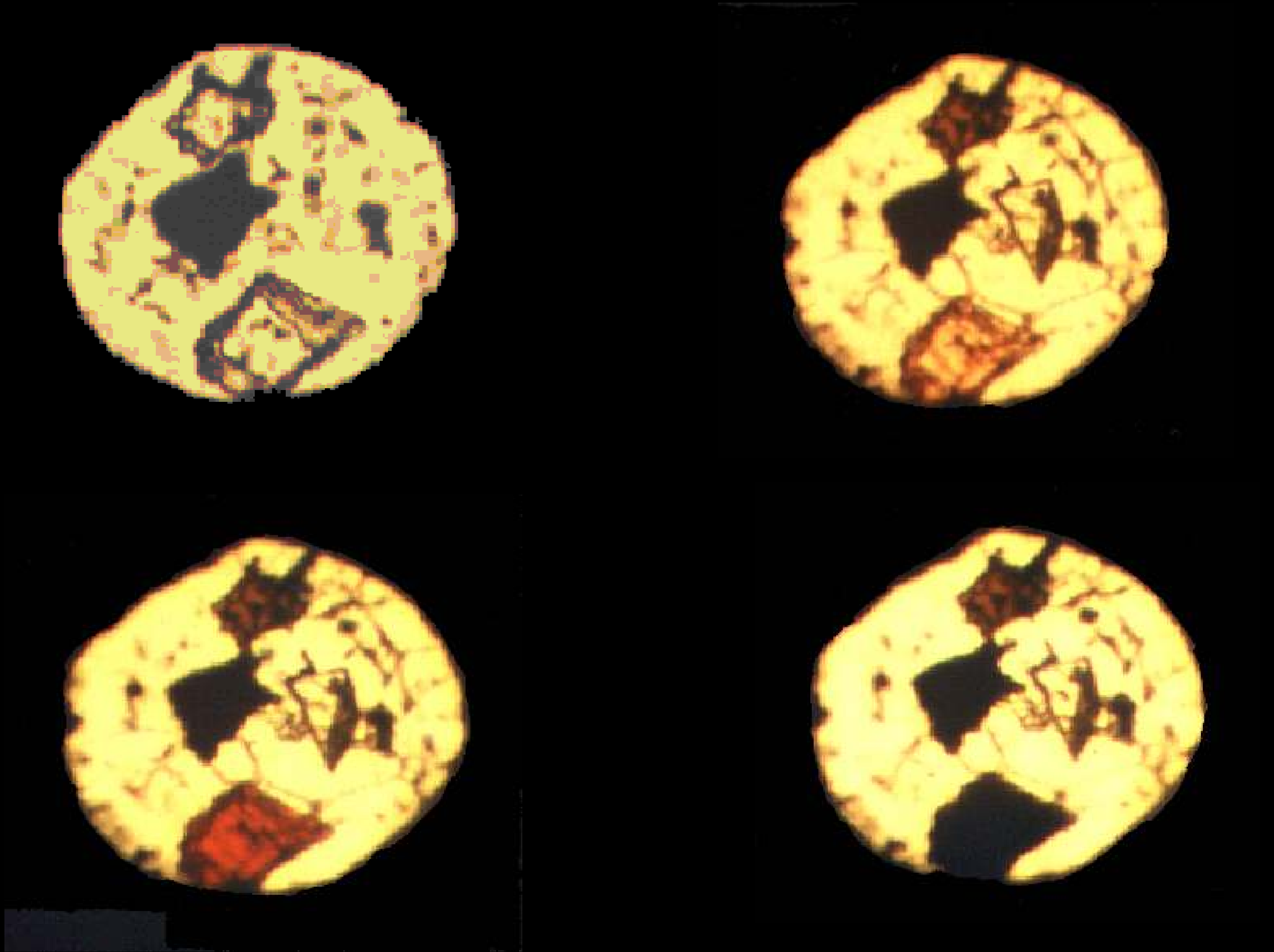

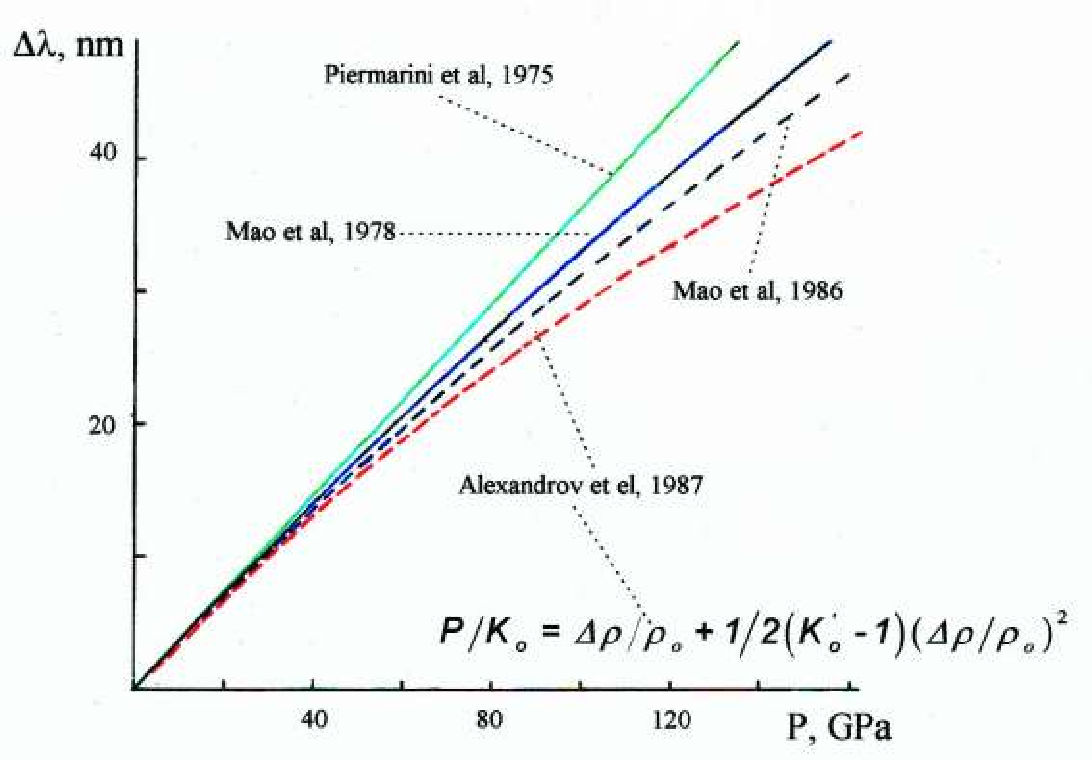

Pressure measurements and High Pressure Scale

- Primary and secondary gauges
- EOS and pressure calibration
- Ruby scale
- Diamond scale
- Pressure medium and pressure calibration

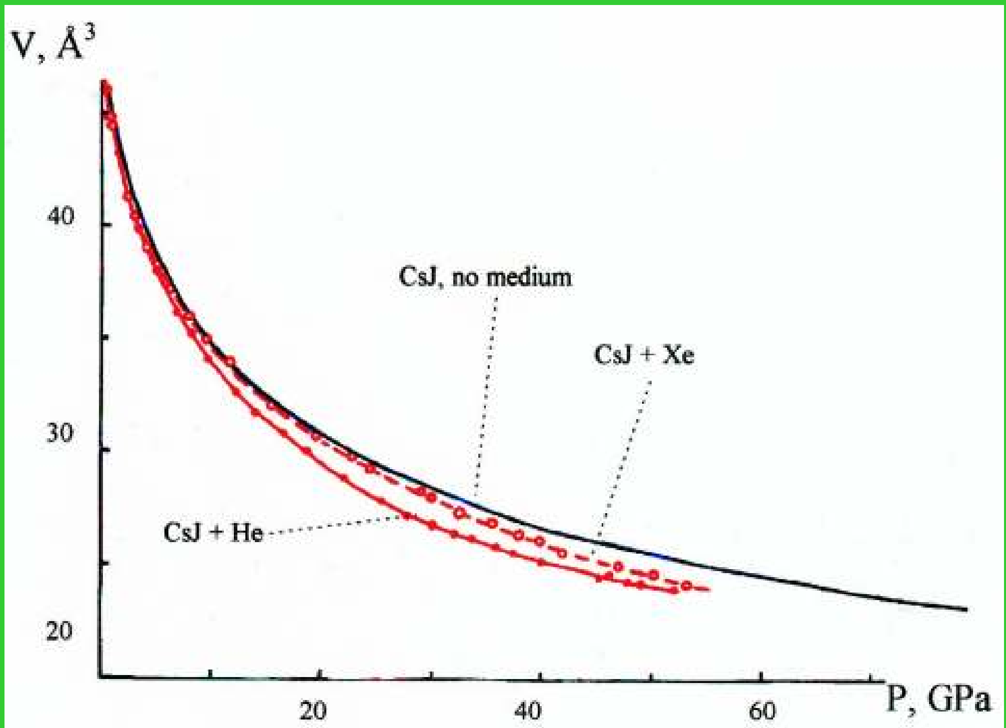

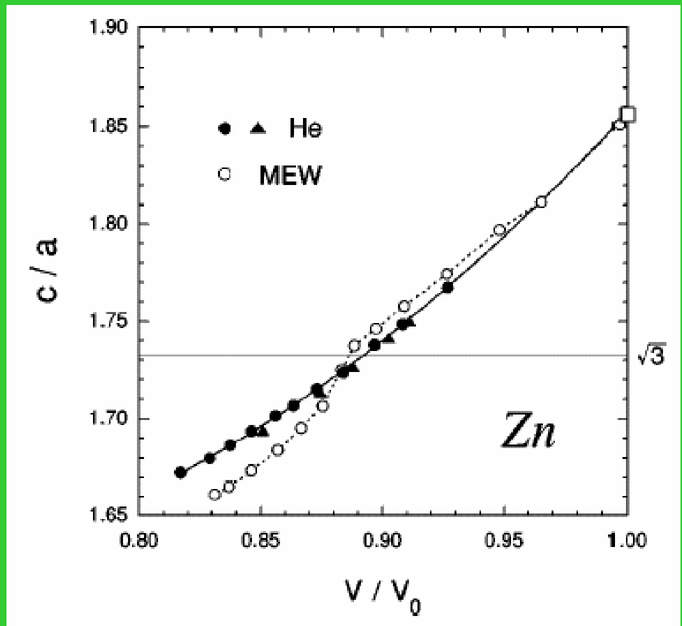

MgO High-Pressure Scale

(Zha, Mao, Hemley, 2000)

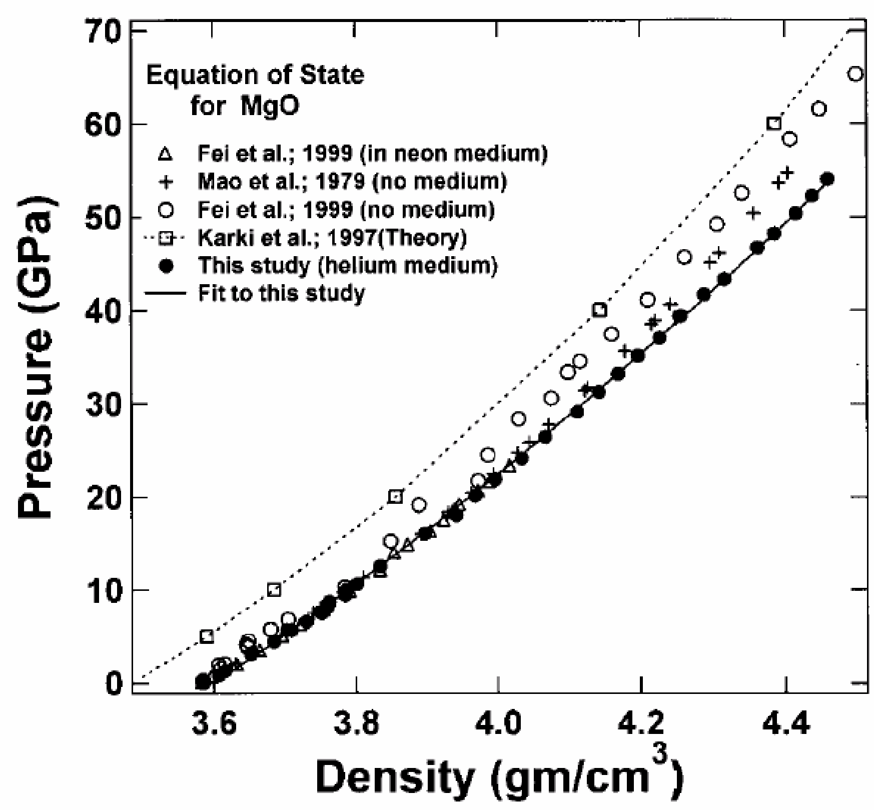

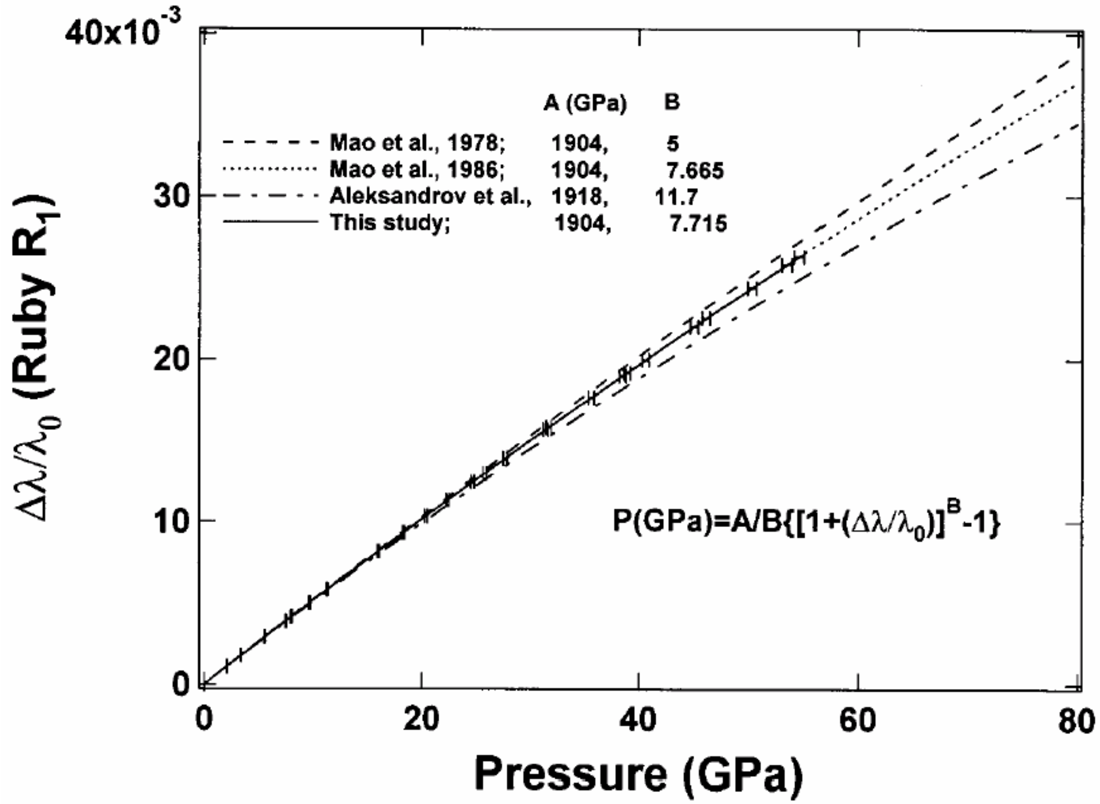

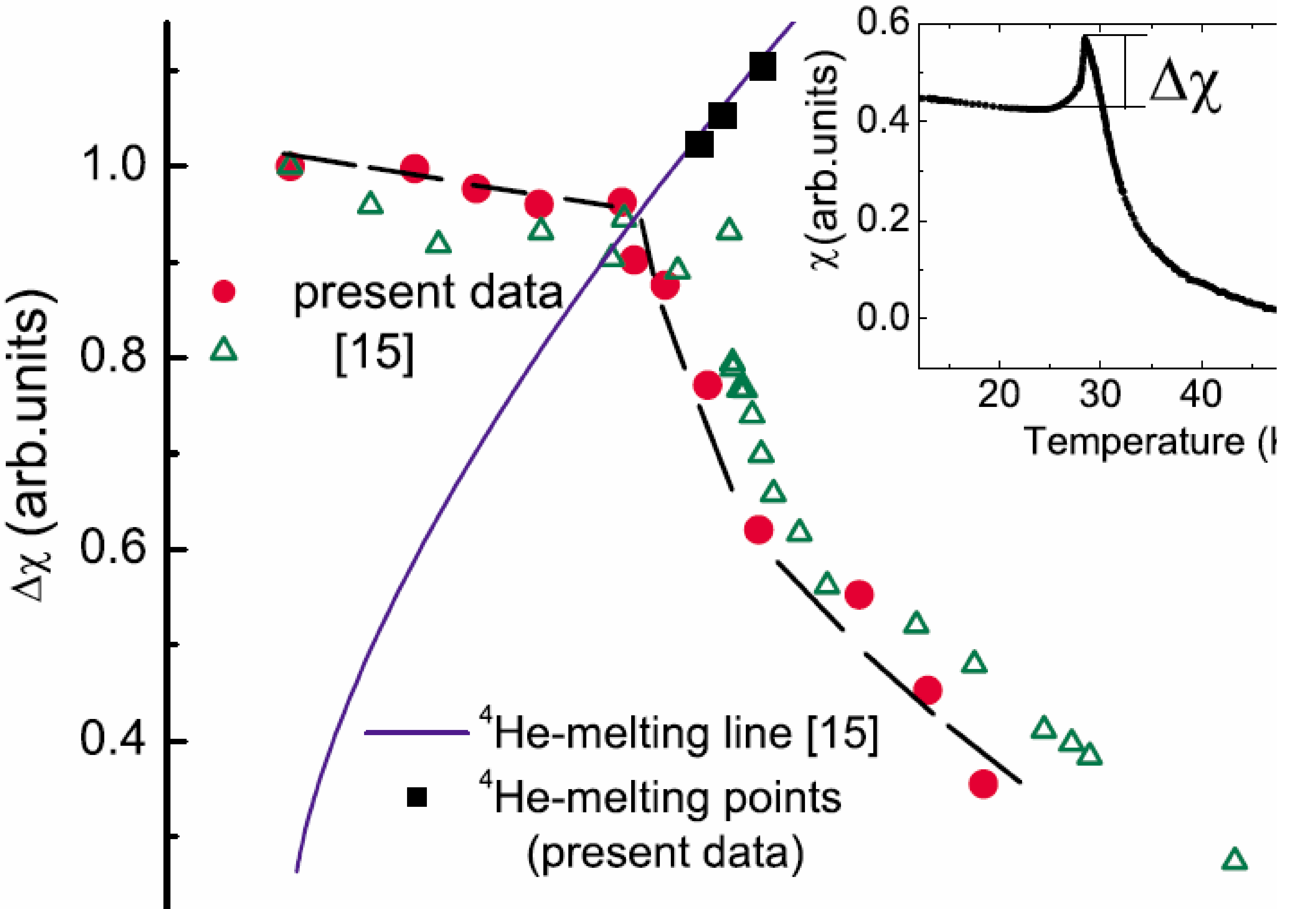

Δχ (arb.units)
1.0
0.8
0.6
0.4
present data
[15]
^{4}He-melting line [15]
^{4}He-melting points
(present data)
χ(arb.units)
0.6
0.4
0.2
0.0
20
30
40
Temperature (
Δχ

Equation of States of Isolectronic Pairs

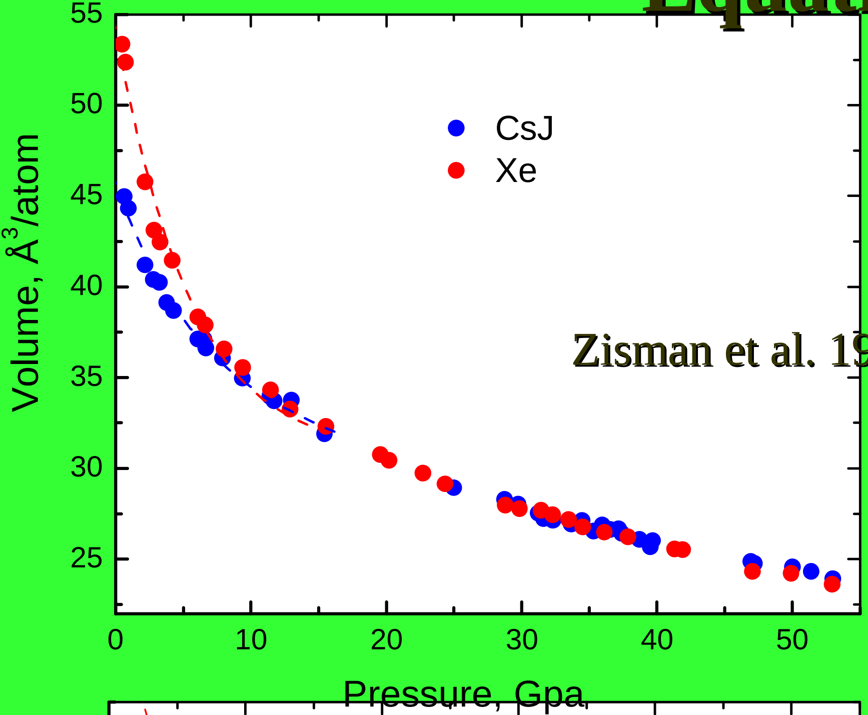

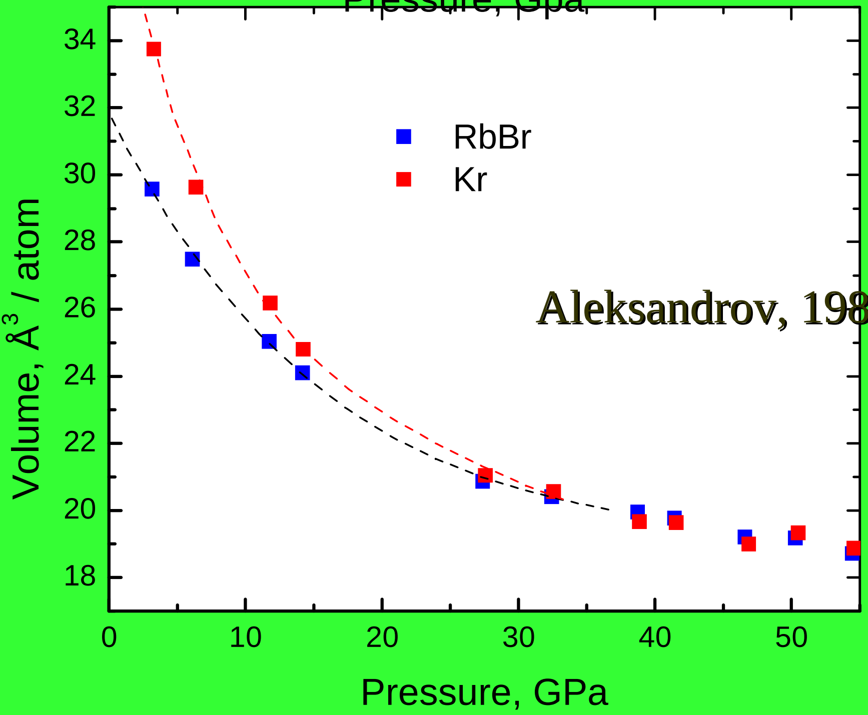

$J^{53}\ Xe^{54}\ Cs^{55}$

$Xe + p = Cs^{+}$

$Xe - p = J^{-}$

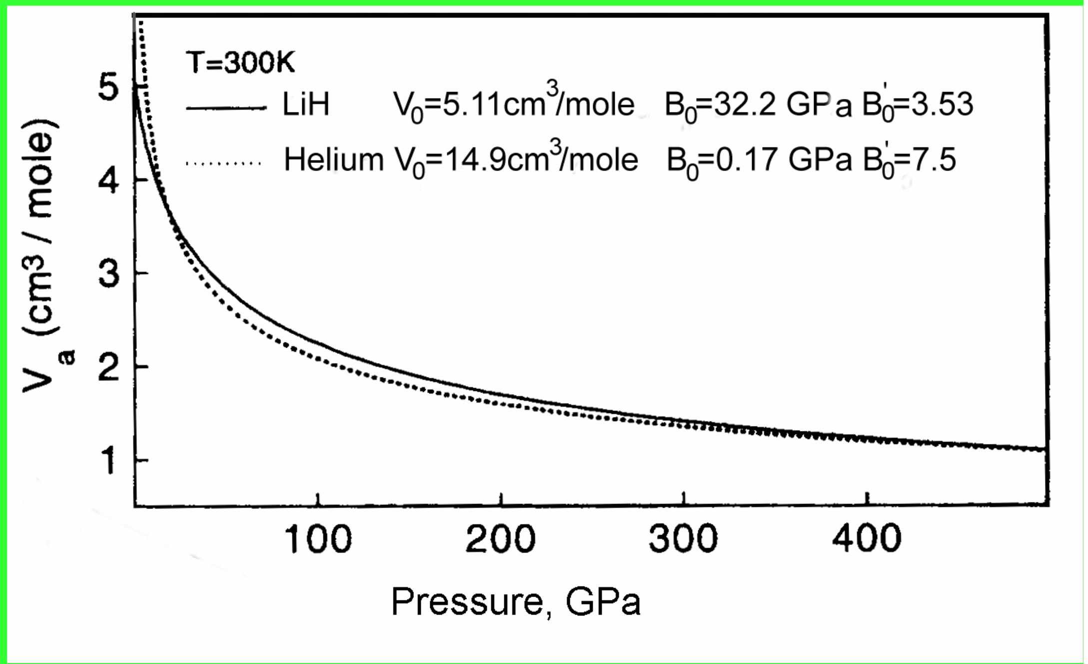

Loubeyre, 1998

Aidun et al. Phys. Rev.B, 29, 2611, 1984

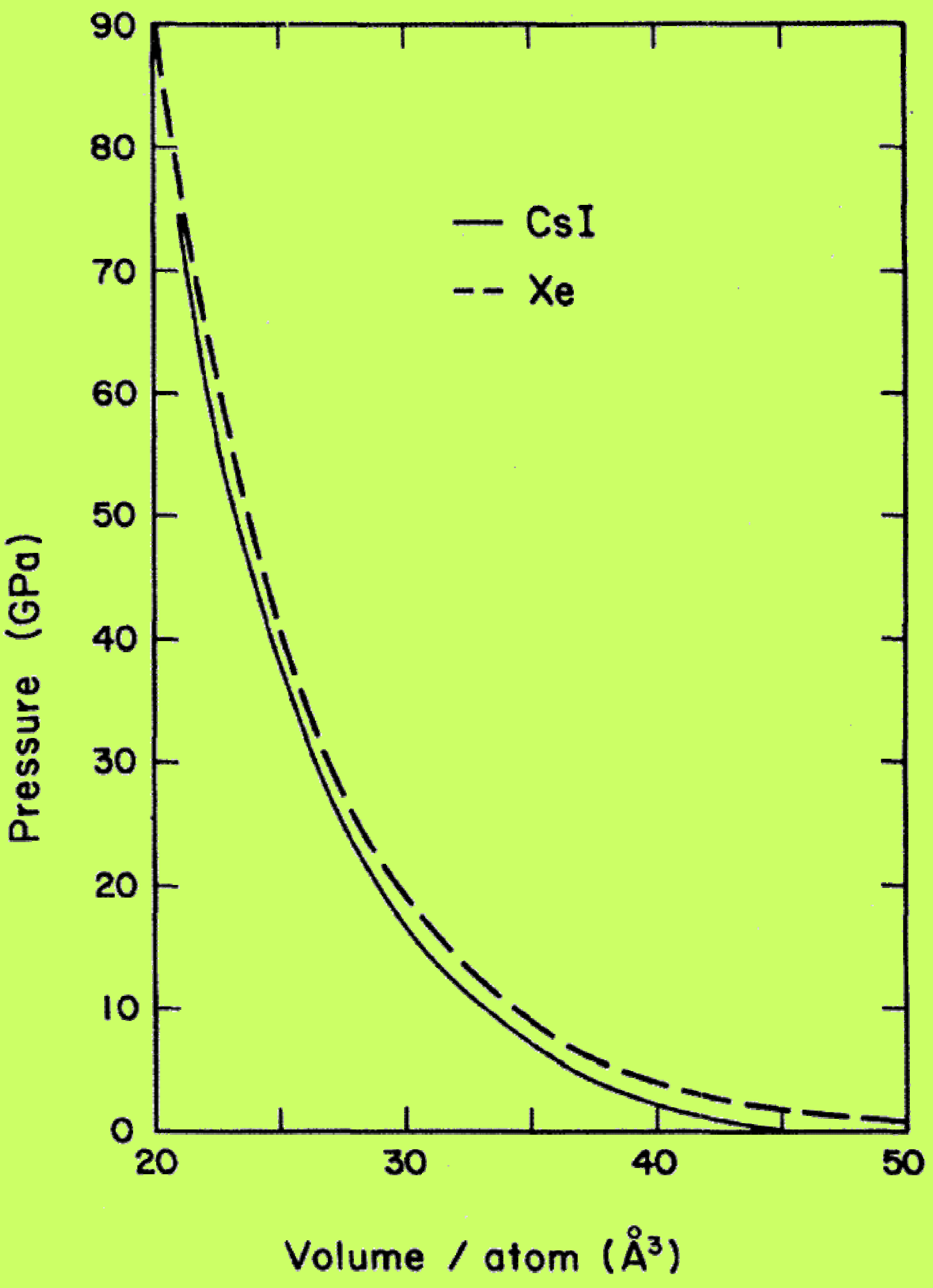

Zisman et al. 1984

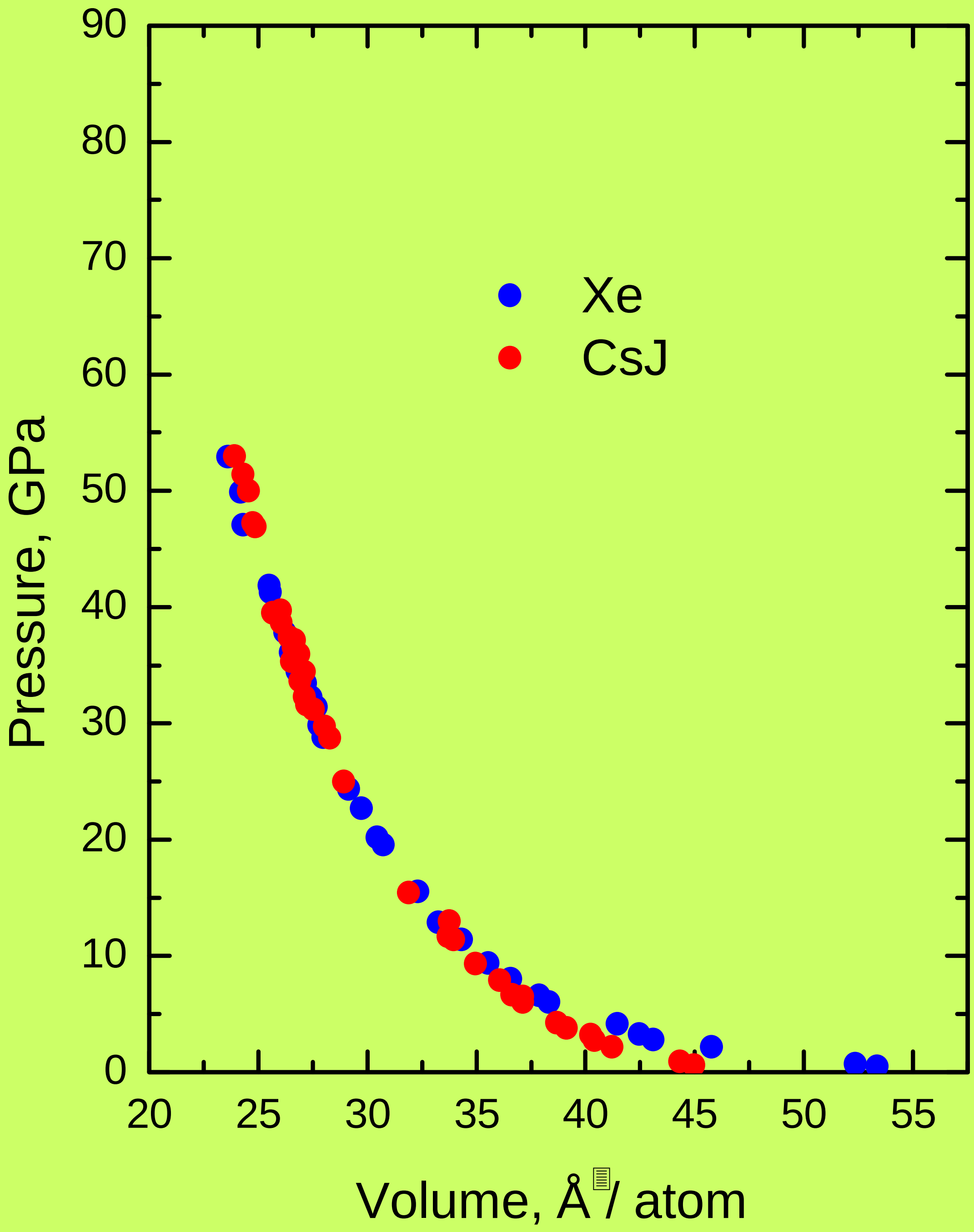

a

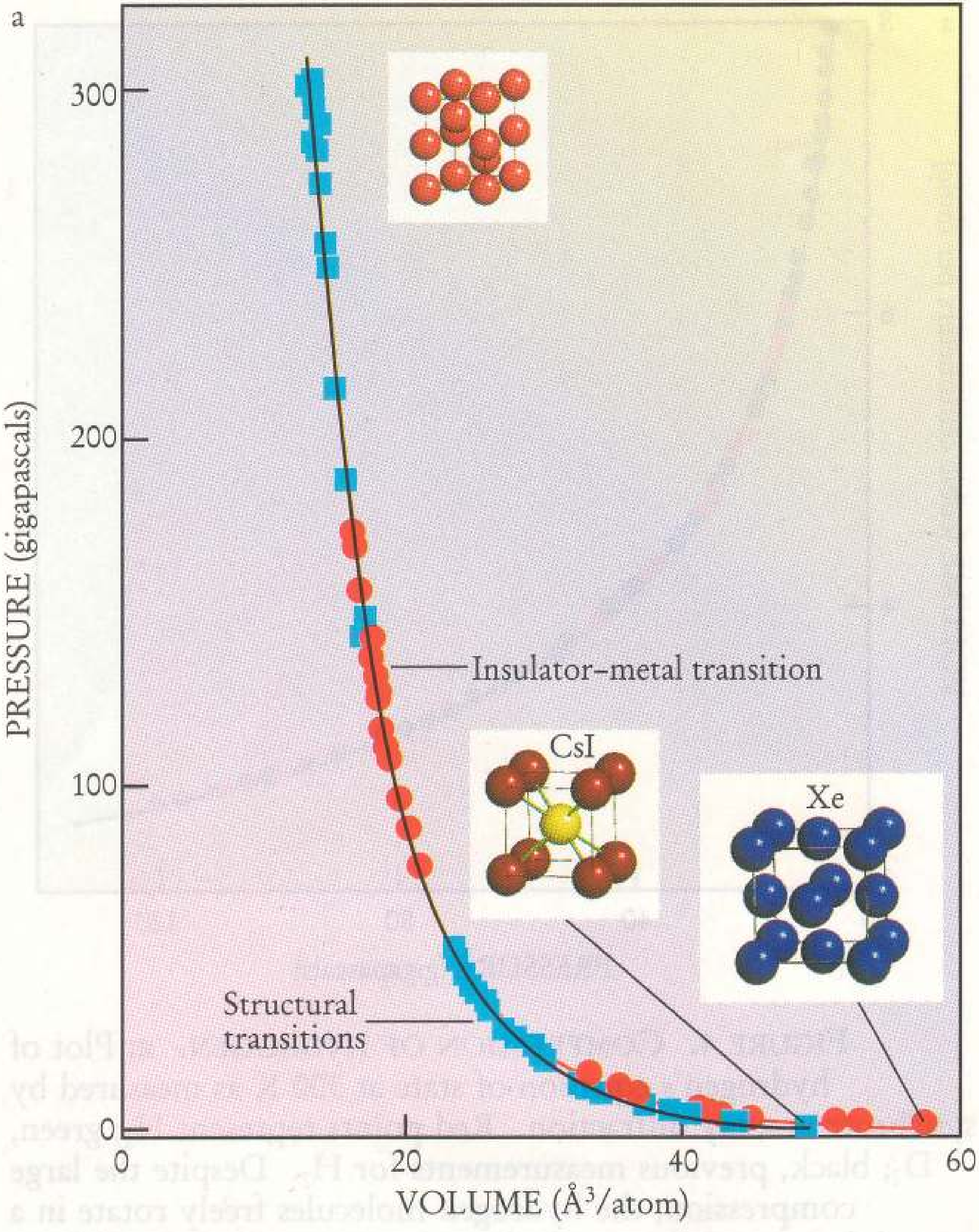

300
200
100
0
0
20
40
60
PRESSURE (gigapascals)
VOLUME (Å³/atom)
Insulator–metal transition
CsI
Xe
Structural
transitions

Solid – solid critical point in Ce

(Ponyatovsky, 1958)

Tsiok, Khvostansev, 2000

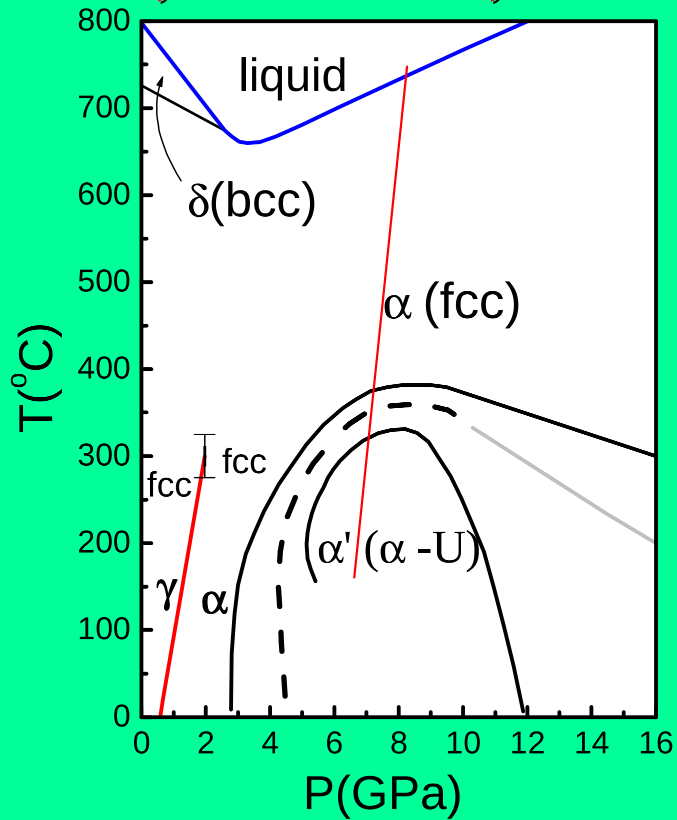

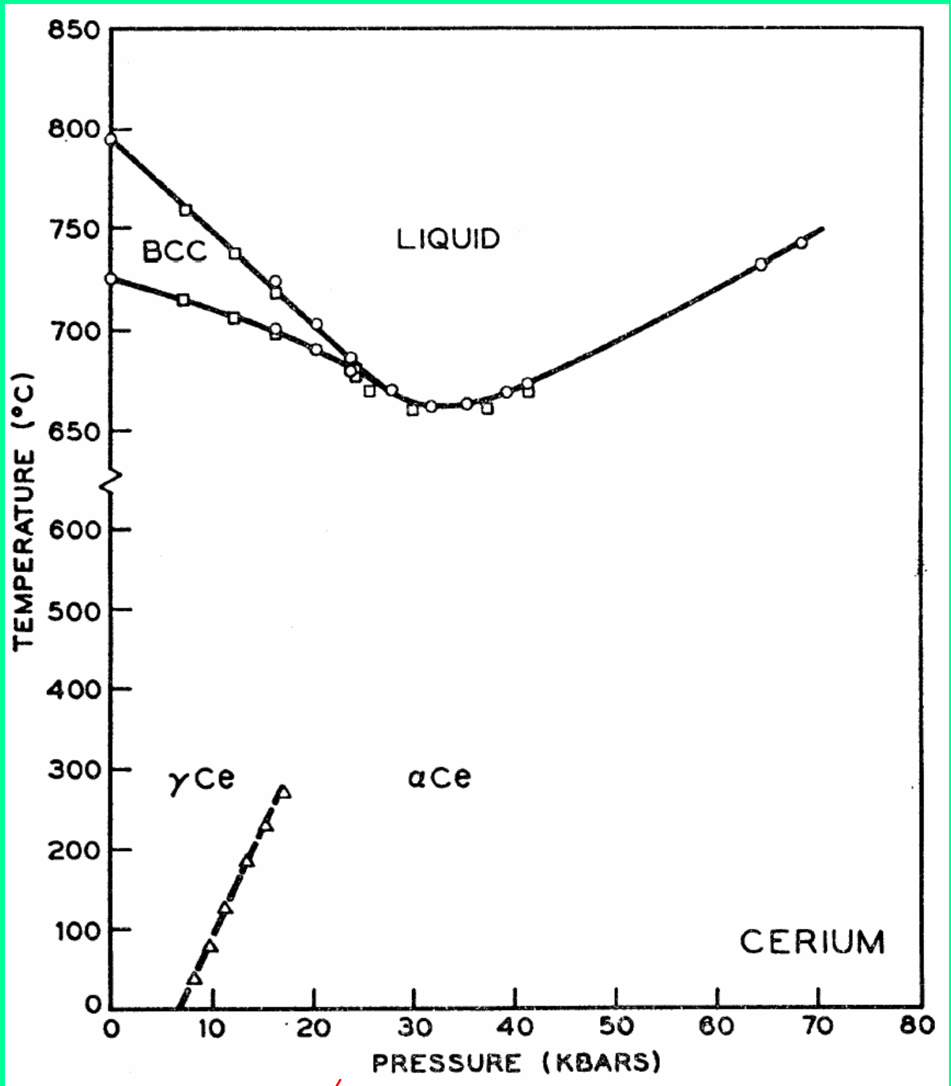

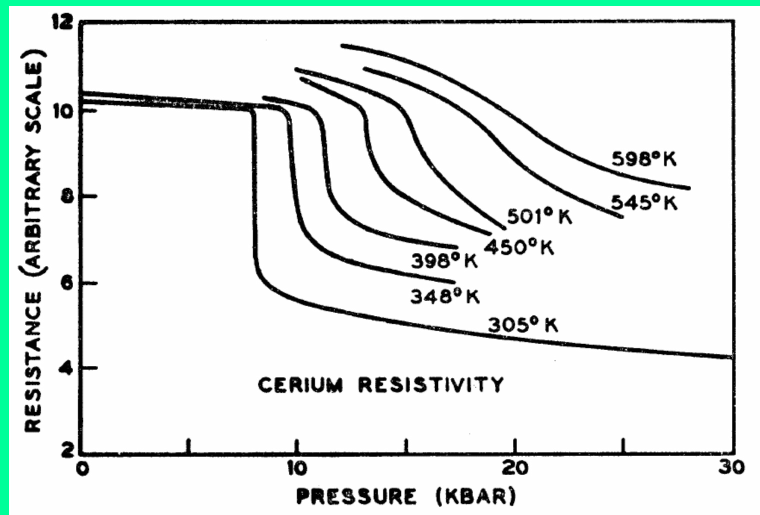

Jayaraman, 1965

to the pressure. The main factor which limits the maximum pressures that can be reached within vessels is the strength of materials. The strongest steels in the most favourable form and size (piano wire, for example) have ultimate tensile strengths of the order of 14,000–21,000 kgm./cm.². Sintered carbides, such as 'Carboloy', have compressive strengths of the order of 50,000 kgm./cm.² or more. The pressure required for reasonably rapid synthesis of diamond was thought by our group to be above the compressive strength of 'Carboloy' in the range 50,000–100,000 kgm./cm.².

Merely making the walls thicker on a pressure vessel contributes very little to its pressure-holding ability after a certain wall thickness is reached. By using multiple support bands on the cylinder part (a technique used years ago in making large gun barrels), and special sealing gasket devices between

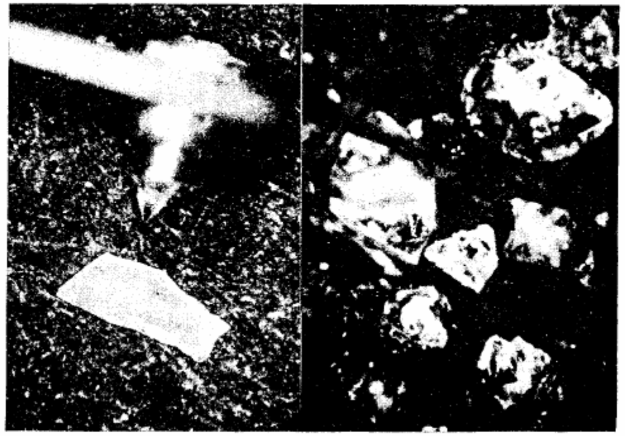

(a) (b)

Fig. 3. Man-made diamonds. (a) 1-mm. diamond shown with phonograph needle. (b) 0·2–0·5-mm. octahedra

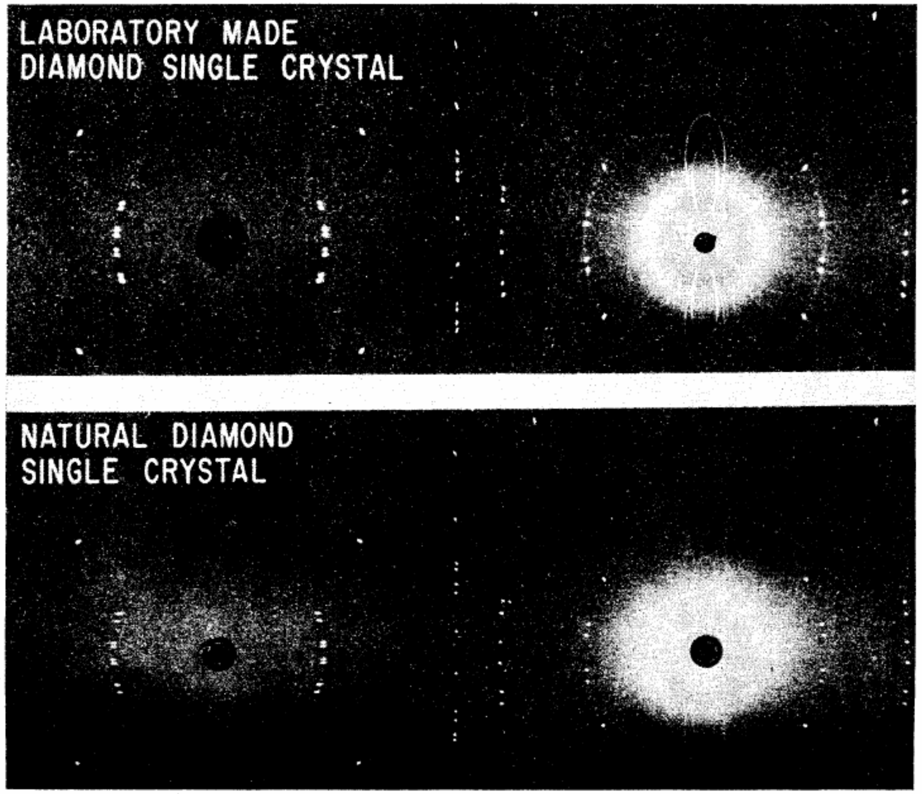

Fig. 4. X-ray diffraction patterns of man-made and natural diamond (powder camera photograph)

Errors in diamond synthesis

SIR — In 1955, some of us announced the first reproducible synthesis of diamond[1], details of which were subsequently published[2]. These results marked the beginning of the present synthetic-diamond industry. But from the outset there were doubts in our team as to whether the first diamond grown by our technique (which we will call the run 151 diamond) was truly synthetic at all, or whether it was instead just a fragment of a natural diamond seed that got into the experiment inadvertently. We have now reanalysed the run 151 diamond using modern spectroscopic techniques and have found that it is indeed a small piece of a natural type Ia diamond.

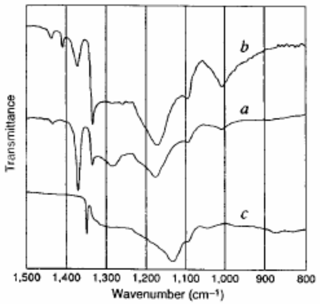

Infrared absorption spectra of: *a*, run 151 diamond; *b*, a type Ia natural diamond with 'B'-form nitrogen; *c*, a typical synthesized diamond (type Ib).

In the early 1950s four of us (H. P. B., F. P. B., H. M. S. and R. H. W.), together with H. T. Hall, developed an approach to diamond synthesis at high pressures and temperatures. The pressure scale used in our experiments was Bridgman's 'resistance-jump' scale, which was suspected to be in error in absolute terms above 30 kbar or so. The proximity of our experimental conditions to the calculated graphite–diamond phase boundary was therefore uncertain.

The run 151 diamond appeared in an experiment using apparatus made of hard steel. According to the Bridgman 'resistance' scale, the pressure in this run was about 53 kbar, within the diamond stability field[3]. But later developments revealed that the true pressure could not have been much above 42 kbar, which is insufficient to stabilize diamond.

To investigate the true nature of the run 151 diamond, we recently removed it from the GE archives, cleaned it with acids and rinsed it with water. An infrared absorption spectrum was measured using an IR PLAN microscope attached to a Nicolet 740 FTIR spectrometer. The portion of this spectrum shown in the figure resembles that of a natural nitrogen-containing type Ia diamond[4]. In particular, there are coincidences of the absorption bands at about 1,365 cm^{-1} (related to nitrogen platelets), 1,330 cm^{-1} (a Raman frequency, rendered infrared-active by defects and impurities), 1,280 cm^{-1} (from nitrogen in the 'A' aggregate form) and 1,175 cm^{-1} (from nitrogen in the 'B' aggregate form). We also show the spectrum of a typical nitrogen-containing synthetic type Ib diamond, which has characteristic bands at 1,130 and 1,343 cm^{-1} (ref. 5); neither of these bands is seen in the run 151 diamond. We conclude that the run 151 diamond is a small piece of a natural type Ia diamond.

How the natural diamond got into the run 151 experiment is not clear, although it came to light only a week later, when the iron pellet from the run was being polished for metallographic examination. After we found this diamond and took it to be synthetic, Hall used a similar synthetic system of iron/iron sulphide/graphite in his 'belt' apparatus, which used a carbide piston and cylinder to achieve high pressures[6]. This led to further successful runs and ultimately to the development of the process for synthesizing diamonds at high pressures and temperatures from graphite reacted with molten group VIII metals and alloys, which we described fully in 1959[2] (after a US Department of Defense secrecy order had been lifted). Our mistake was therefore clearly a most serendipitous one, as it provided the impetus to experiment with that system at higher pressures, leading quickly to the "right" and "reproducible" results.

H. P. Bovenkerk
F. P. Bundy
R. M. Chrenko
P. J. Codella
H. M. Strong
R. H. Wentorf Jr
GE Corporate Research and Development, Schenectady, New York 12301, USA

1. Bundy, F. P., Hall, H. T., Strong, H. M. & Wentorf, R. H. Jr *Nature* **176**, 51–54 (1955).
2. Bovenkerk, H. P., Bundy, F. P., Hall, H. T., Strong, H. M. & Wentorf, R. H. Jr *Nature* **184**, 1094–1098 (1959).
3. Strong, H. M. *Am. J. Phys.* **57**, 794–802 (1989).
4. Clark, C. D., Mitchell, E. W. J. & Parsons, B. J. in *The Properties of Diamond* (ed. Field, J. E.) 28 (Academic, London, 1979).
5. Chrenko, R. M., Tuft, R. E. & Strong, H. M. *Nature* **270**, 141–144 (1977).
6. Hall, H. T. *Rev. sci. Instr.* **31**, 125–131 (1960).

Galaxies and magnetic fields

SIR — The observed flat rotation curves of spiral galaxies constitute one of the most important facts suggesting the existence of large amounts of so-called dark matter in the Universe. However, if the galactic gas could be held in equilibrium by forces other than gravity alone, then an important argument for excess galactic mass would be weakened. Battaner *et al.*[1] suggest that stresses from an azimuthal magnetic field at the peripheries of a galactic disk can provide the confining stress needed. Here we reconsider the question of magnetic-field and gas equilibrium, and point out that the simple success of the one-dimensional Battaner *et al.* model depends on their incomplete treatment of the three-dimensional equilibrium. Application of the well-known virial theorem shows that the addition of magnetic field to their system would require more dark matter to maintain equilibrium, not less.

The pertinent steady-state virial theorem is[2,3]

$$2\,(T+T_t) + M + \int_V d^3\mathbf{r}\, x_i F_i = S \qquad (1)$$

where $T = \int_V d^3\mathbf{r}\rho v^2/2$ is the sum of directed kinetic energies; $T_t = \int_V d^3\mathbf{r}\rho\langle u^2\rangle/2$ is the sum of thermal or random kinetic energies; $M = \int_V d^3\mathbf{r}B^2/8\pi$ is the total magnetic field energy, and F_i is the force of gravity. $S = \int_S dS_k x_i\{-p\delta_{ik} + M_{ik}\}$ is the surface stress integral, with p the particle pressure and M_{ik} the Maxwell stress tensor.

Following Battaner *et al.*, consider an isolated system with $S = 0$. The terms T, T_t and M in equation (1) are positive definite; only the last term on the left of the equation, the gravity integral, is negative. Regardless of the configuration or geometry, in the overall dynamical balance of a physical system, magnetic field is an expansive stress. Equation (1) shows explicitly that the only confining stress for large, isolated, astrophysical systems is gravity.

Applying equation (1) to the specific situation addressed by Battaner *et al.*, we first consider the case in which magnetic field stresses can be neglected ($M = 0$). Focusing only on the super-keplerian gas — treating it as an isolated system immersed in external gravity — it is clear that virial equilibrium requires a dynamical balance between the expansive tendency of the gas motions and the confining influence of gravity acting on that gas. The need for dark matter is already encapsulated in this analysis.

Now, with everything else unchanged, assume that the gas is magnetized. According to Battaner *et al.*, assuming a special field configuration, the magnetic stresses should take up some of the expansive tendency of the gas motion, so that the strength of gravity needed diminishes. But, from the more general virial rela-

Diamond: stability, elastic properties

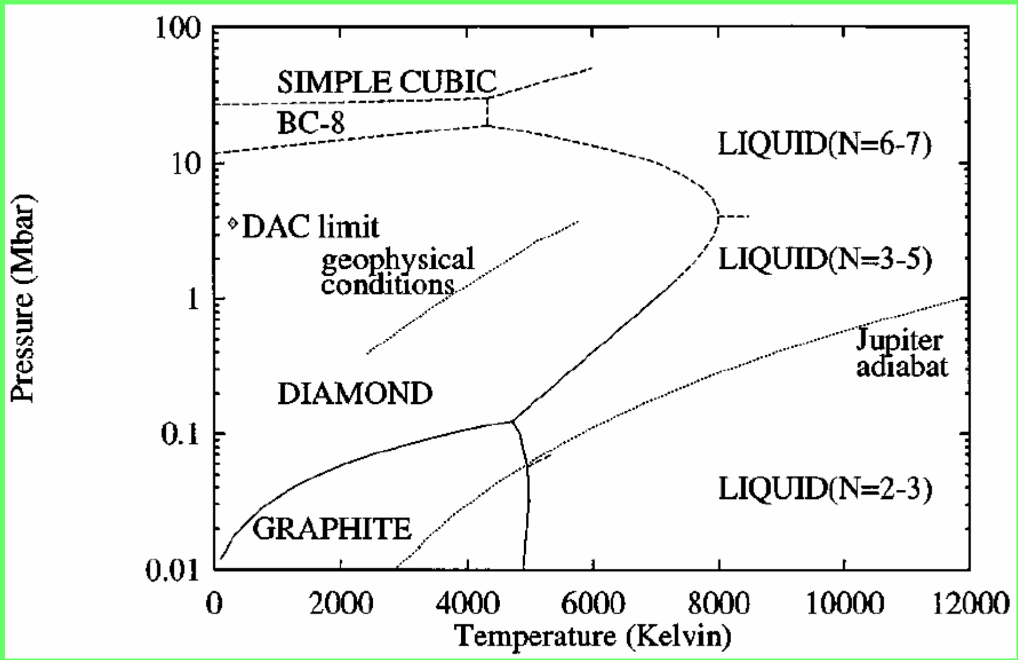

Grumbash, Martin, 1996

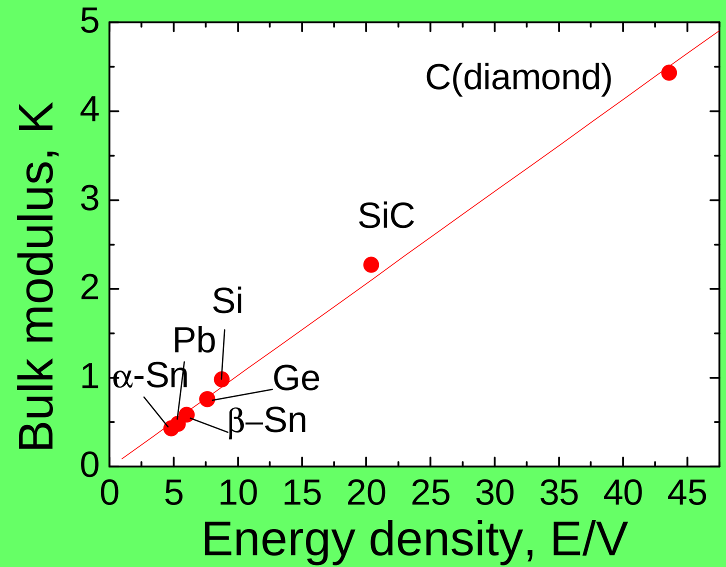

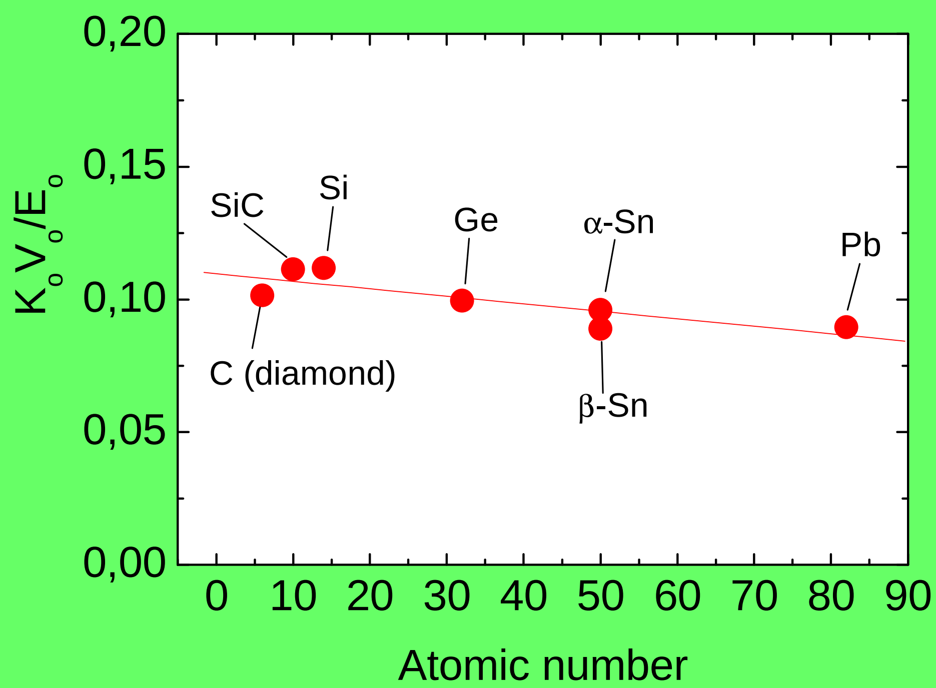

Stishov, 2000

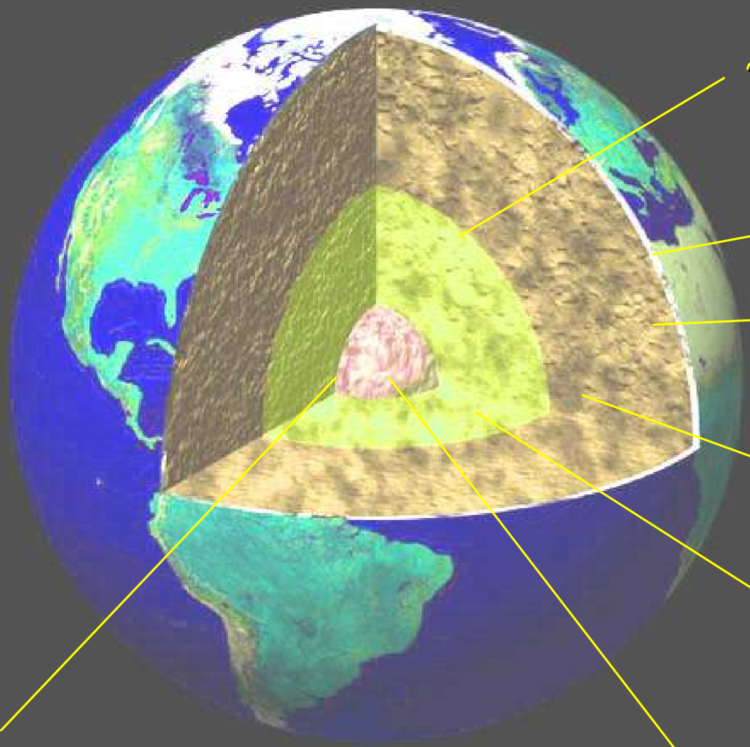

Earth radius ~ 6380 km

Average density ~ 5.5 g / cm^3

Crust average density ~ 2.8 g / cm^3

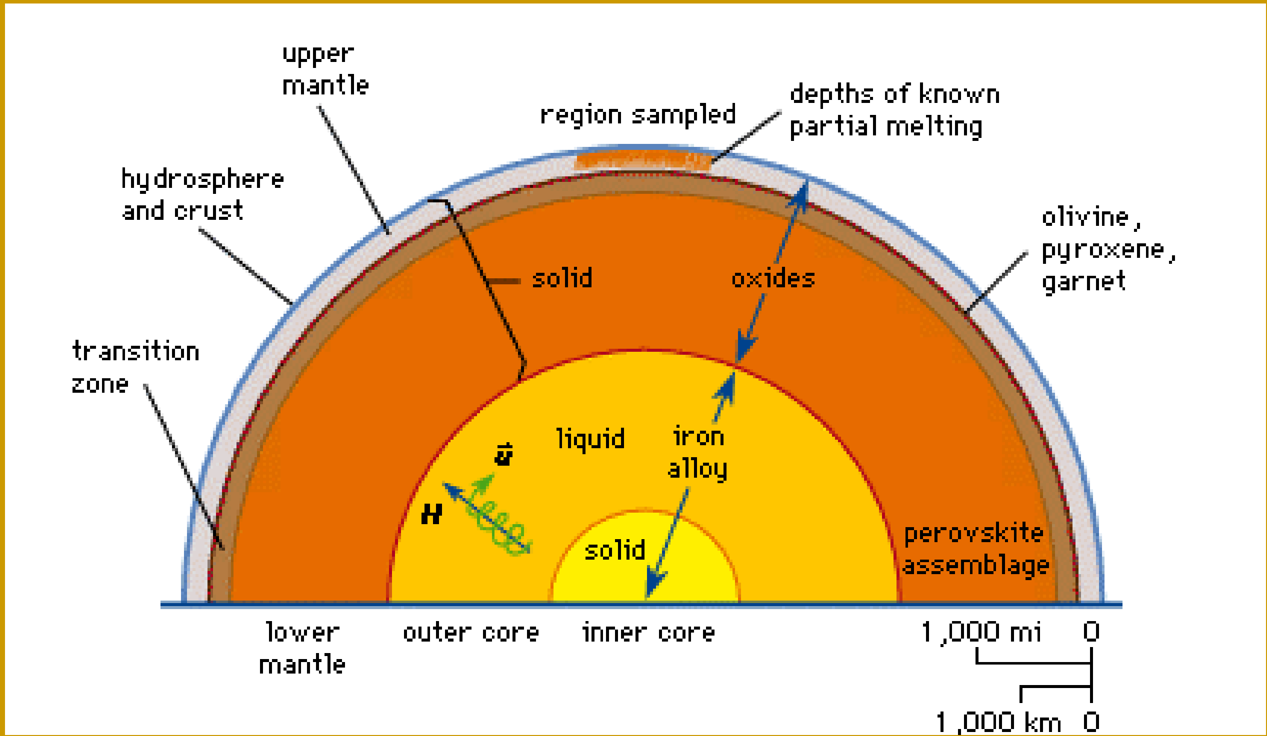
upper mantle
region sampled
depths of known partial melting
hydrosphere and crust
olivine, pyroxene, garnet
solid
oxides
transition zone
liquid
iron alloy
H
solid
perovskite assemblage
lower mantle
outer core
inner core
1,000 mi 0
1,000 km 0

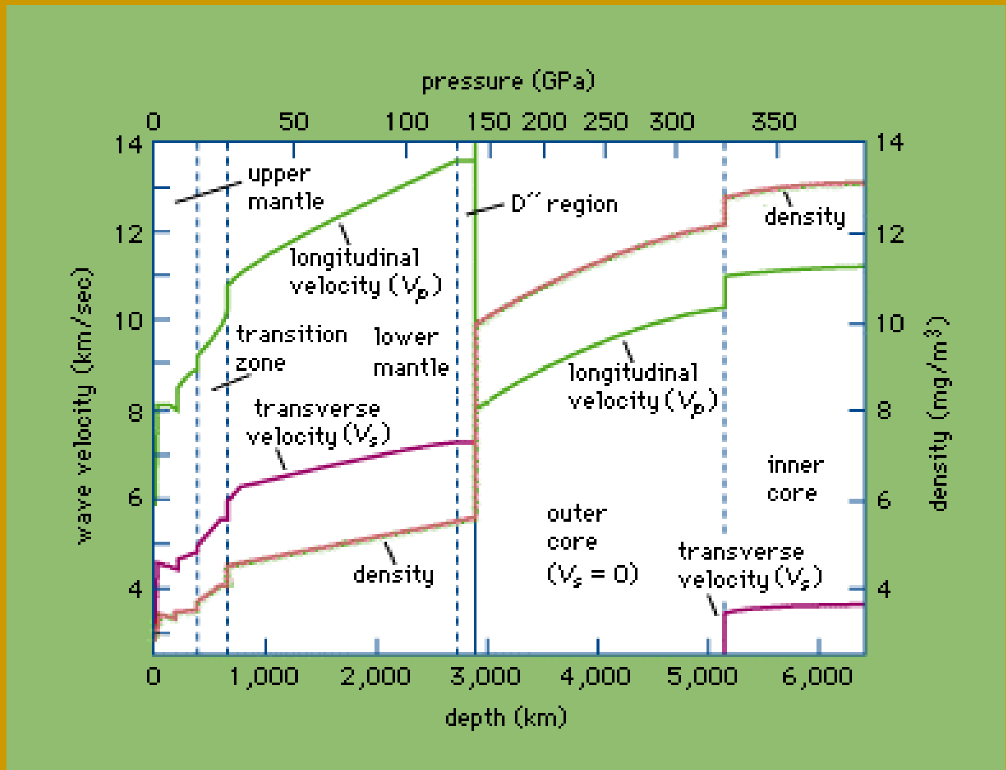
pressure (GPa)
0 50 100 150 200 250 300 350
upper mantle
D´´ region
density
longitudinal velocity (V_p)
transition zone
lower mantle
longitudinal velocity (V_p)
transverse velocity (V_s)
inner core
outer core (V_s = 0)
transverse velocity (V_s)
density
wave velocity (km/sec)
density (mg/m^3)
0 1,000 2,000 3,000 4,000 5,000 6,000
depth (km)

ALBERT FRANCIS BIRCH
1903-1992

JOURNAL OF GEOPHYSICAL RESEARCH VOLUME 57, NO. 2 JUNE, 1952

ELASTICITY AND CONSTITUTION OF THE EARTH'S INTERIOR*

By FRANCIS BIRCH

Harvard University, Cambridge, Massachusetts

(Received January 18, 1952)

ABSTRACT

The observed variation of the seismic velocities with depth, below the crust, is examined with reference to the variation to be expected in a homogeneous medium. A general equation is derived for the variation of the quantity, $\phi = V_P^2 - 4/3\, V_S^2$, in a homogeneous gravitating layer with an arbitrary gradient of temperature. The parameters of this equation are then discussed in terms of the experimental and theoretical relations for solids. The principal parameter is $(\partial K_T/\partial P)_T$, the rate of change of isothermal incompressibility with pressure, which can be found for large compressions from Bridgman's measurements. Comparison of observed and expected rates of variation of ϕ throughout the Earth's interior leads to conclusions regarding homogeneity and, with a larger uncertainty, to estimates of temperature.

Dense silica

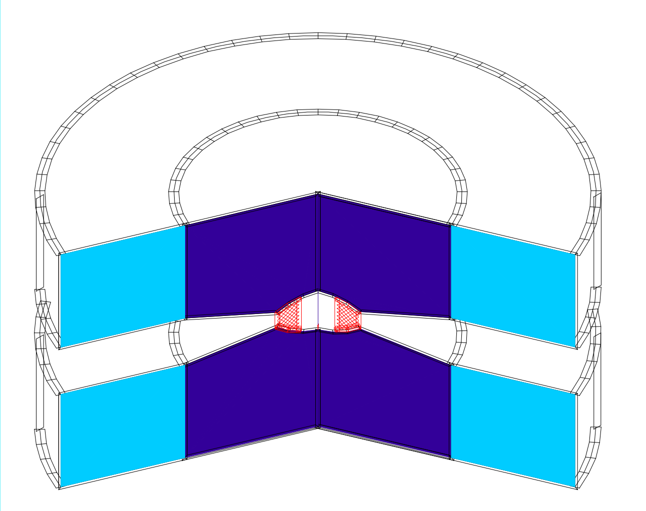

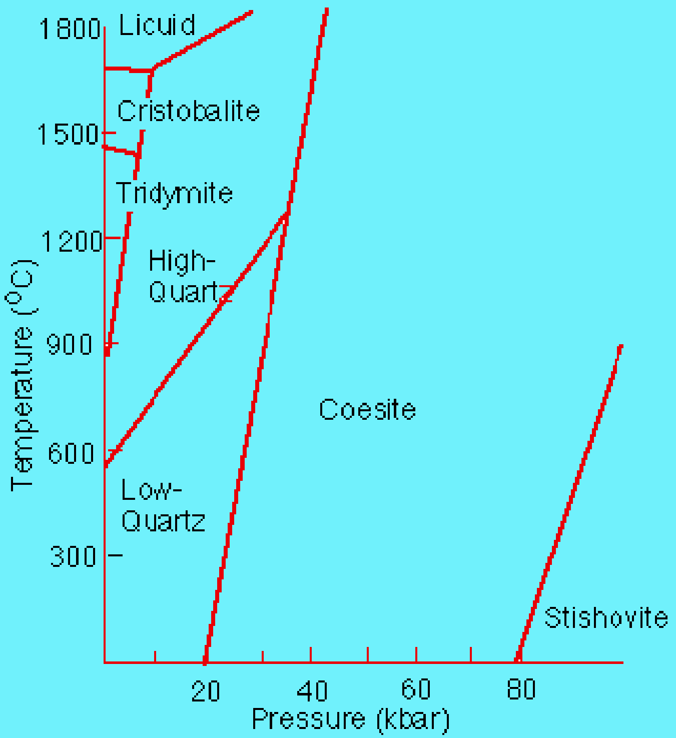

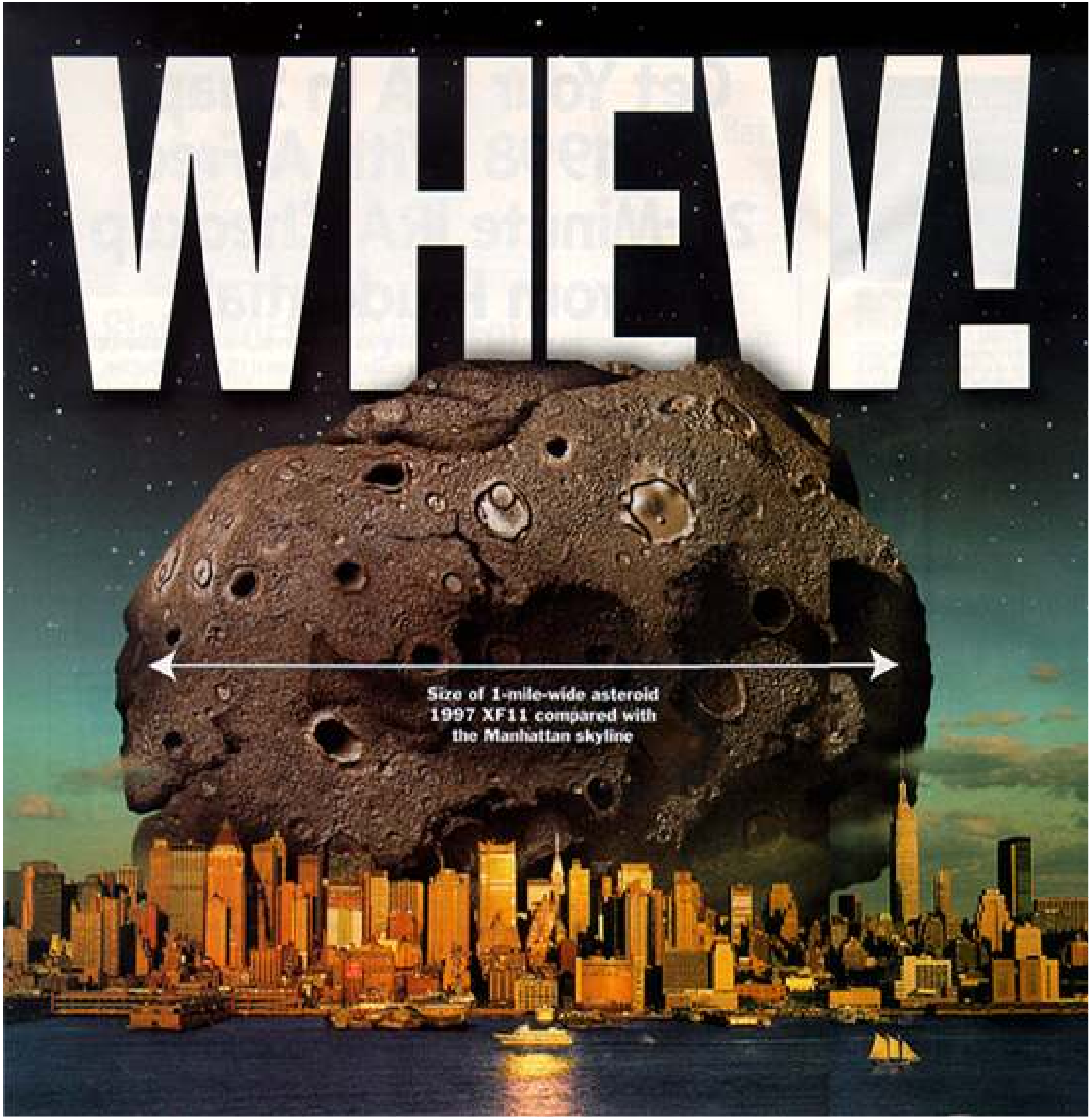
WHEW!
Size of 1-mile-wide asteroid
1997 XF11 compared with
the Manhattan skyline

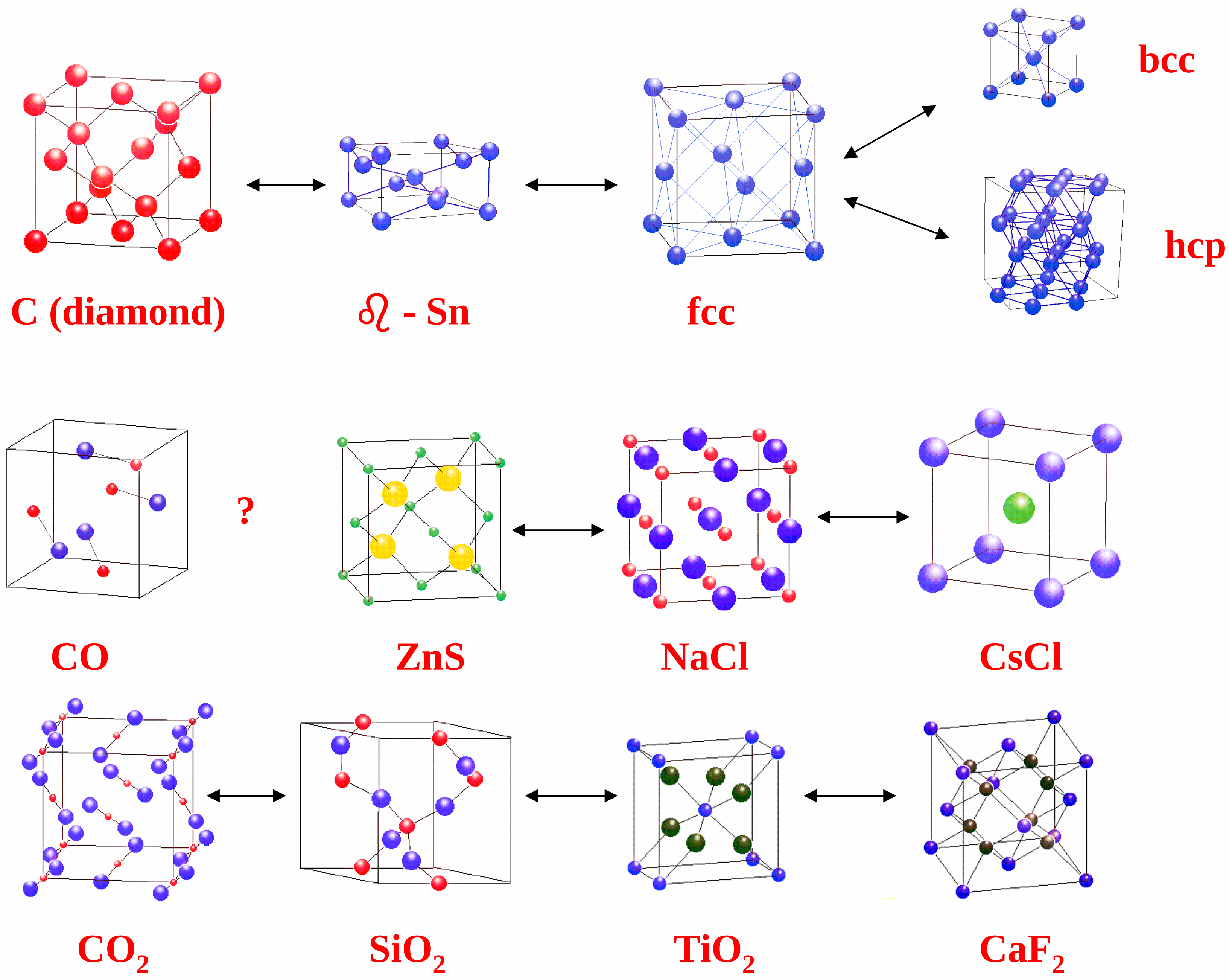
C (diamond)
β - Sn
fcc
bcc
hcp
CO
?
ZnS
NaCl
CsCl
CO_2
SiO_2
TiO_2
CaF_2

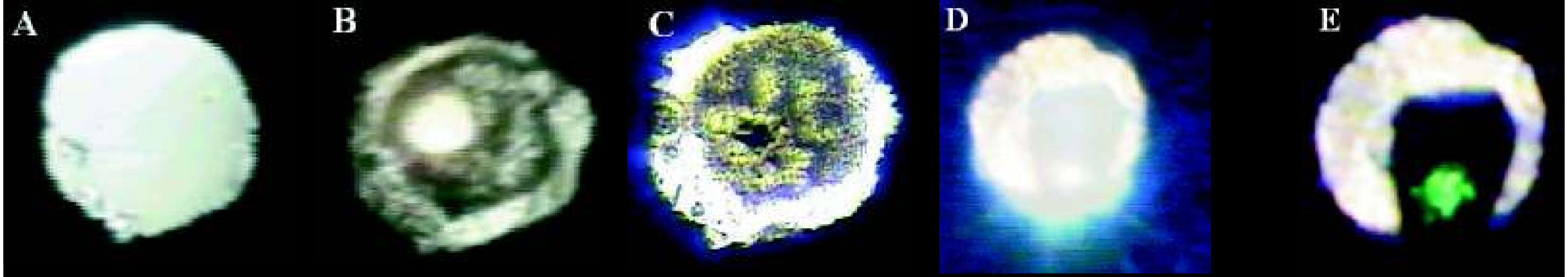

Quartz-like CO_2 (Iota, Yoo, Cynn, 1999)

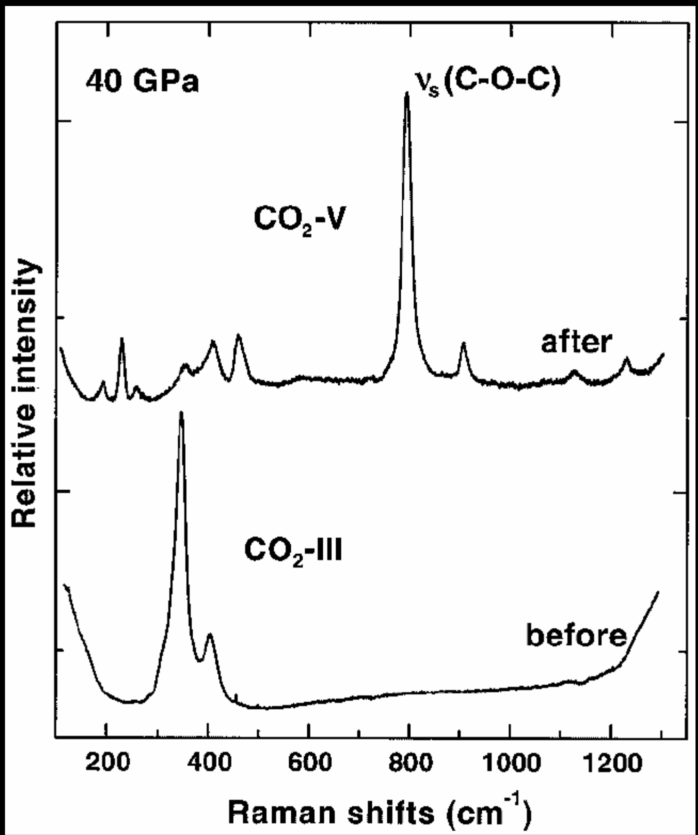

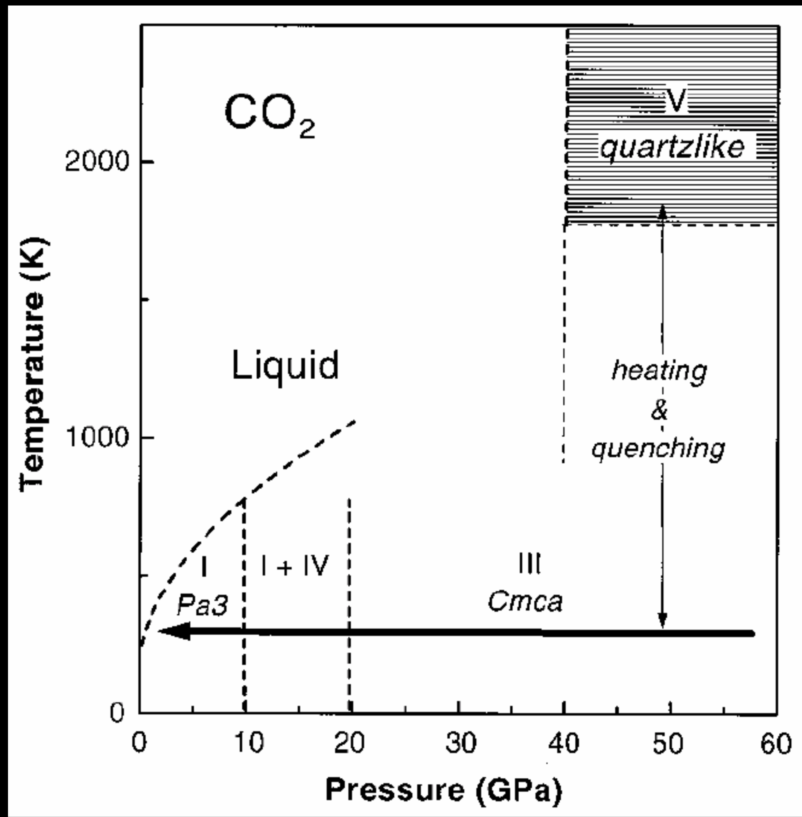

Эволюция кристаллической структуры *SiO$_2$* при высоком давлении

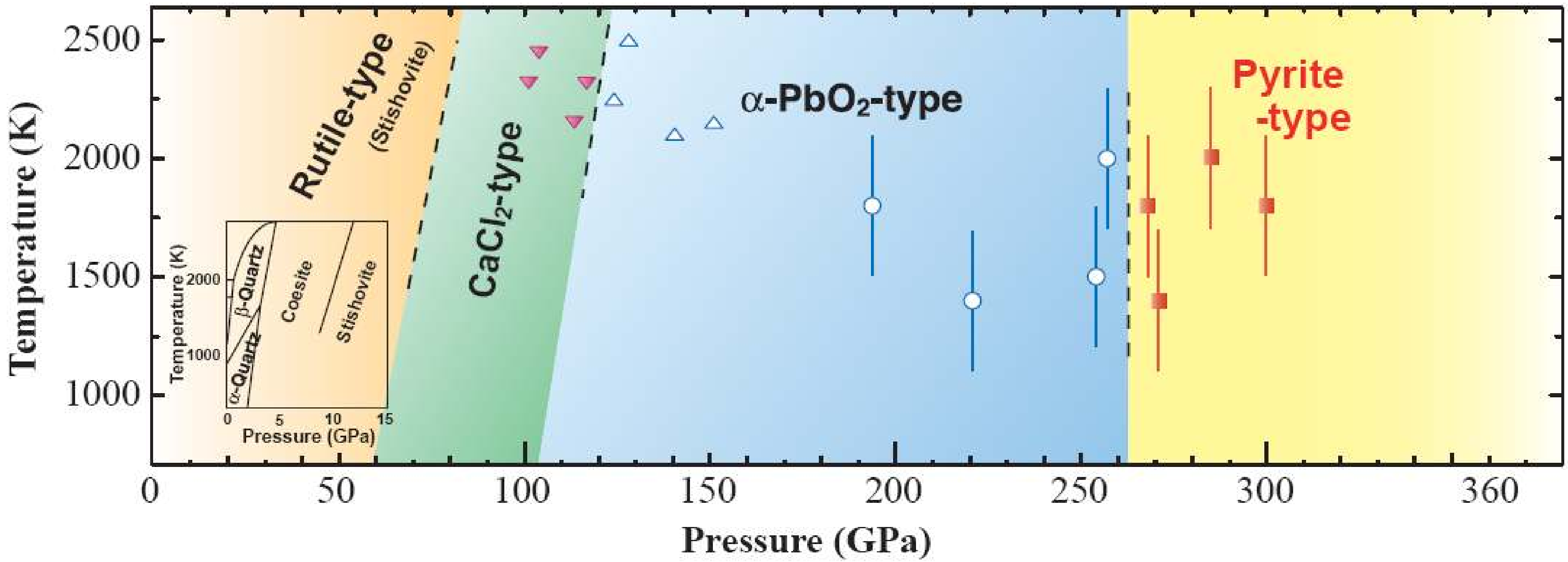

Фазовый переход в перовските $MgSiO_3$ при P ≈ 100 ГПа

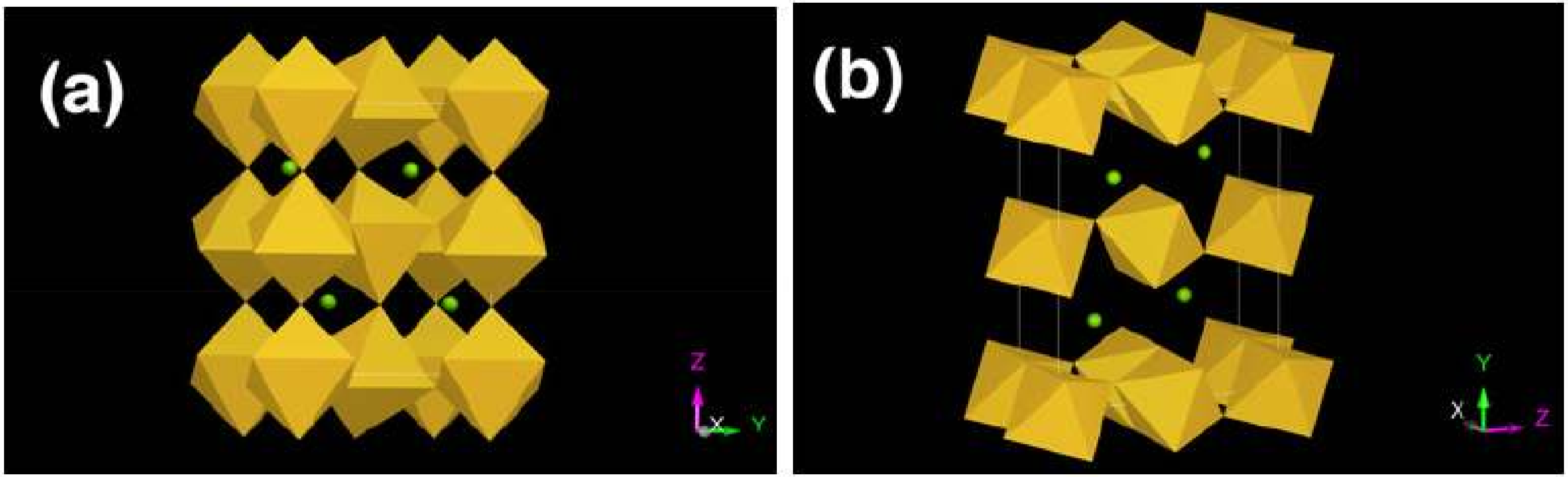

The unit cell structures of $MgSiO_3$. a) Perovskite; b) postperovskite.

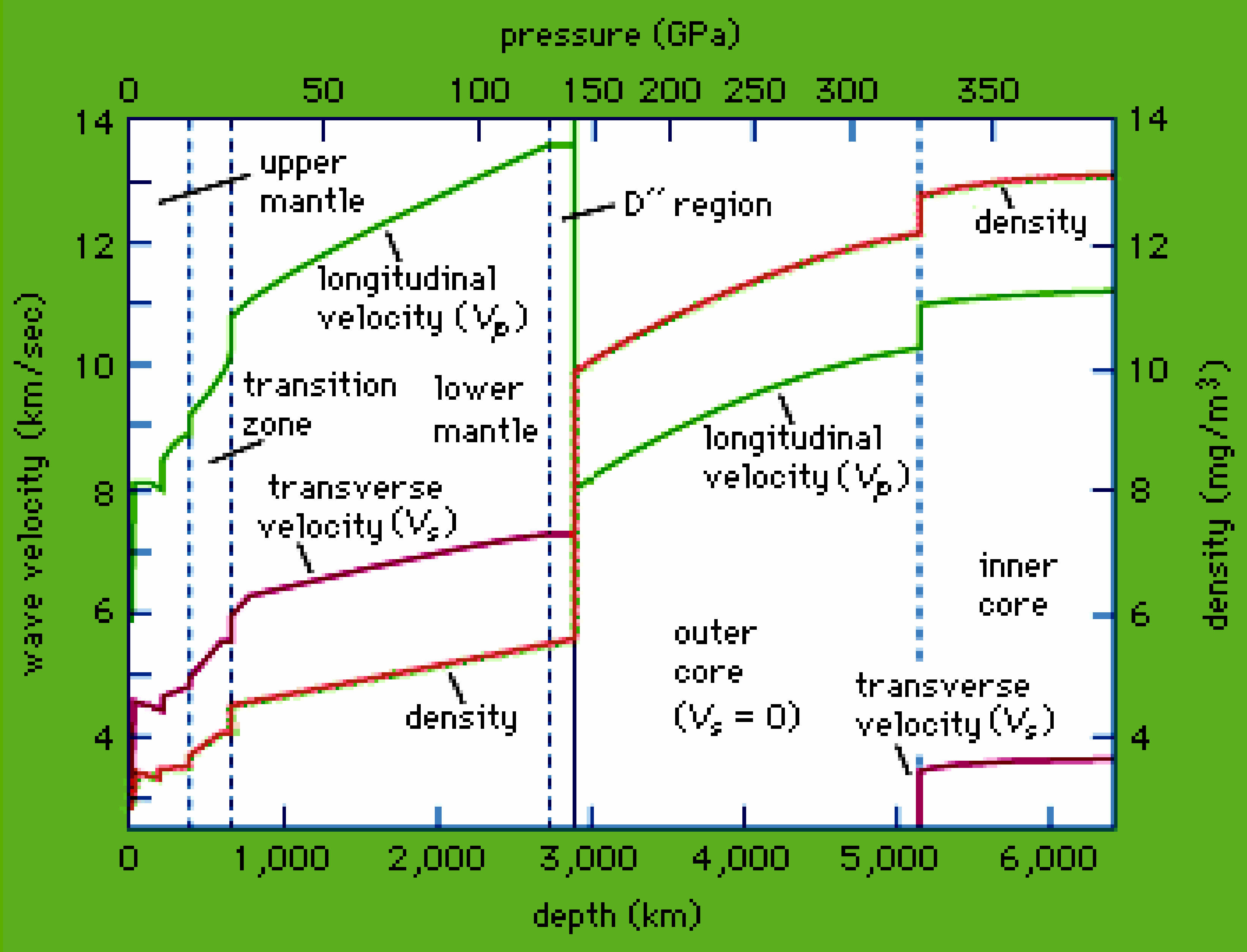
pressure (GPa)
0
50
100
150
200
250
300
350
14
12
10
8
6
4
wave velocity (km/sec)
density (mg/m3)
upper
mantle
D'' region
density
longitudinal
velocity (Vp)
transition
zone
lower
mantle
longitudinal
velocity (Vp)
transverse
velocity (Vs)
inner
core
outer
core
(Vs = 0)
density
transverse
velocity (Vs)
0
1,000
2,000
3,000
4,000
5,000
6,000
depth (km)

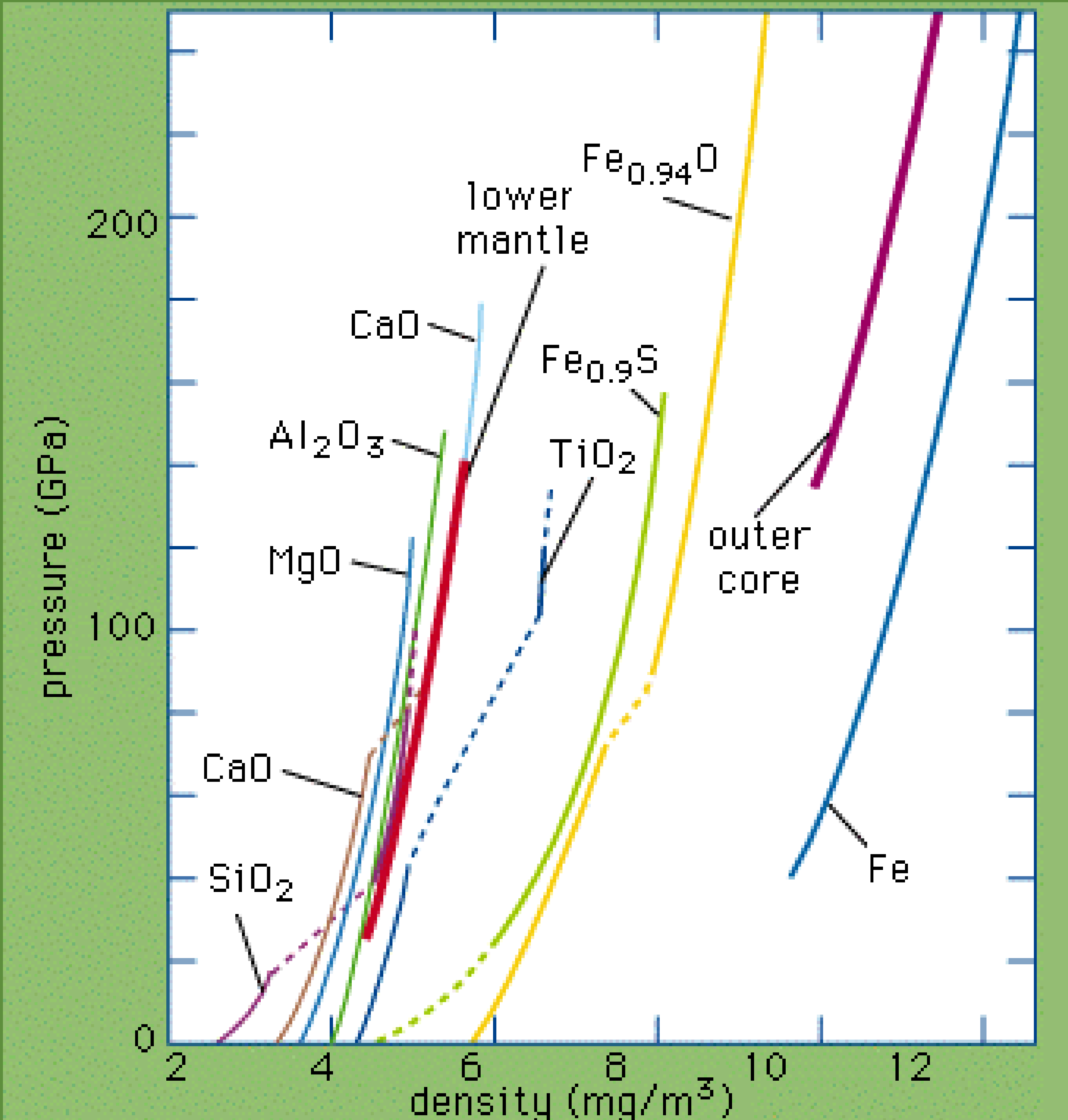

pressure (GPa)
200
100
0
2
4
6
8
10
12
density (mg/m^3)
$Fe_{0.94}O$
lower mantle
CaO
$Fe_{0.9}S$
Al_2O_3
TiO_2
MgO
outer core
CaO
SiO_2
Fe

Iron EOS (Dubrovinsky, Saxena et al., 2000)

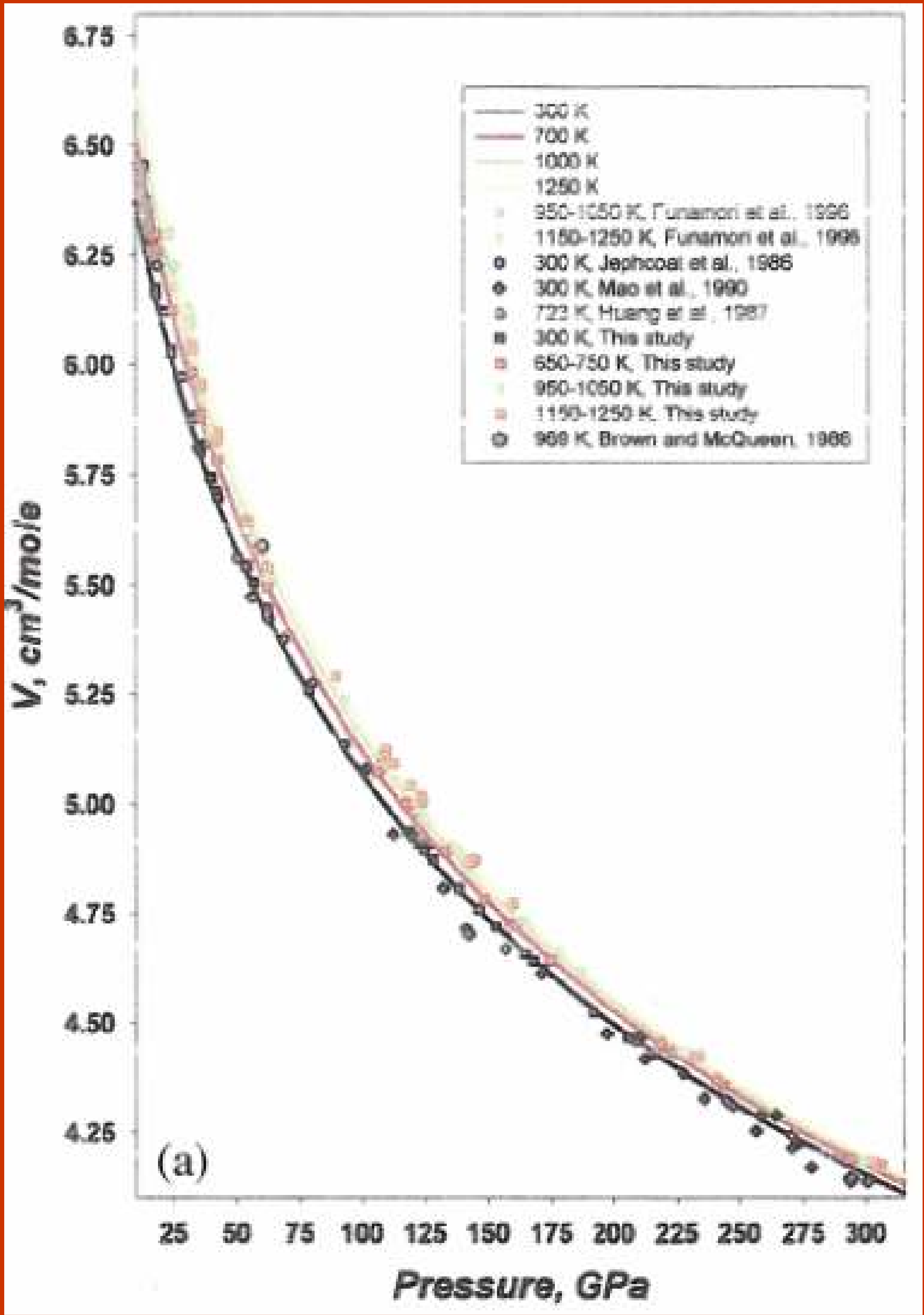

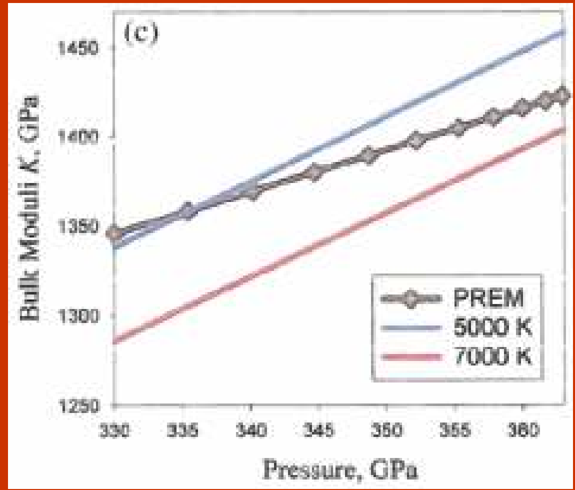

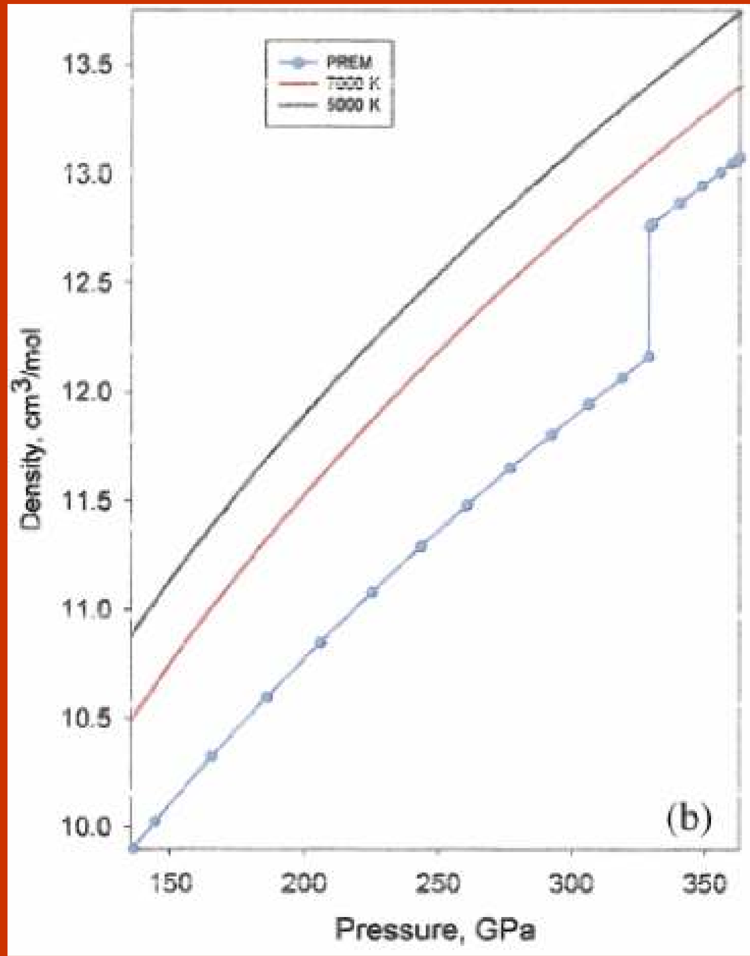

Hydrogen at High Pressure

MaO, Hemley, 1994

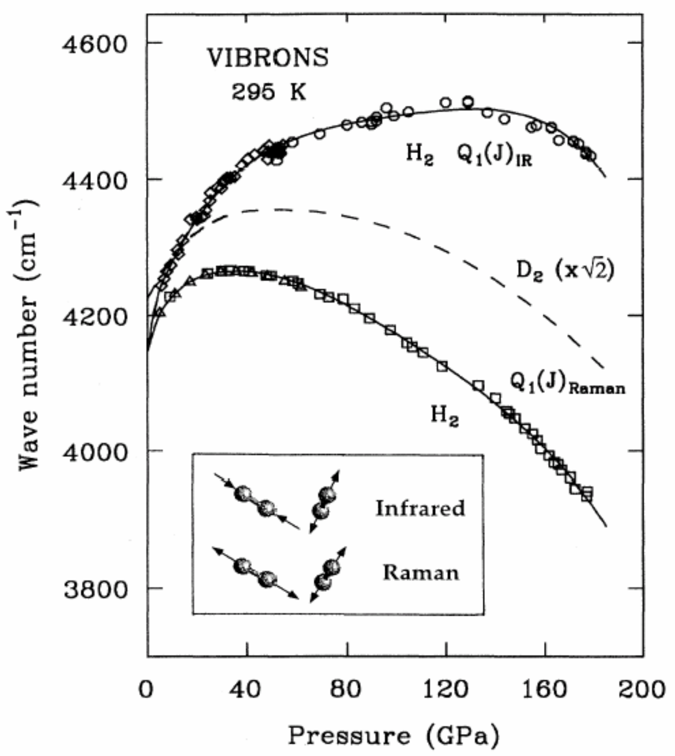

Weir, Mitchell, Nellis, 1996

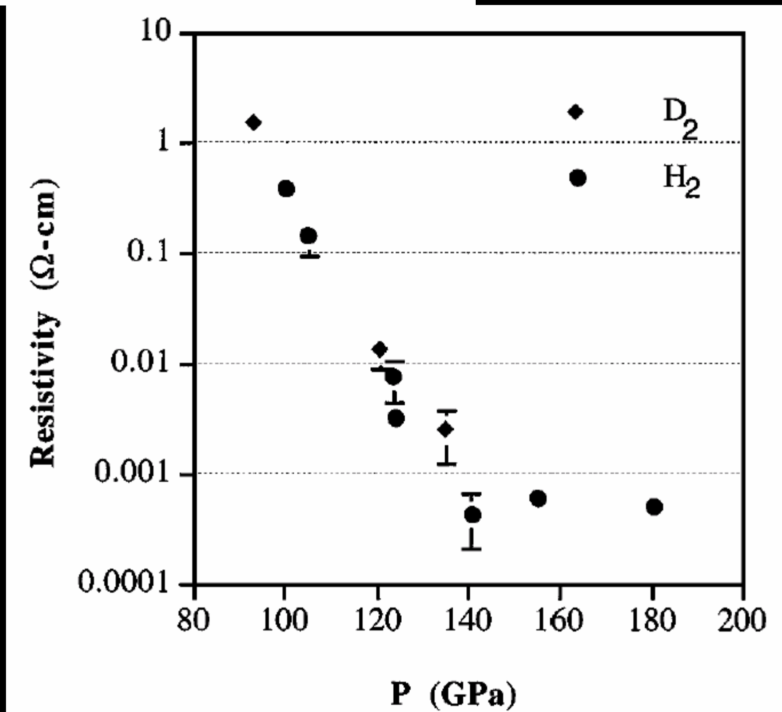

Loubeyre et al., 1996

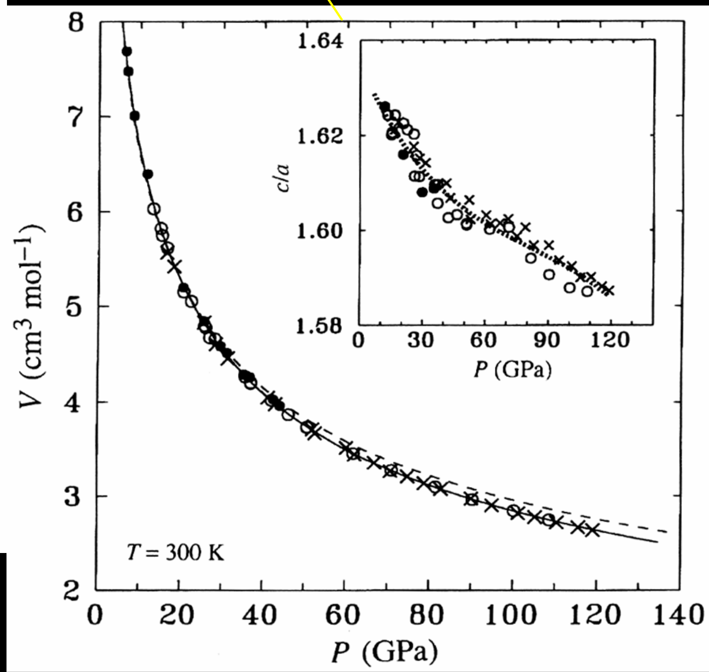

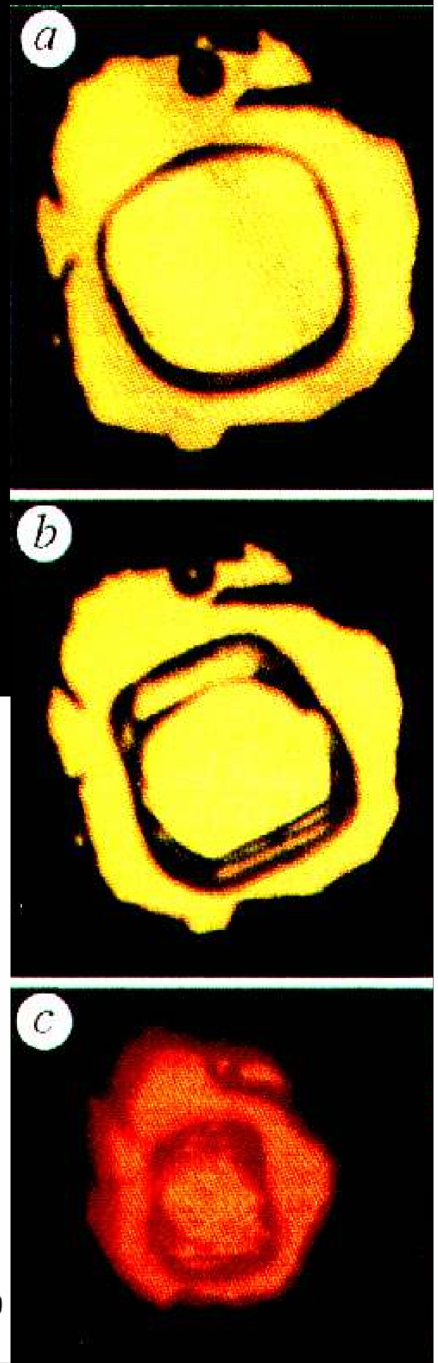


6 μm H_2 at 290 GPa
35 μm Tip
165 μm flattened

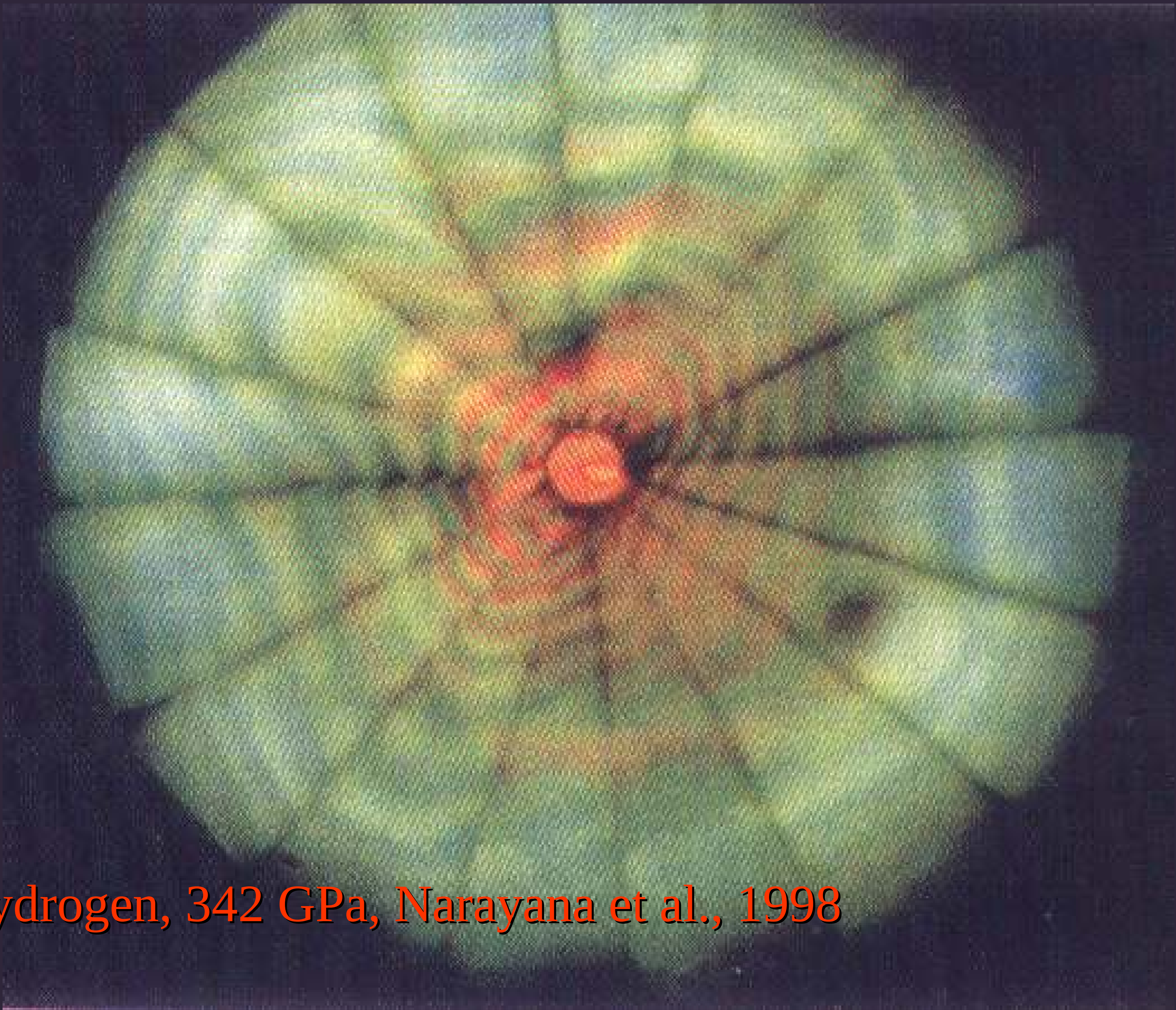

Hydrogen, 342 GPa, Narayana et al., 1998

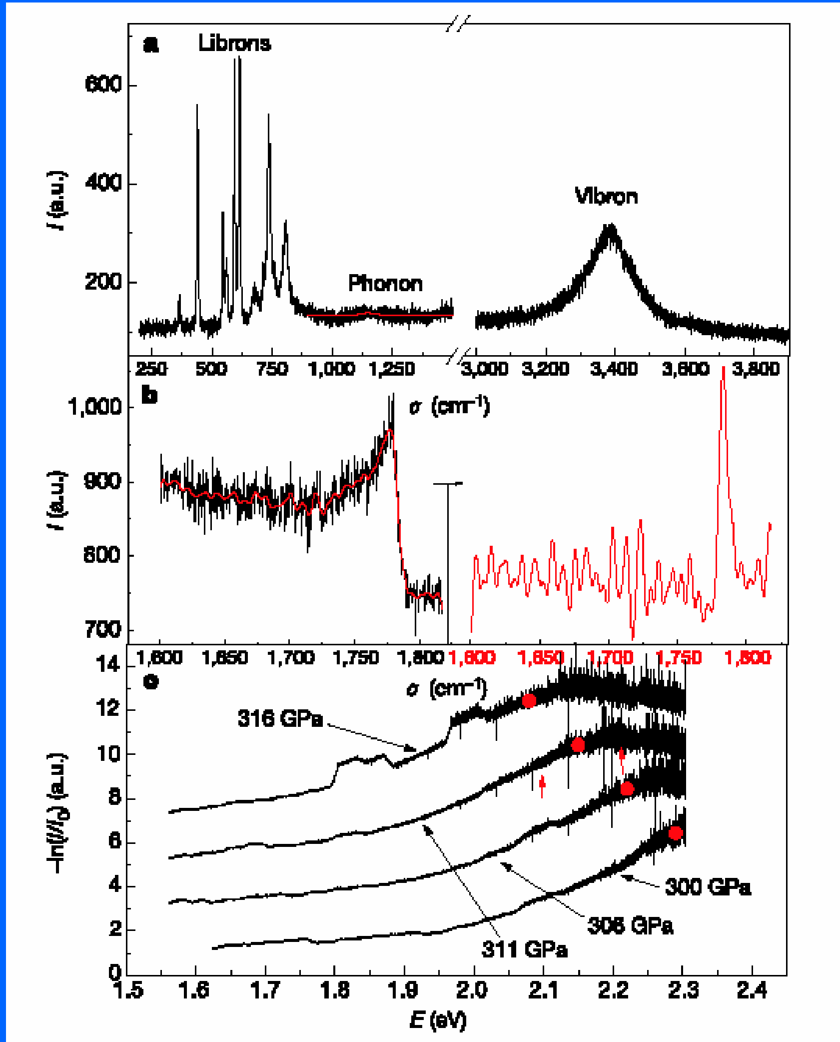

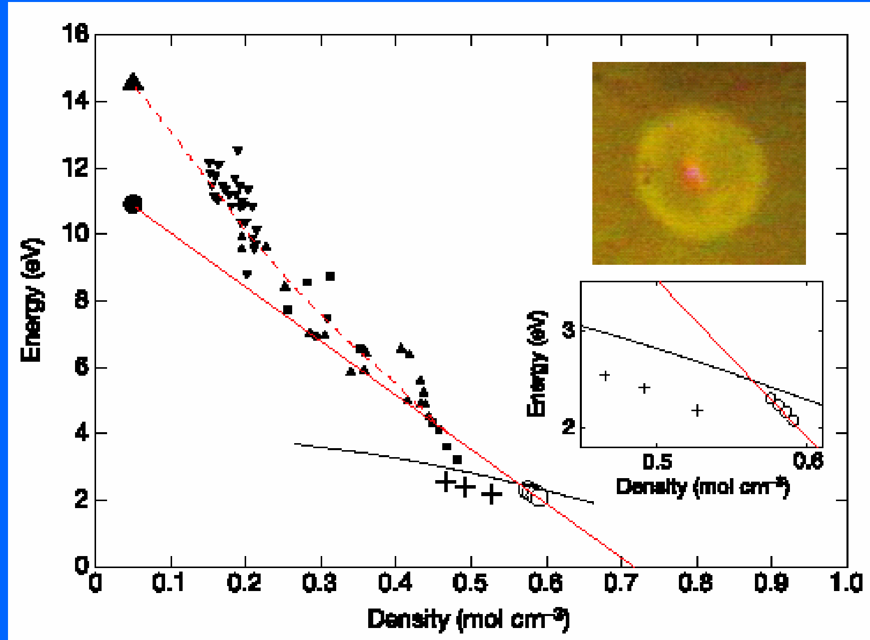

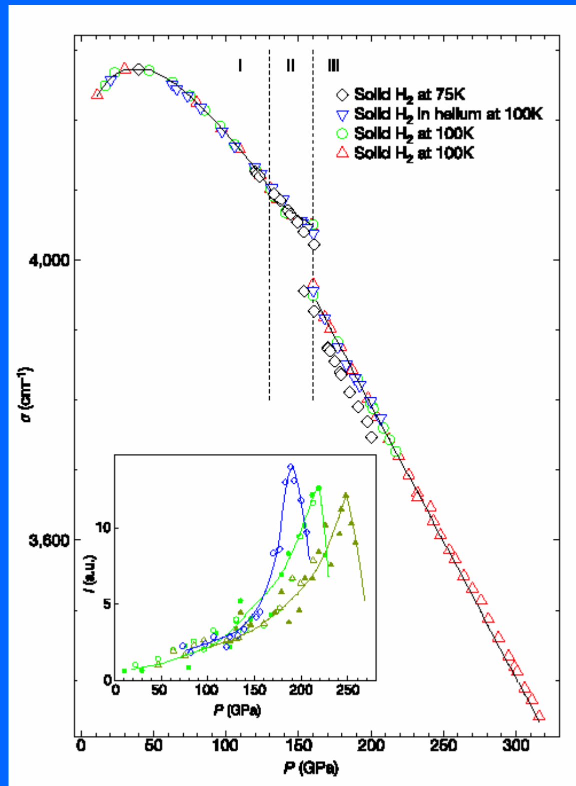

Loubeyre et al. Nature,416,613,2002

Goncharov et al., 2003

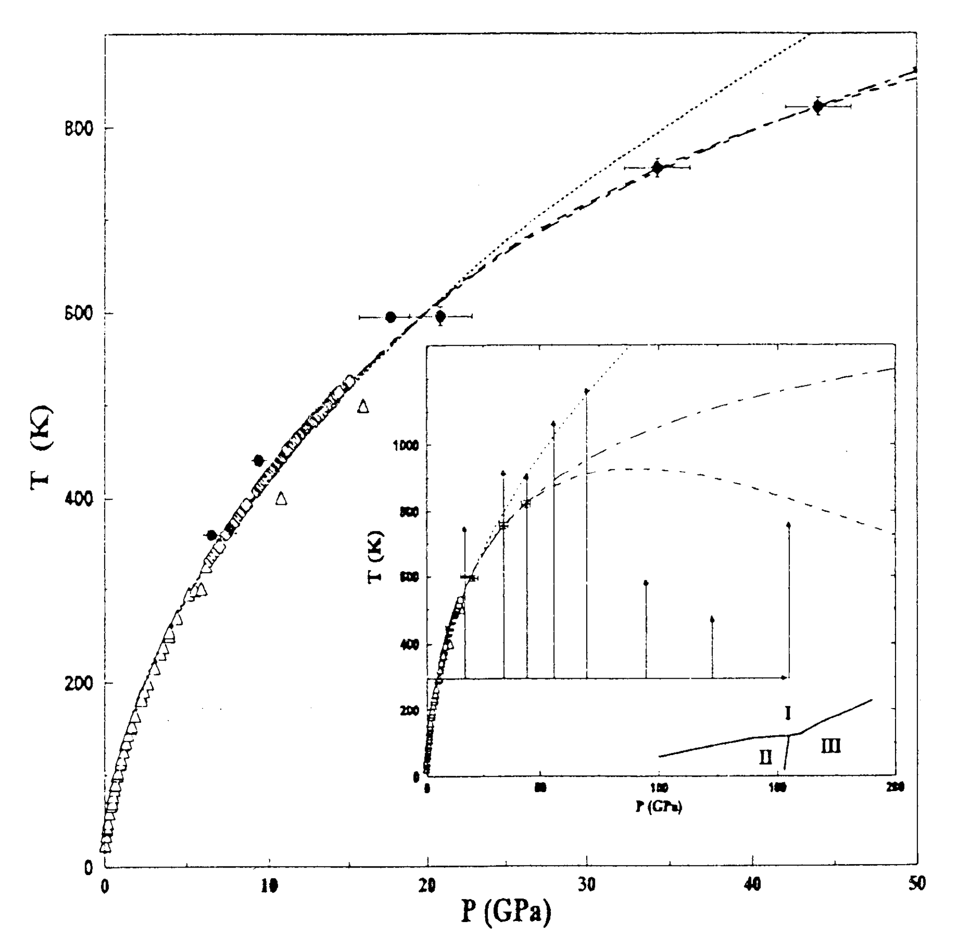

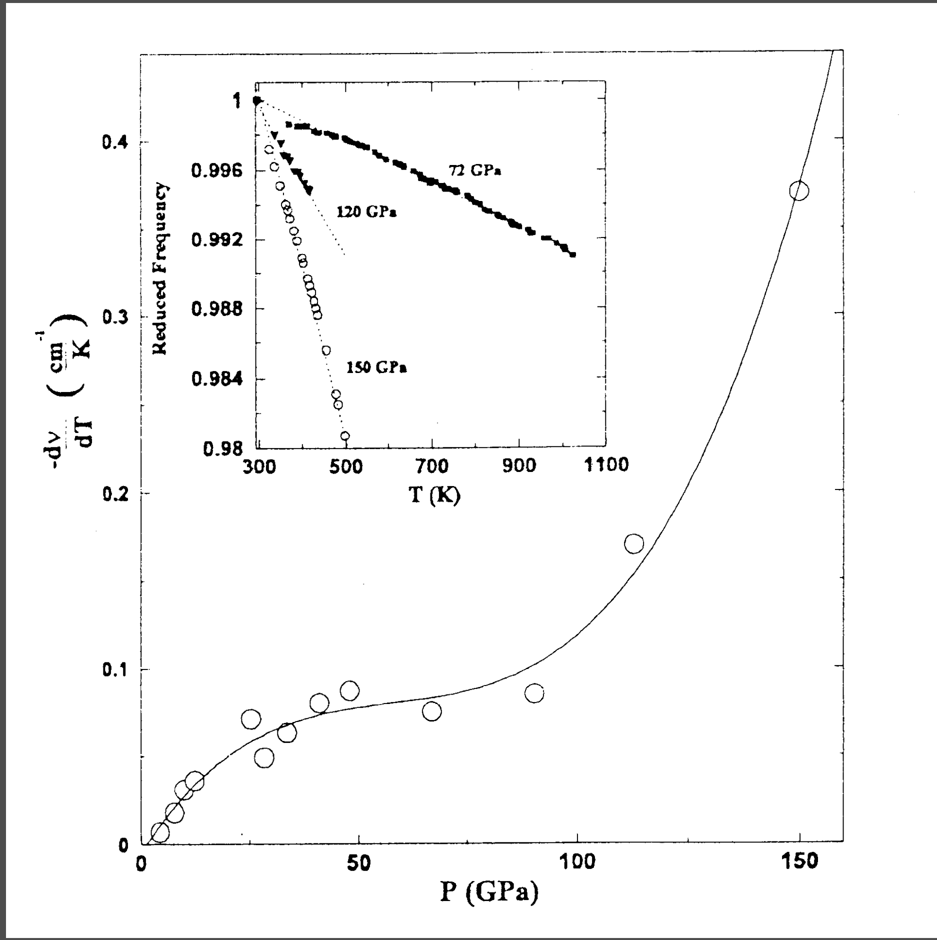

H_2 - melting curve

Temperature dependence of the H_2 vibron frequency at high pressure

Полимеризованный азот

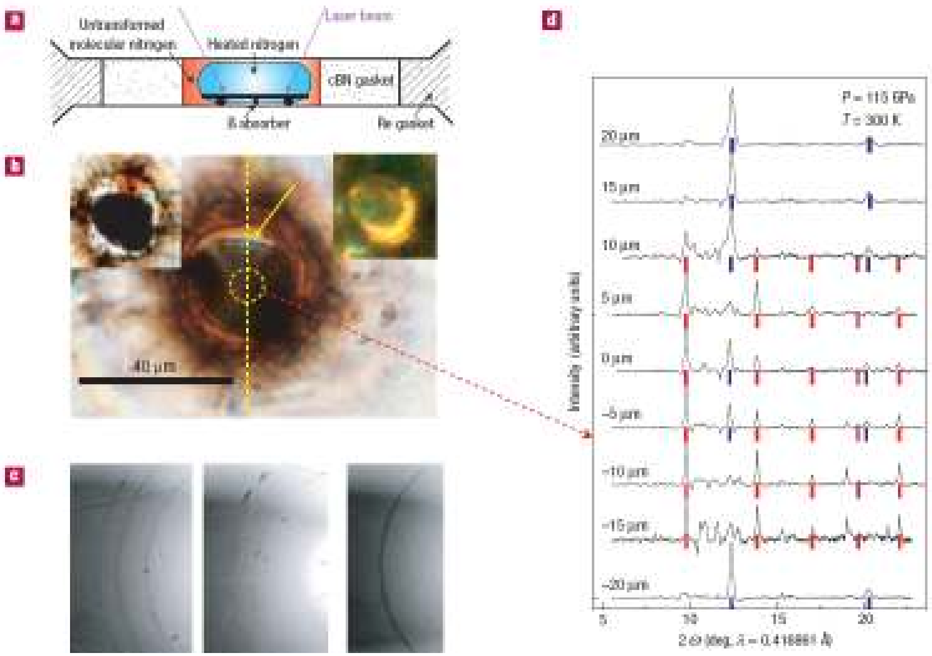

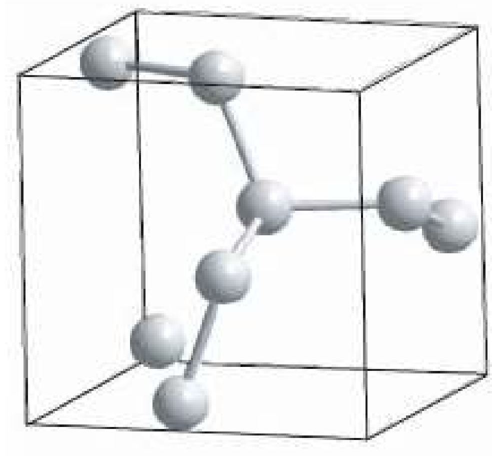

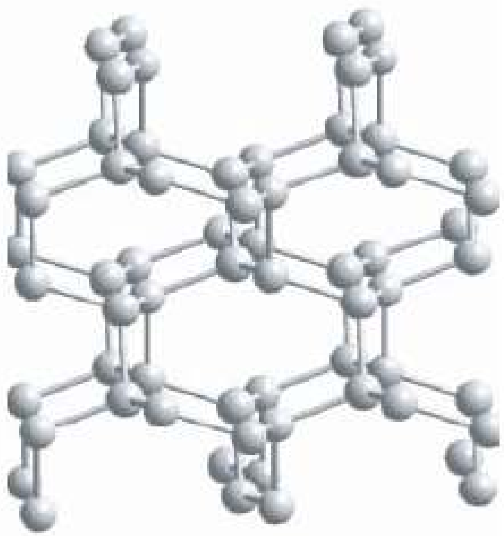

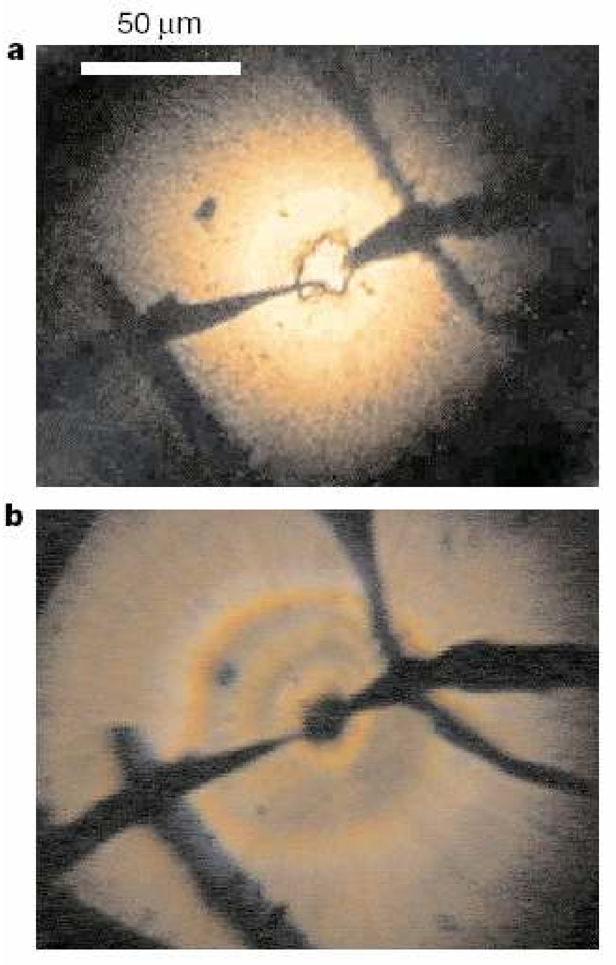

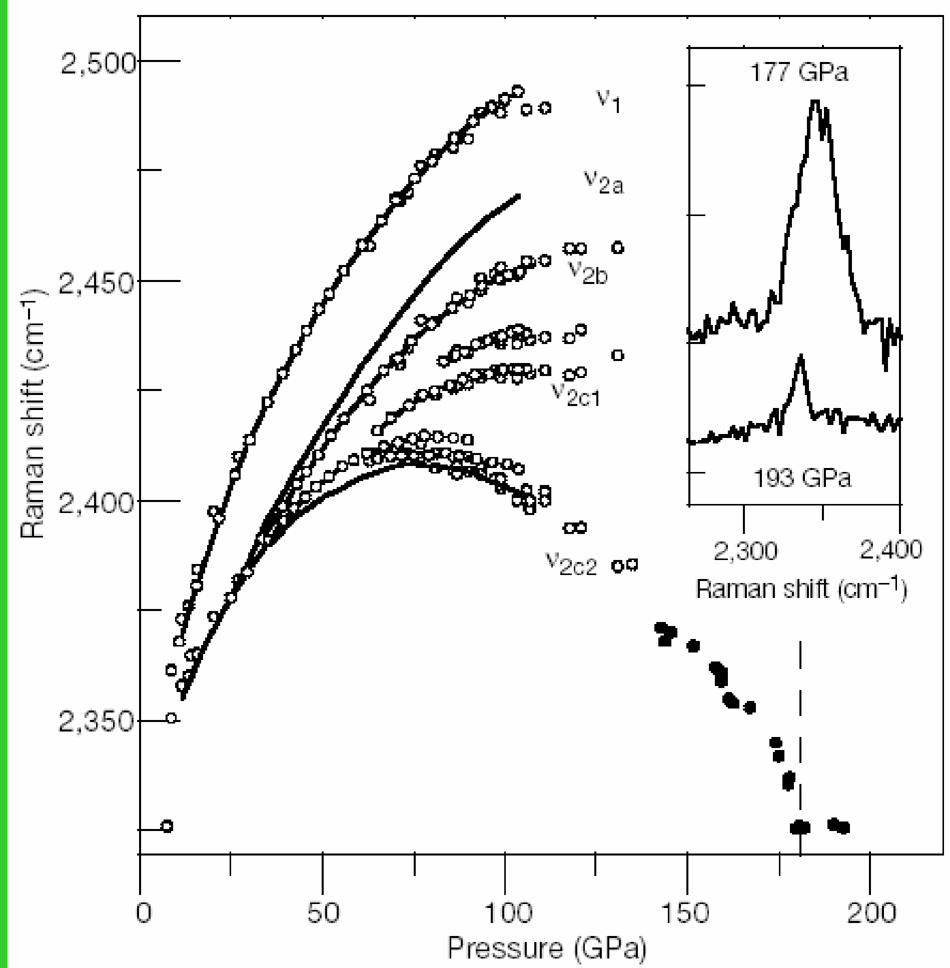

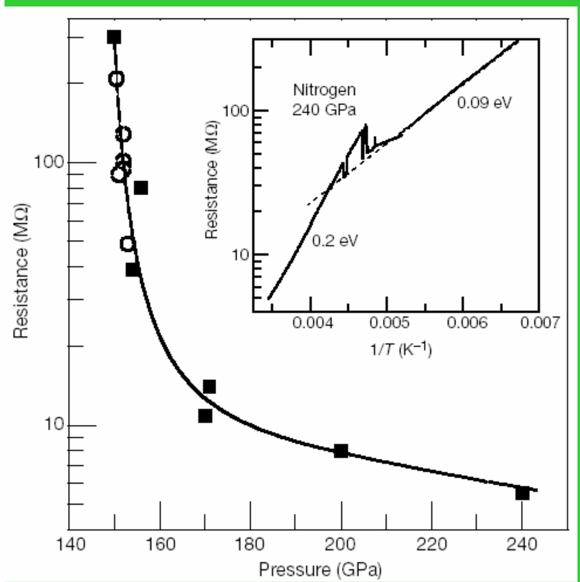

Semiconducting Nitrogen

(Eremetz et al., 2001)

Transformations in Ice

(after Hemley and Ashcroft, 1998)

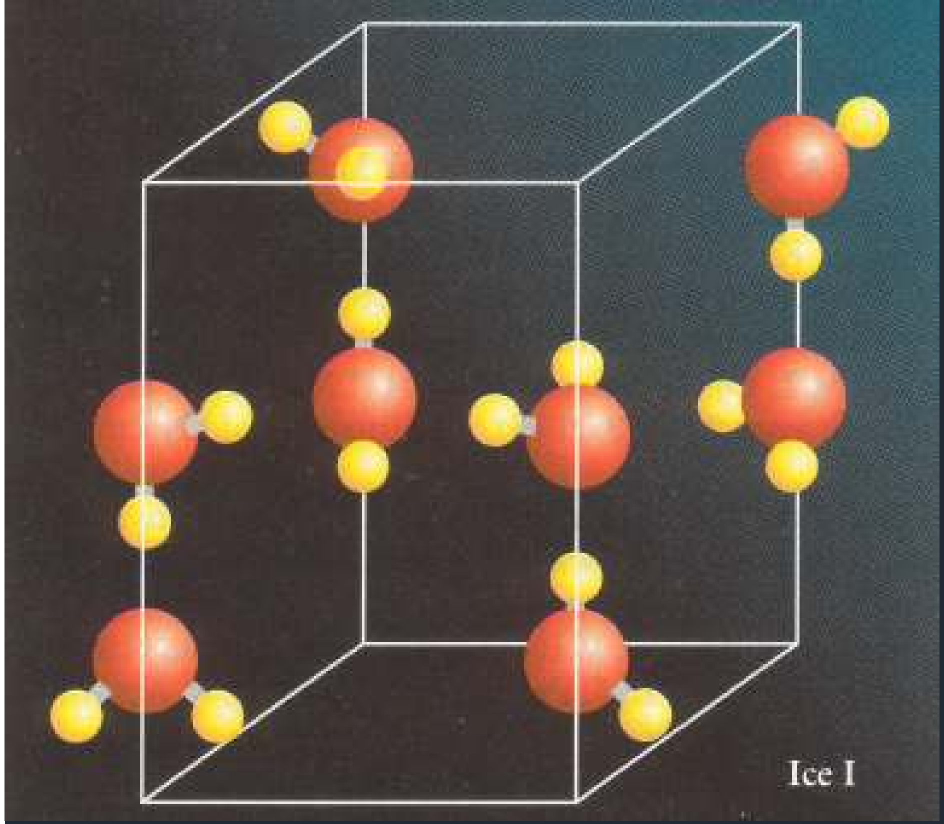

Ordinary Ice (Ice I)

Ice VII, 2GPa

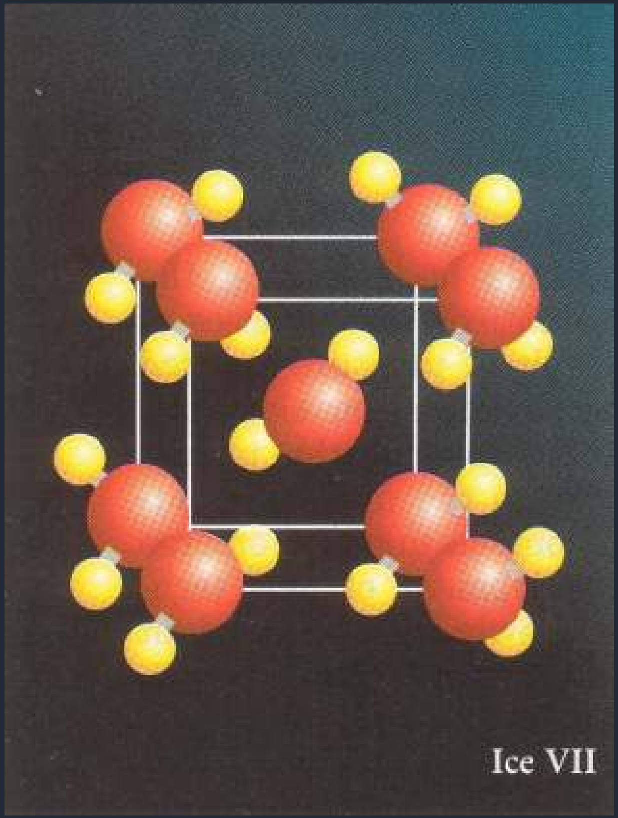

Ice X, 60 GPa

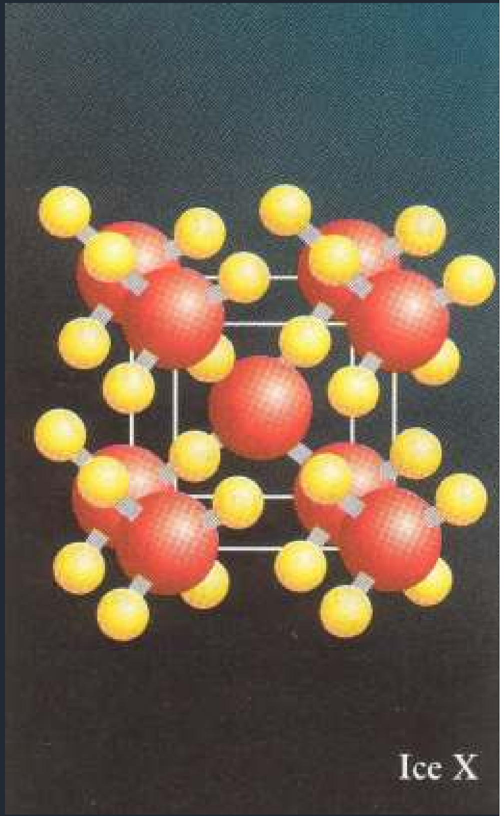

Pairing in dense lithium

Neaton & Ashcroft, 1999

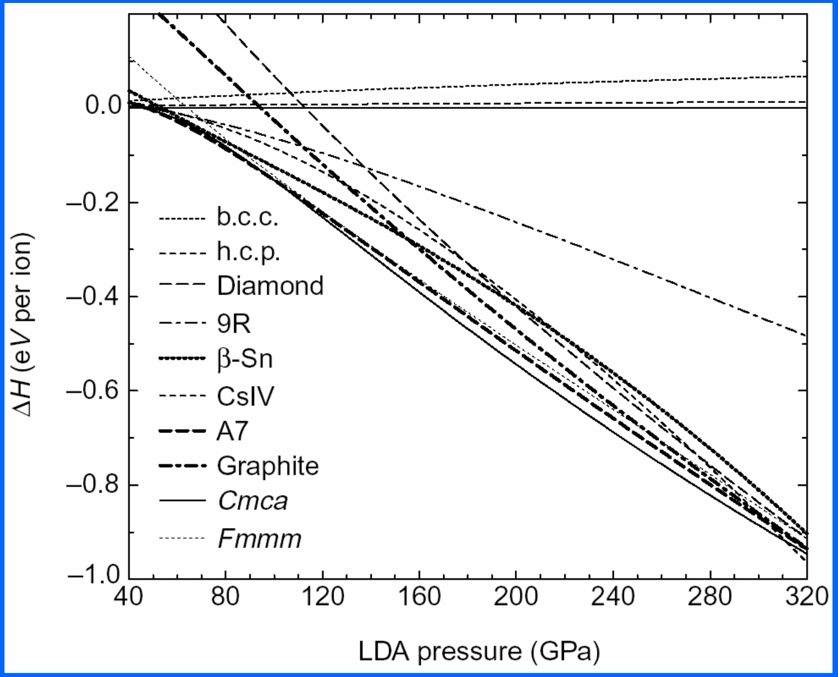

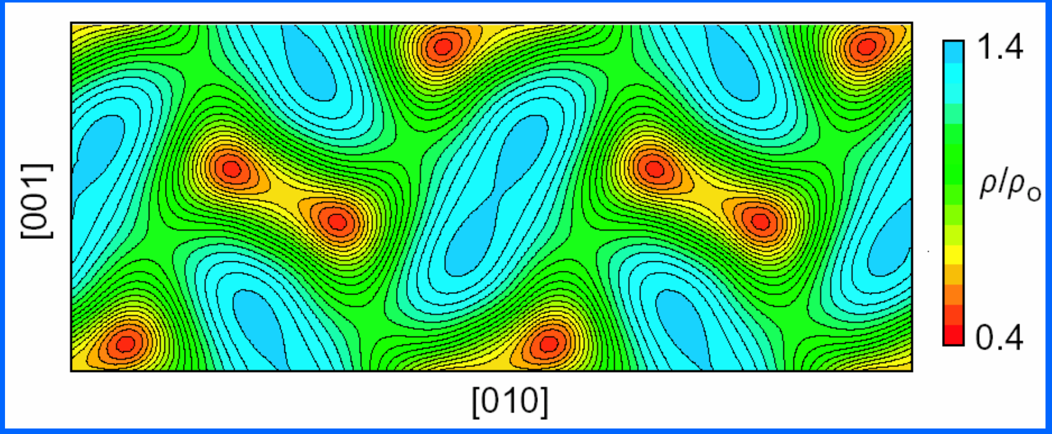

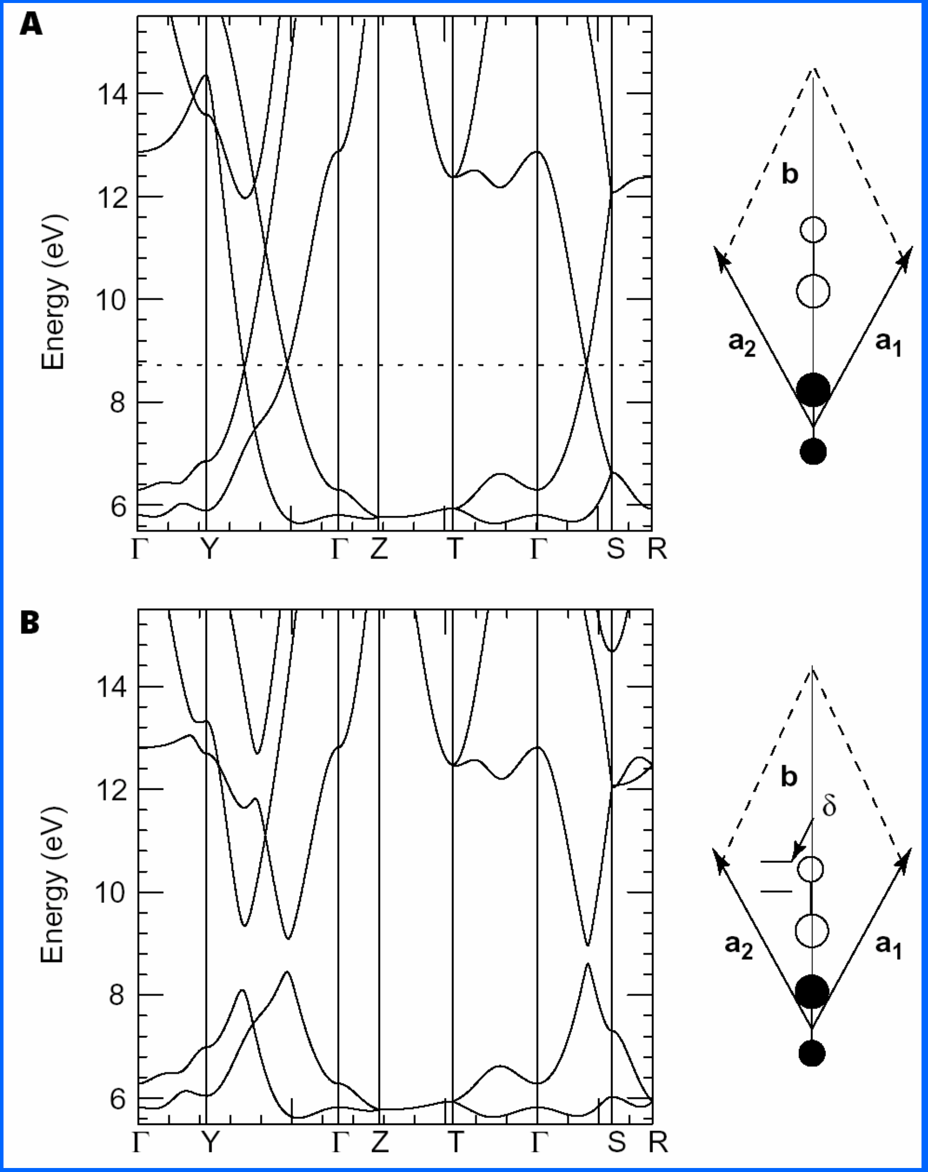

New high –pressure phases of lithium

Hanfland, Syassen, Christensen, Novikov, 2000

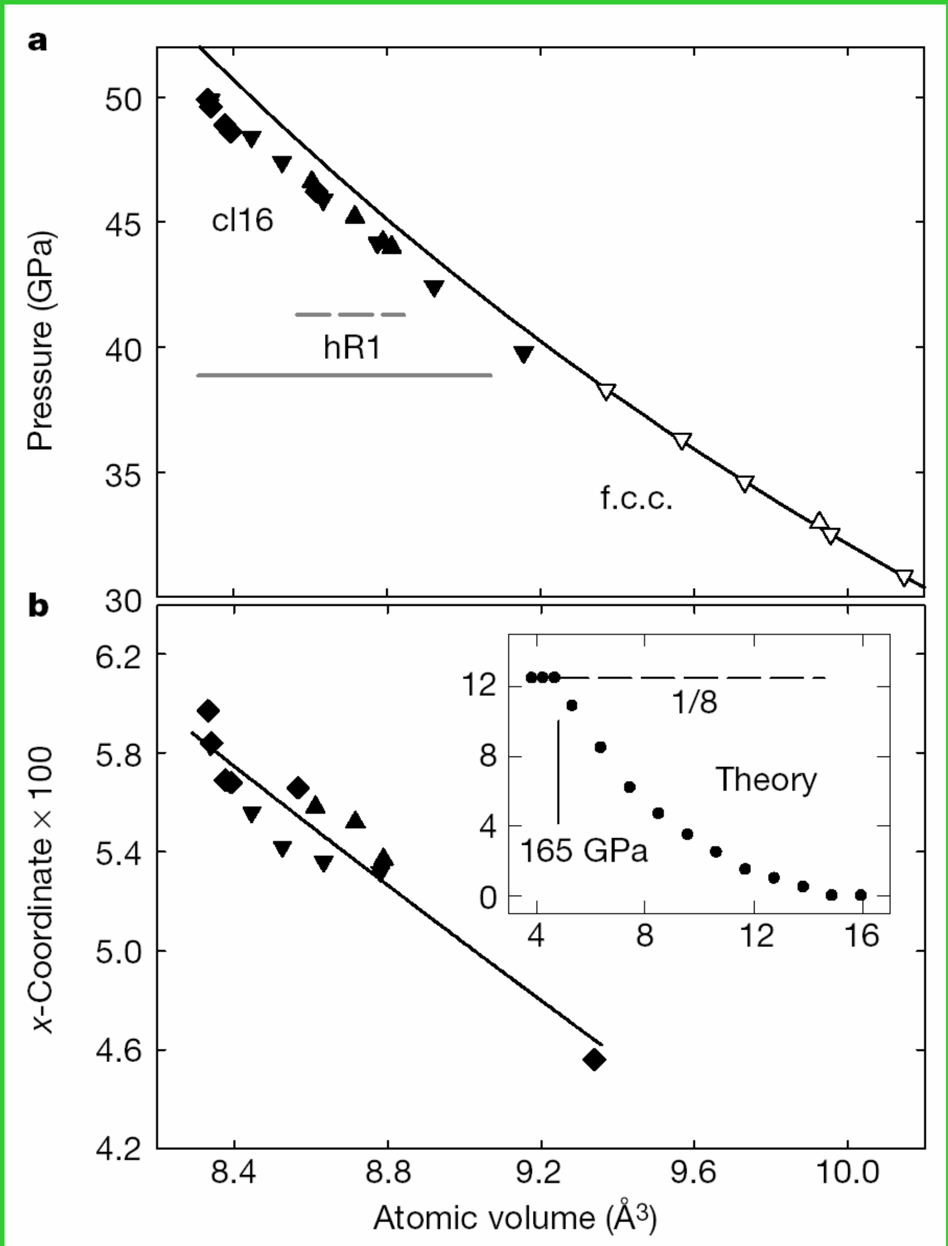

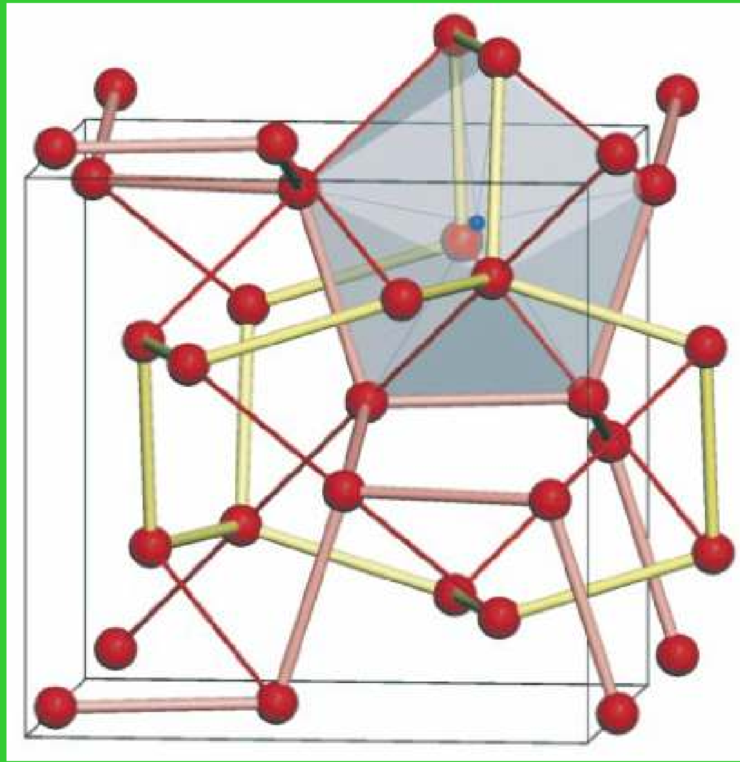

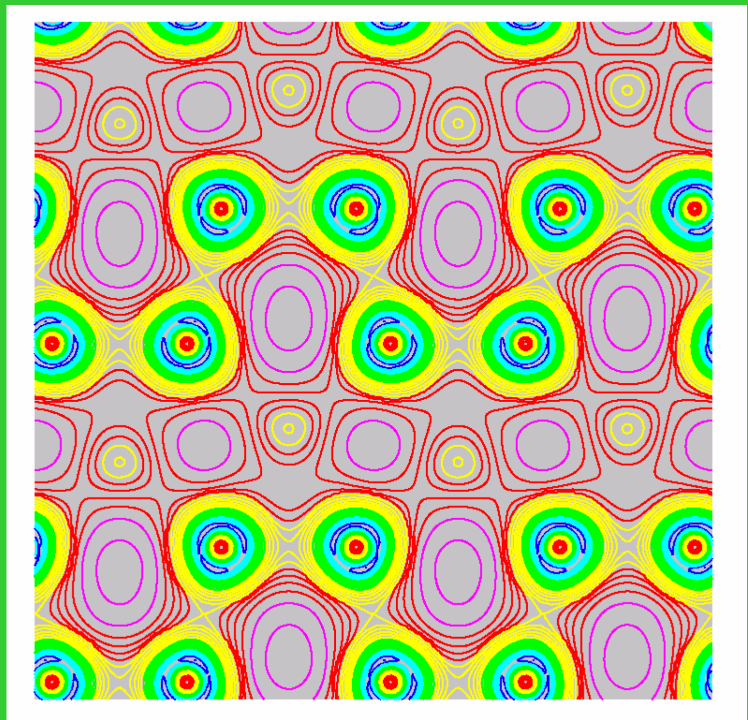

Sodium (Na)

(Neaton, Ashcroft, 2000)

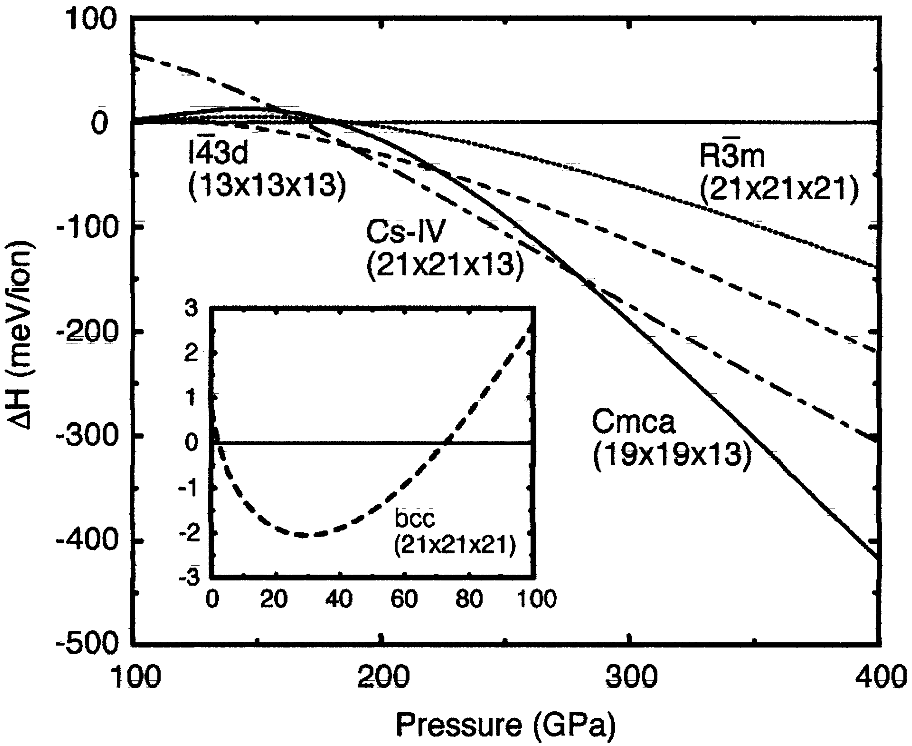

Rubidium (Rb)

(Schwartz, Crzechnik, Syassen, Loa, Hanfland, 1999)

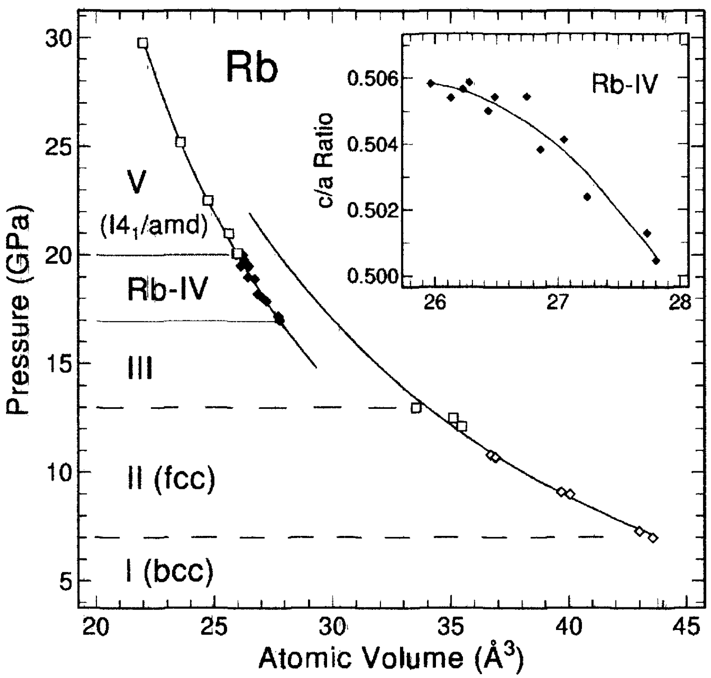

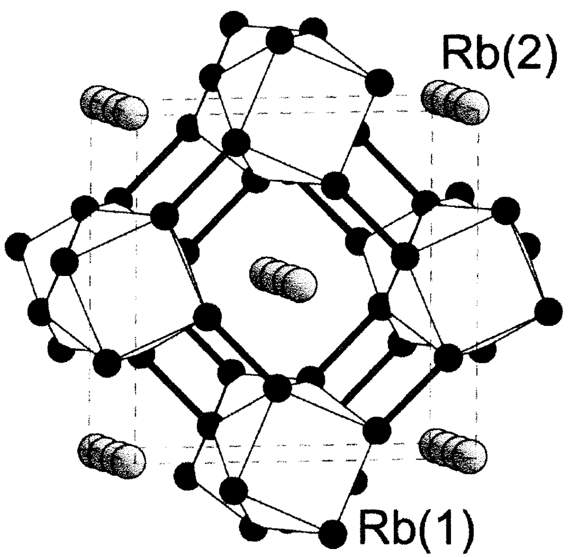

Фазовая диаграмма Na

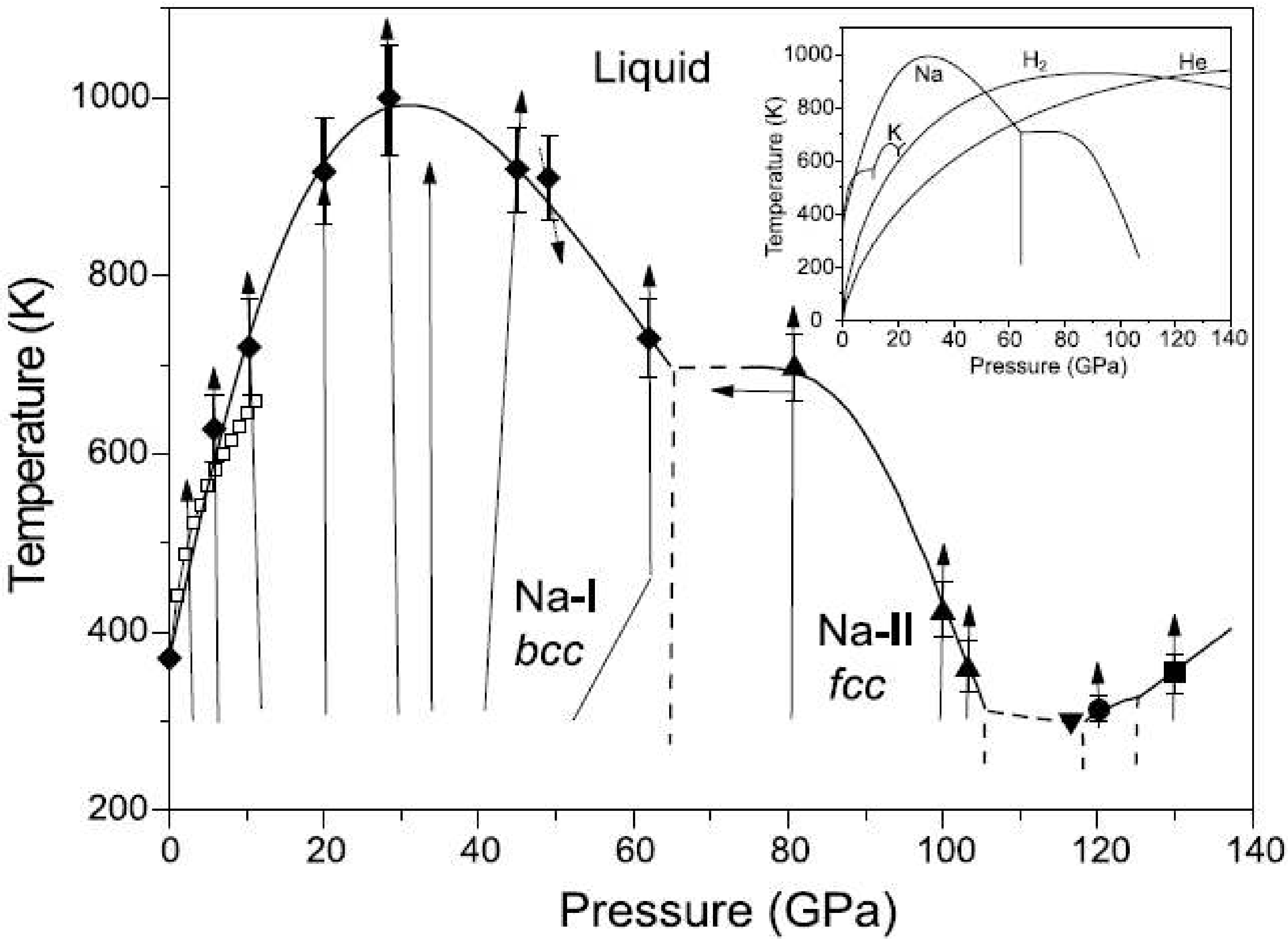

Разнообразие кристаллических структур Na при высоких давлениях

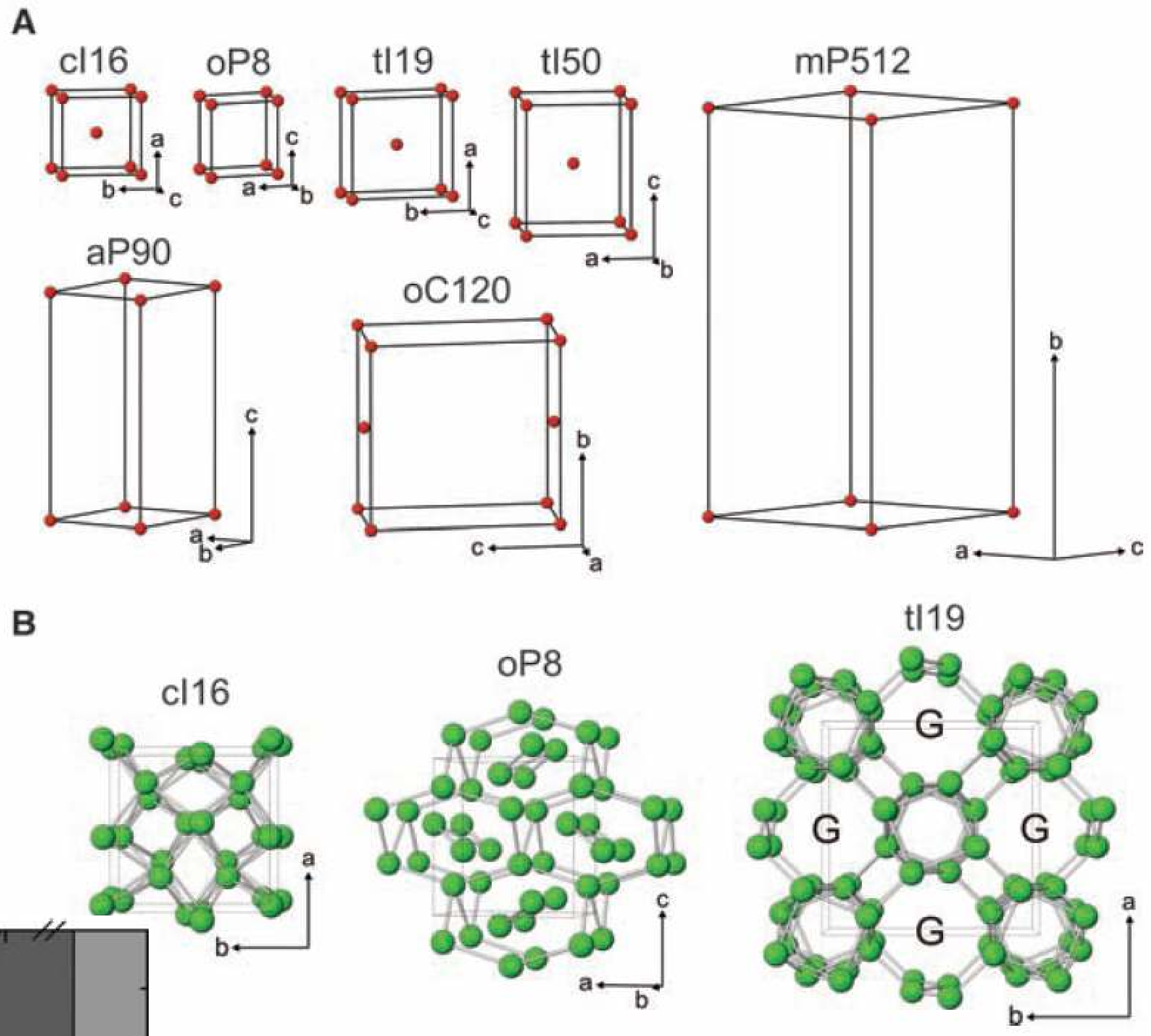

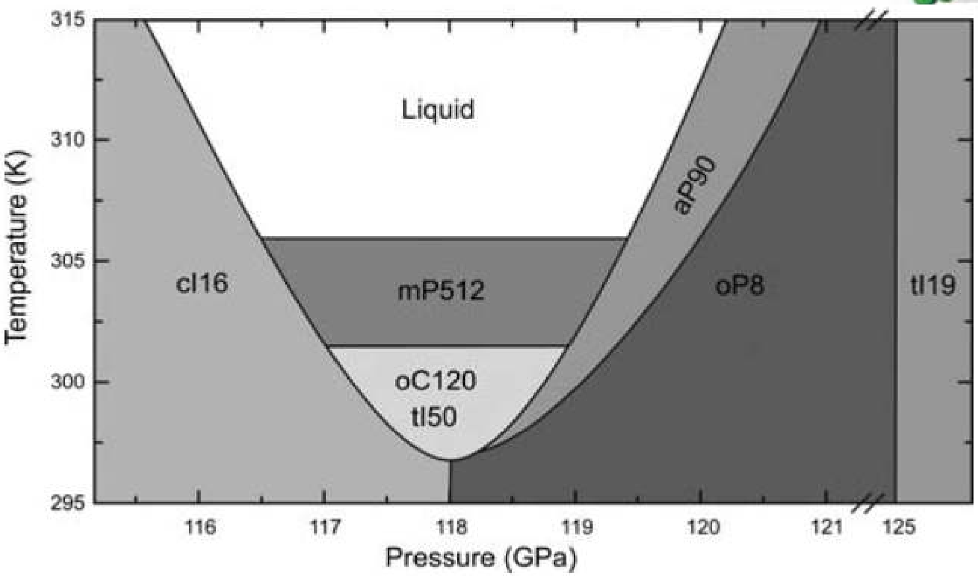

Прозрачный натрий

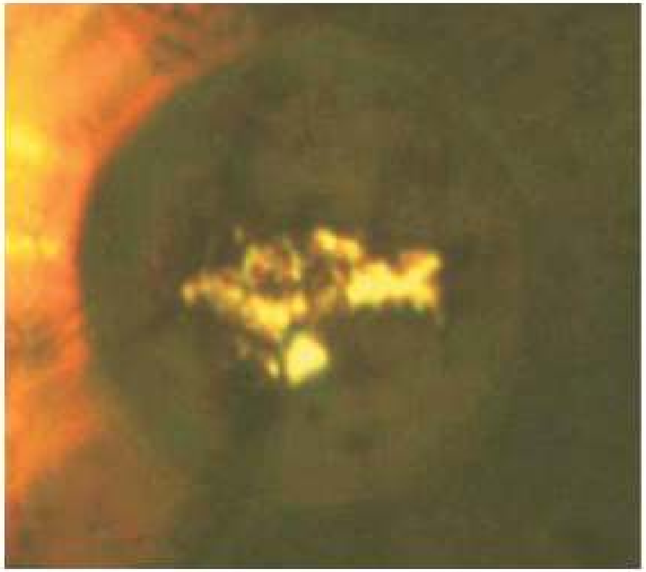

199 GPa

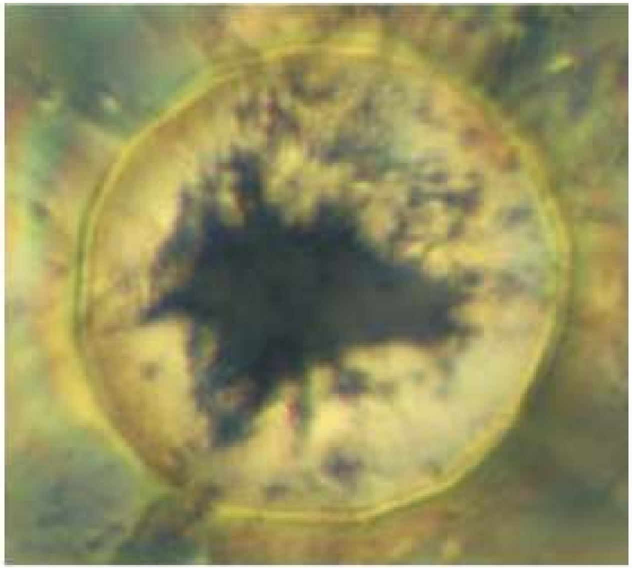

156 GPa

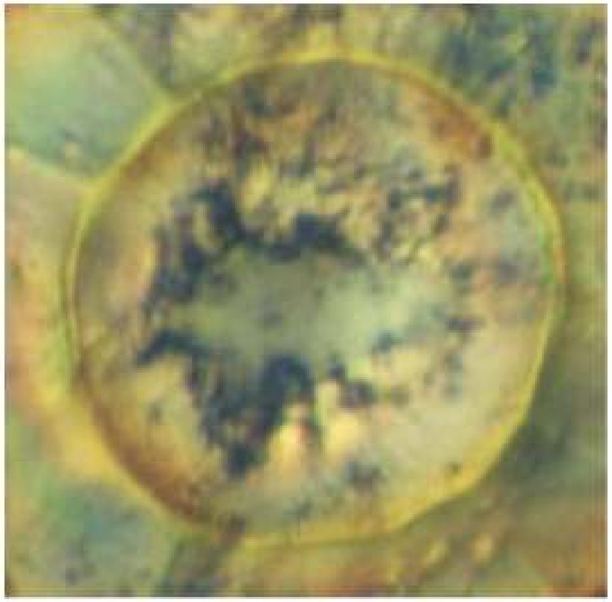

124 GPa

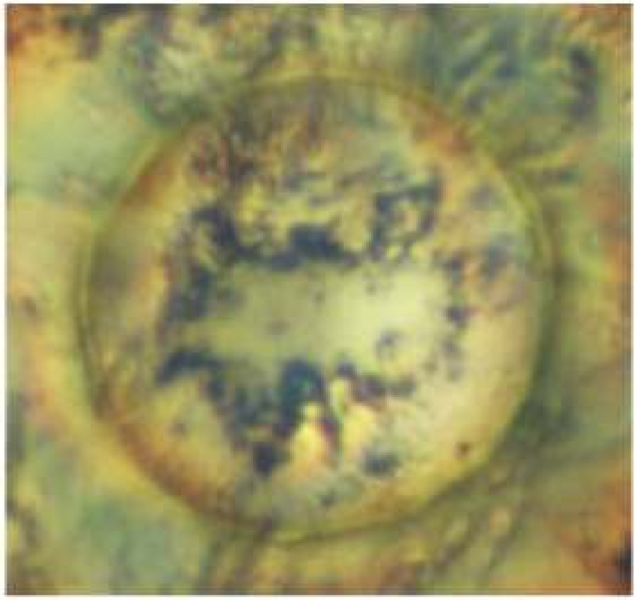

120 GPa

Graphite at High Pressure

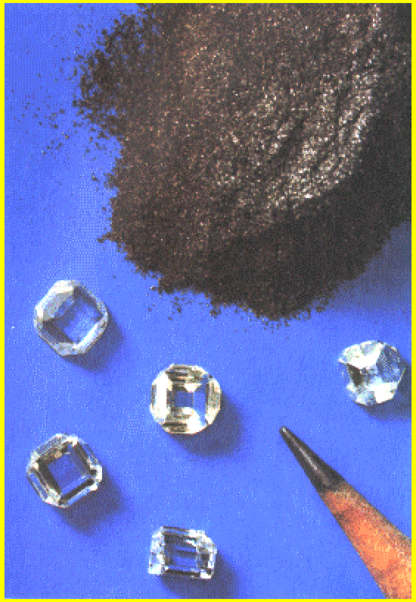

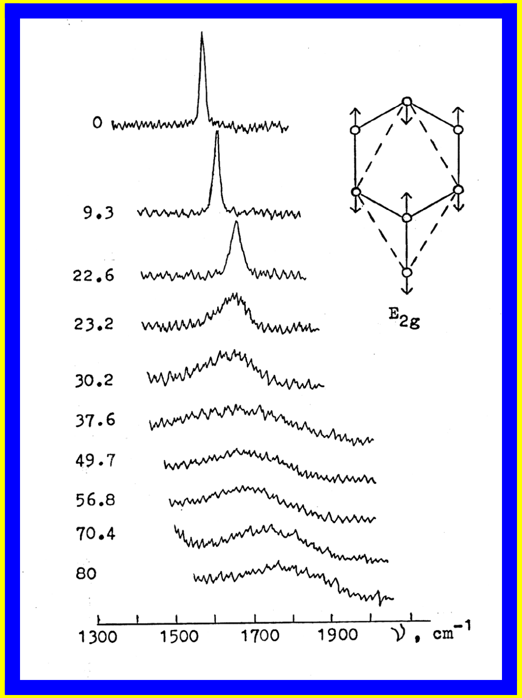

Raman spectra of graphite single crystal

Light can be seen through graphite single crystal at pressure ~ 20 GPa

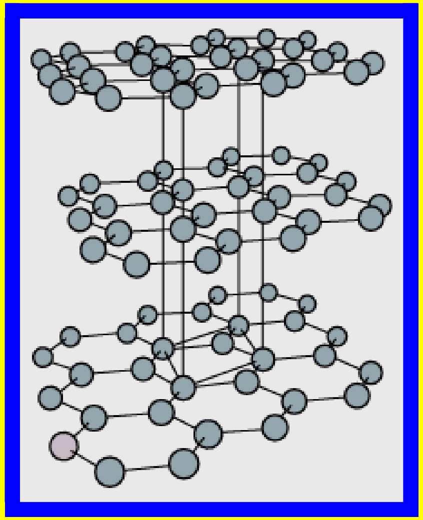

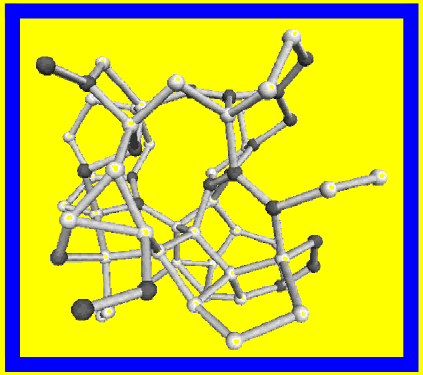

Structures of graphite and amorphous carbon

Goncharov, Makarenko, Stishov, 1989

QuickTime™ and a
YUV420 codec decompressor
are needed to see this picture.

van der Waals compounds

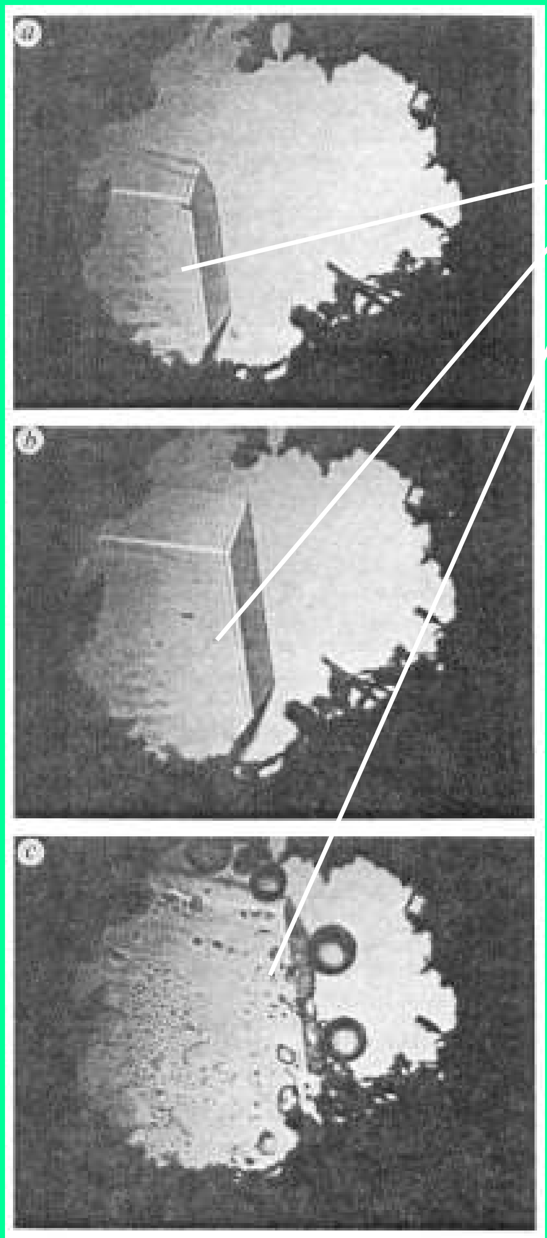

$He(N_2)_{11}$, P ~ 8.9 GPa

(Vos et al., 1992)

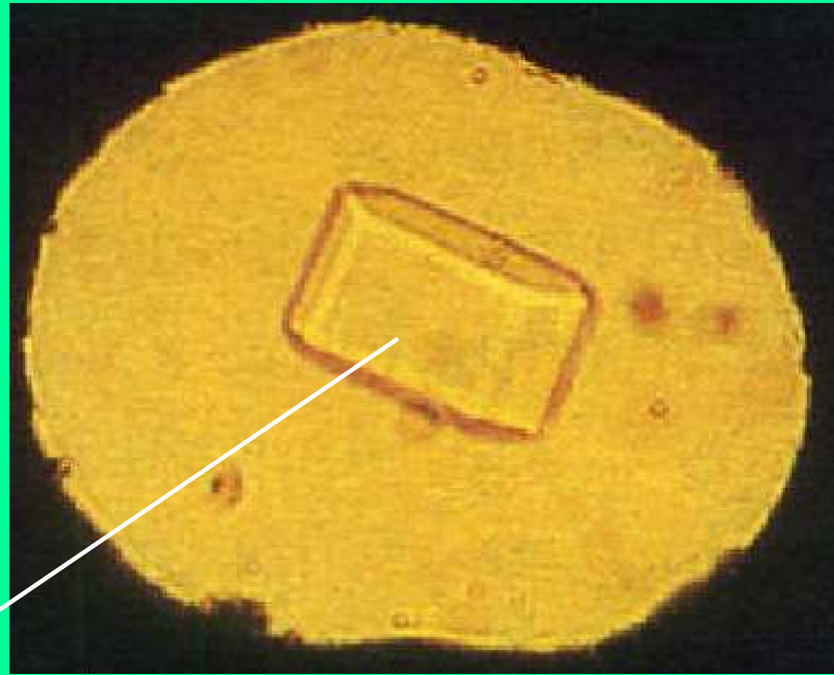

$Ar(H_2)_2$, 4.3 GPa

(Loubeyre, 1994)

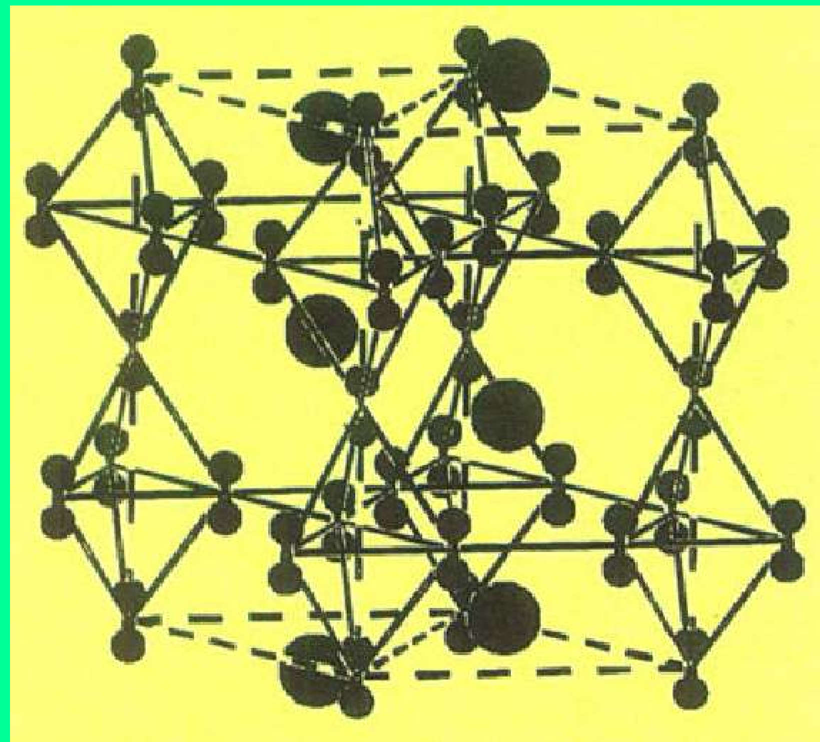

Phase transition in Liquid Selenium (!?)

Brazhkin, Popova, Voloshin, 1989, Endo et al., 1987

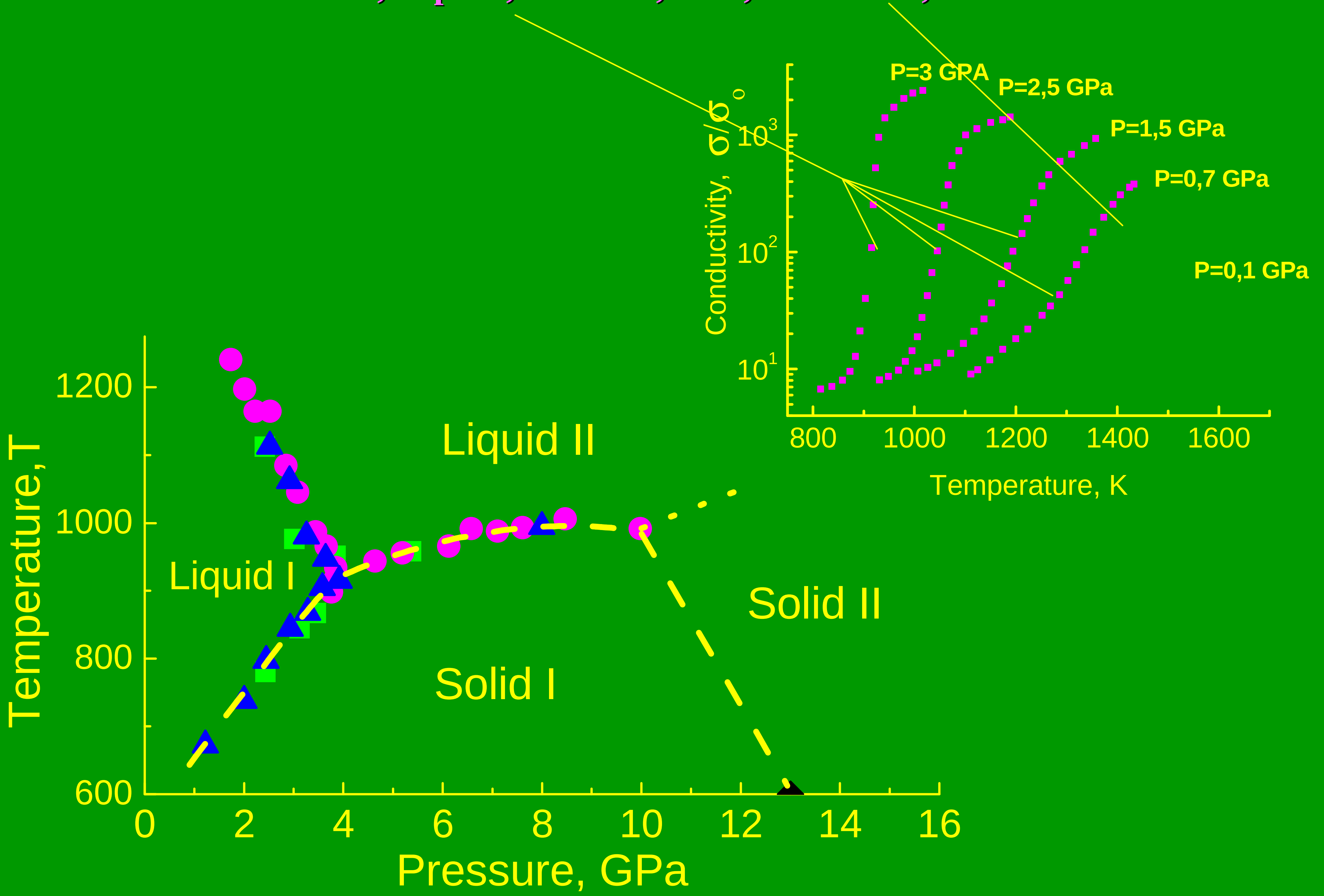

Phase transition in liquid carbon

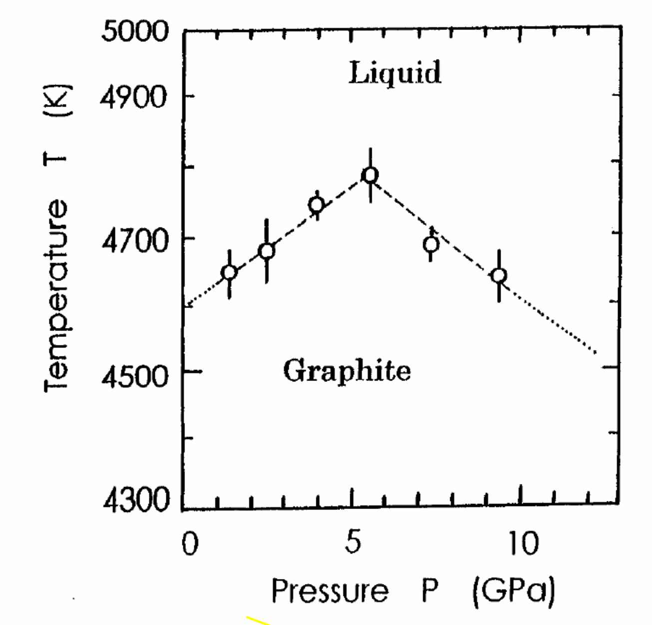

Togaya, 1997

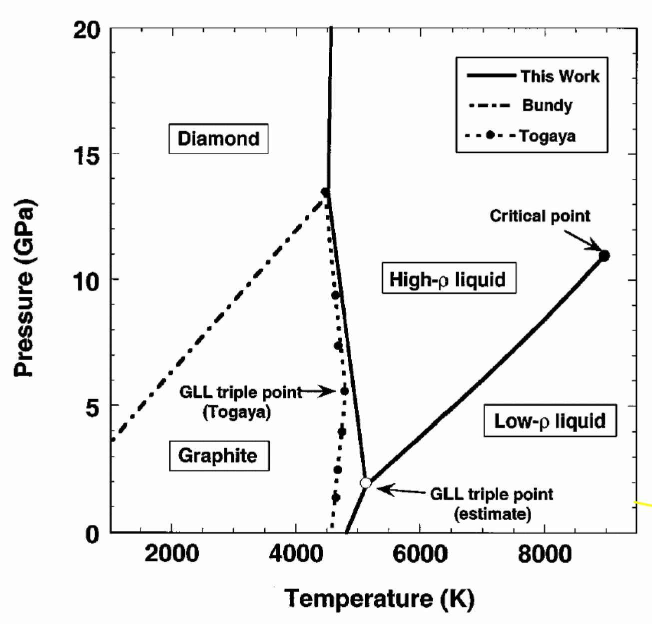

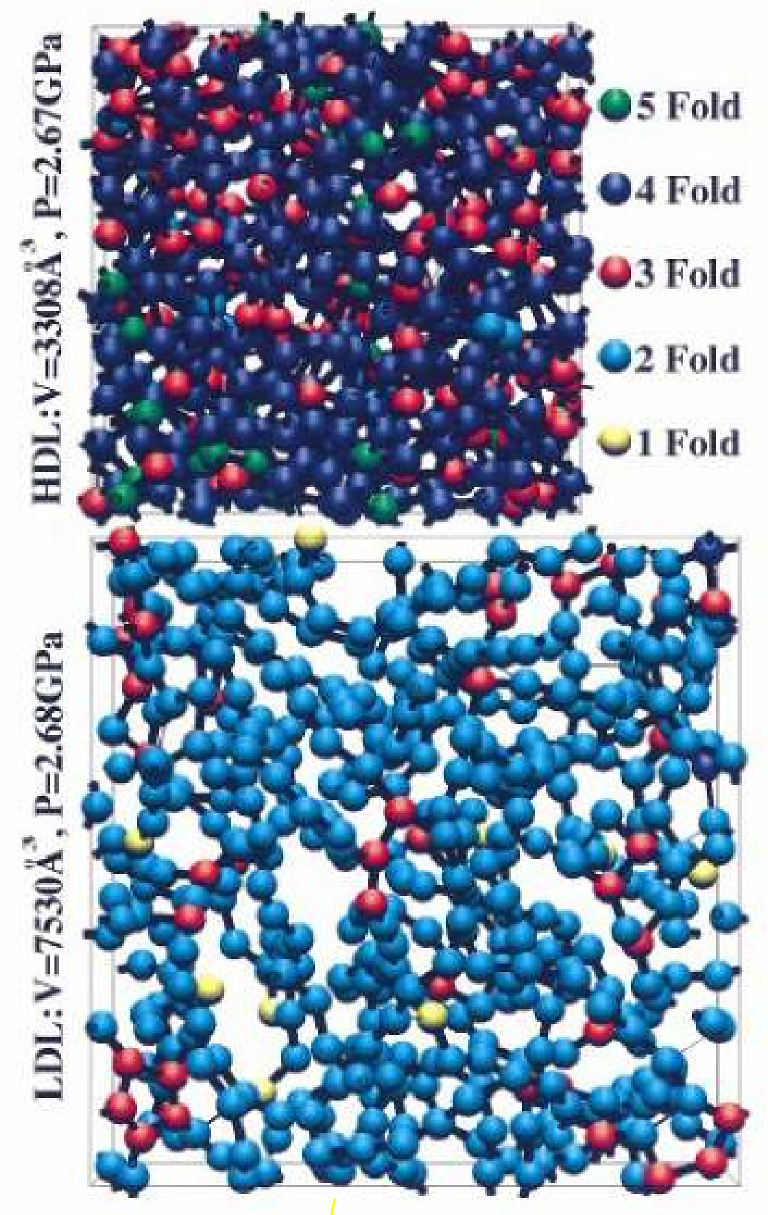

Glosli, Ree, 1998

First-Principle Calculations of the carbon compression isotherm at 6000 K (Wu, Glosli, Galli, and Ree, 2002)

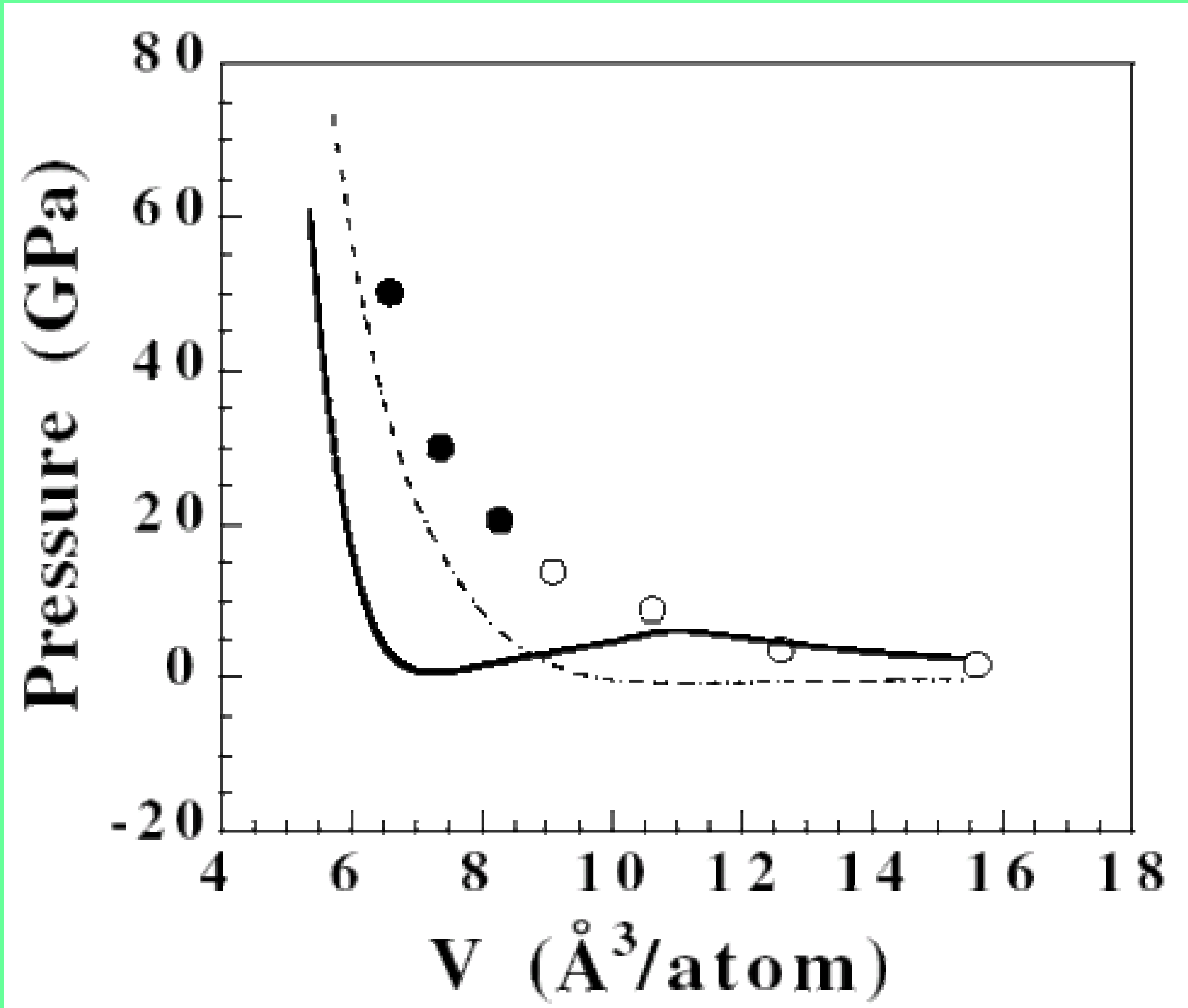

Liquid – liquid first order phase transition in black phosphorus !!!

Morishita, PRL, 87, 105701, 2001

Katayama et al., Nature,403, 170, 2000

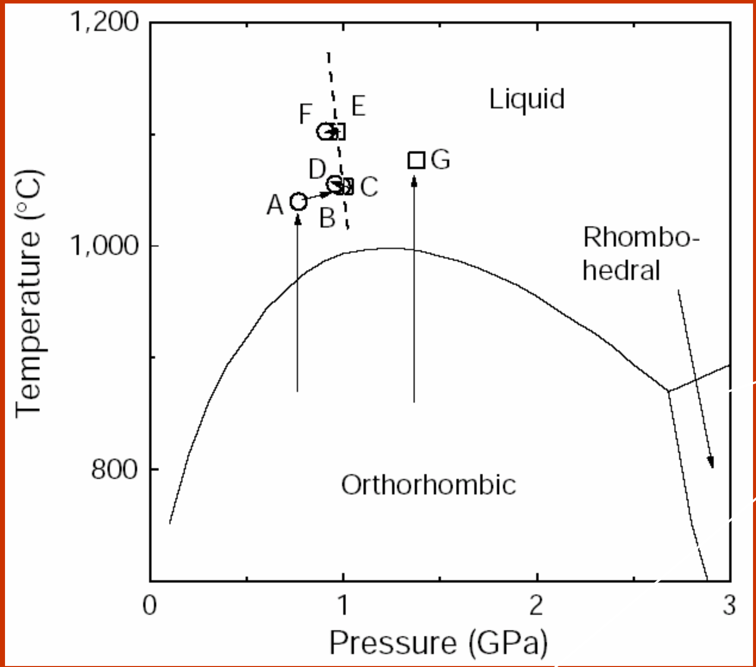

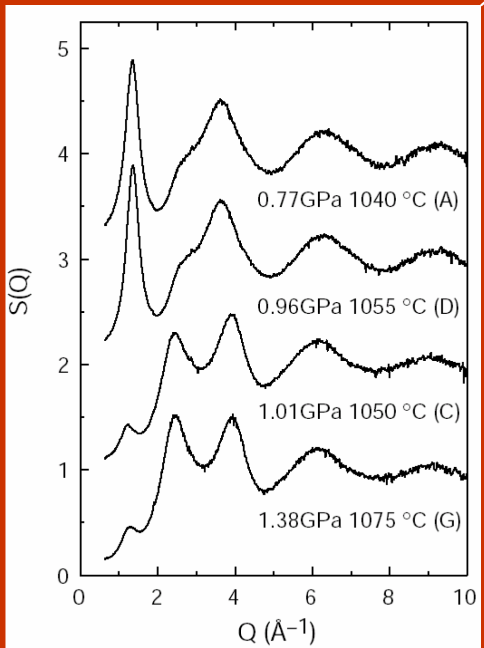

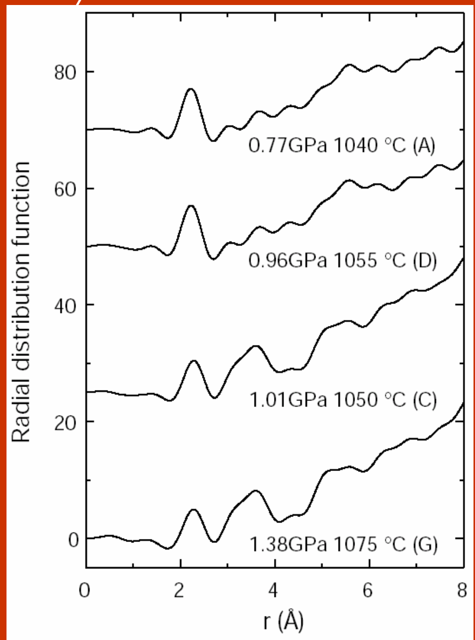

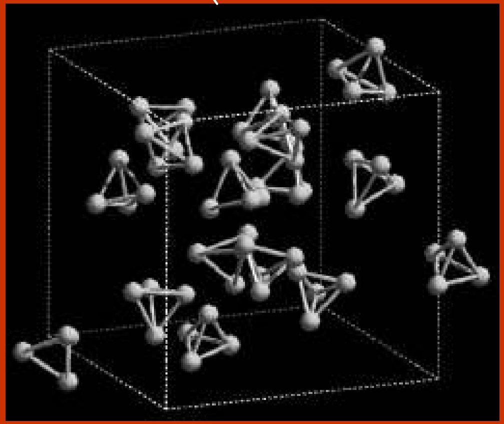

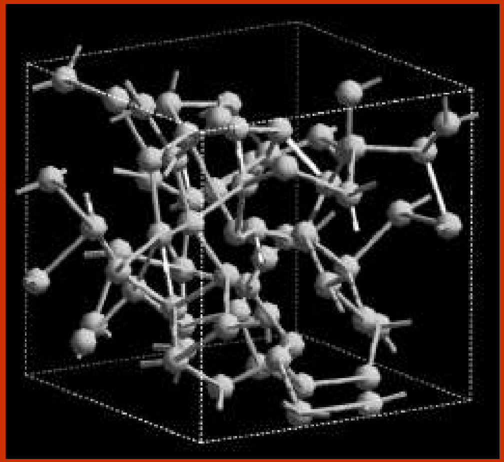

Superconductivity of simple substances at High Pressure

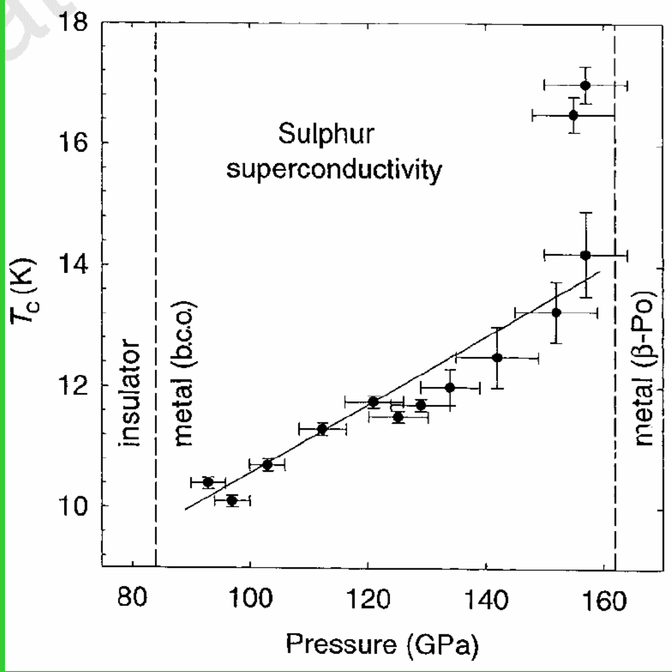

Struzhkin et al., 1997

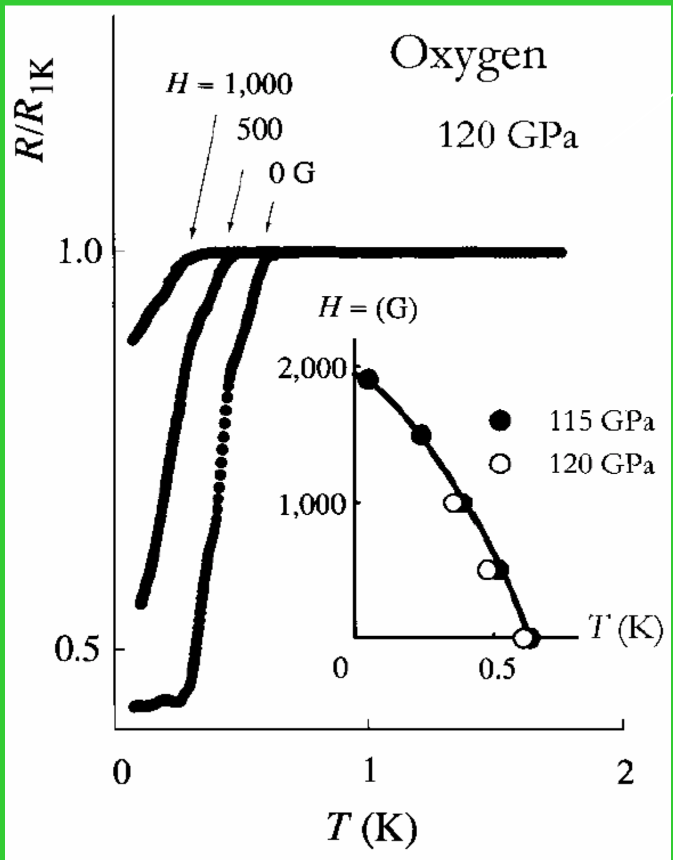

Shimizu et al., 1998

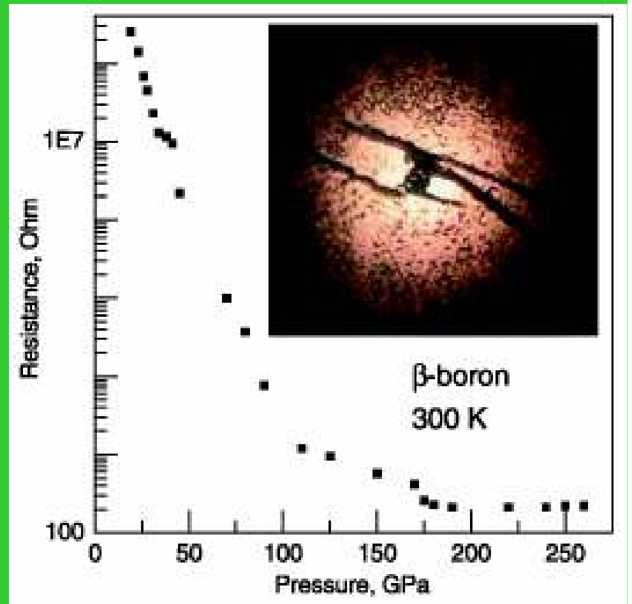

Eremets et al. 2001

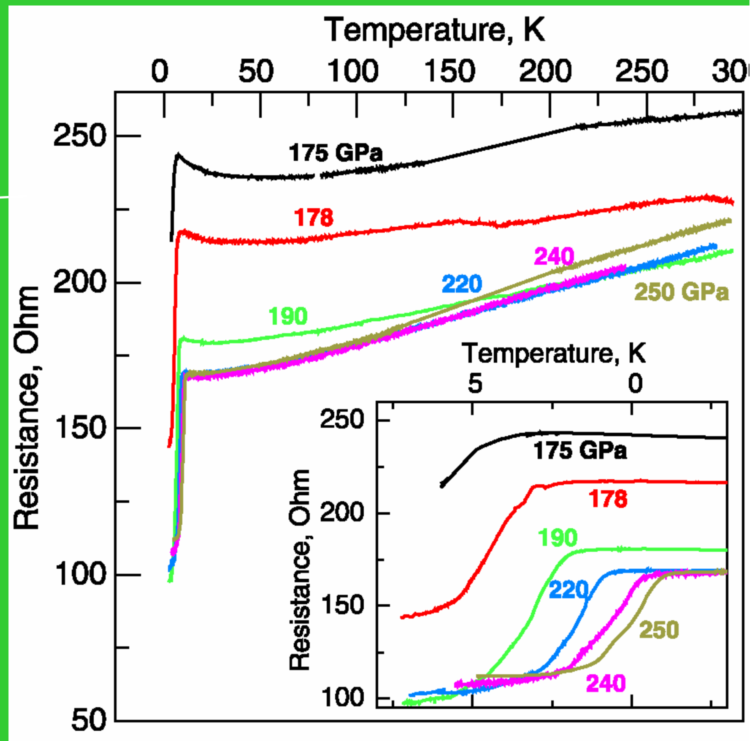

Xe metallization

(Eremetz et al., 2000)

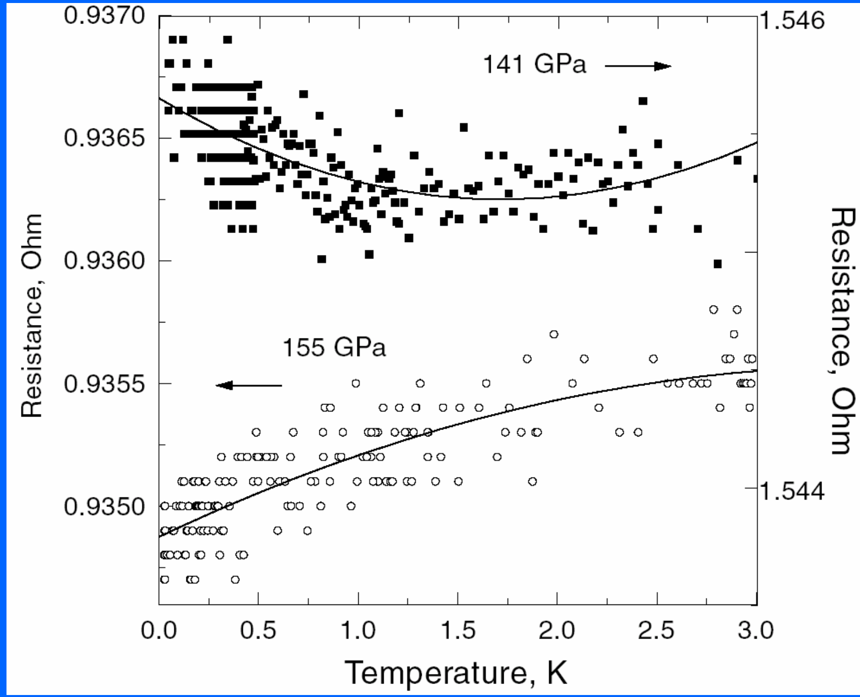

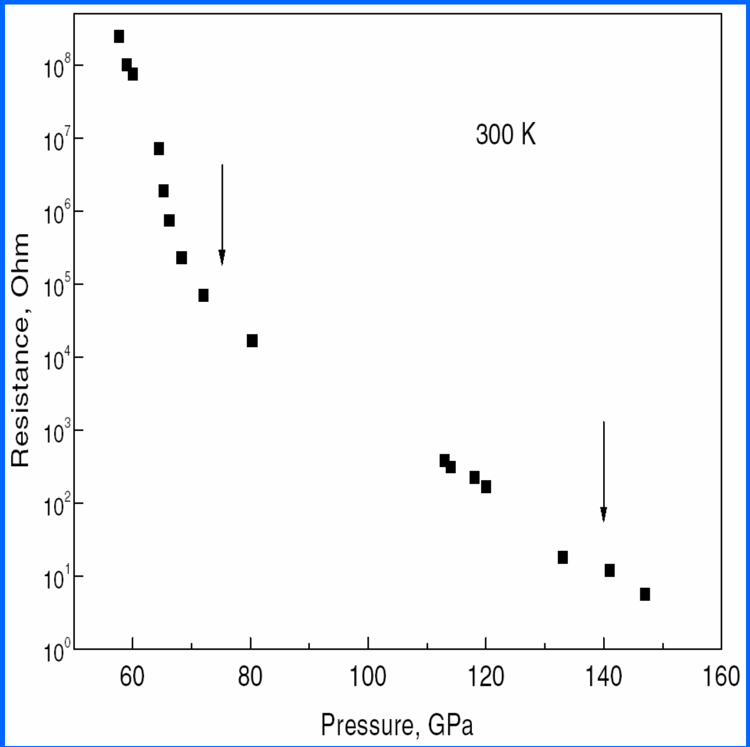

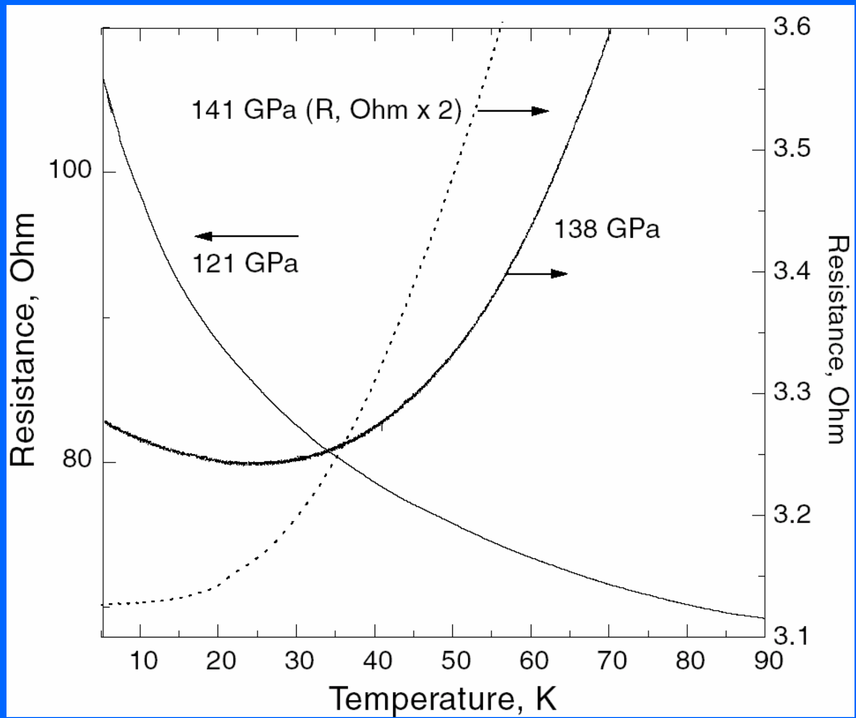

CsJ: metallization and and superconductivity

(Eremetz et al., 1998)

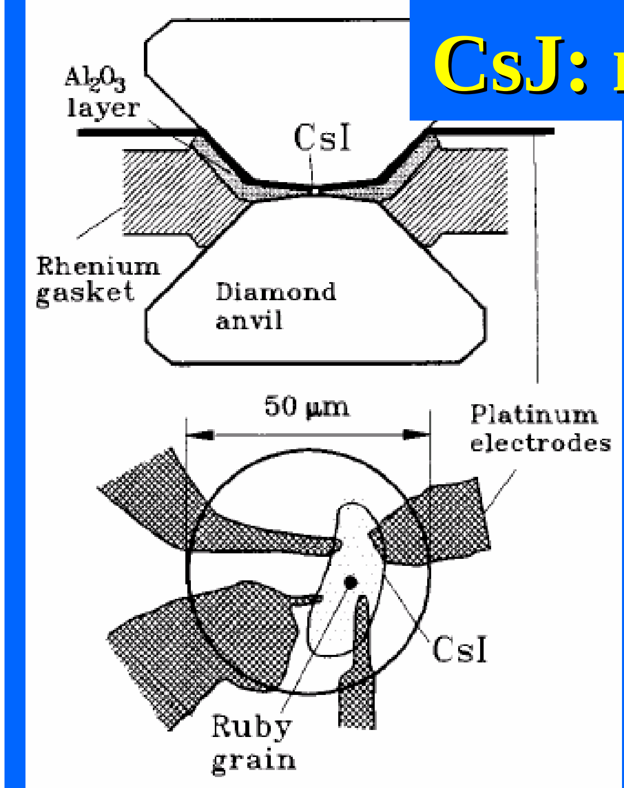

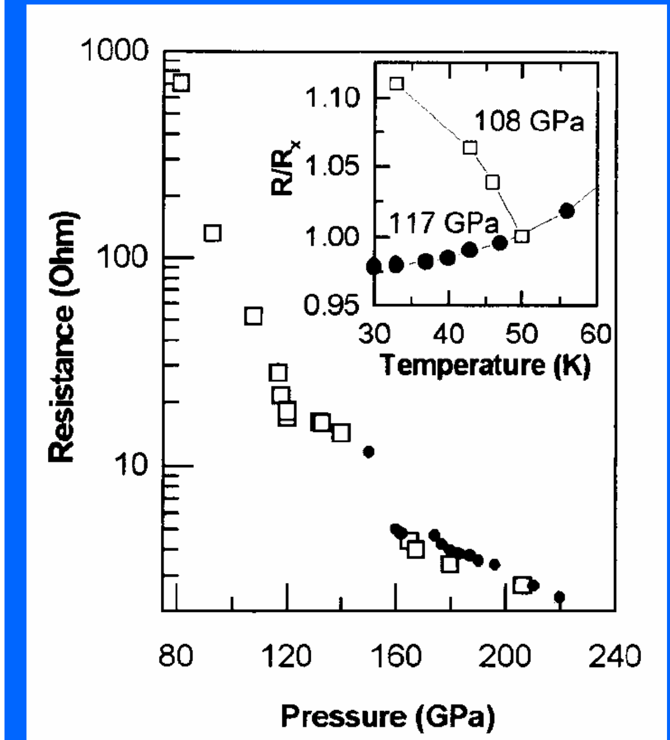

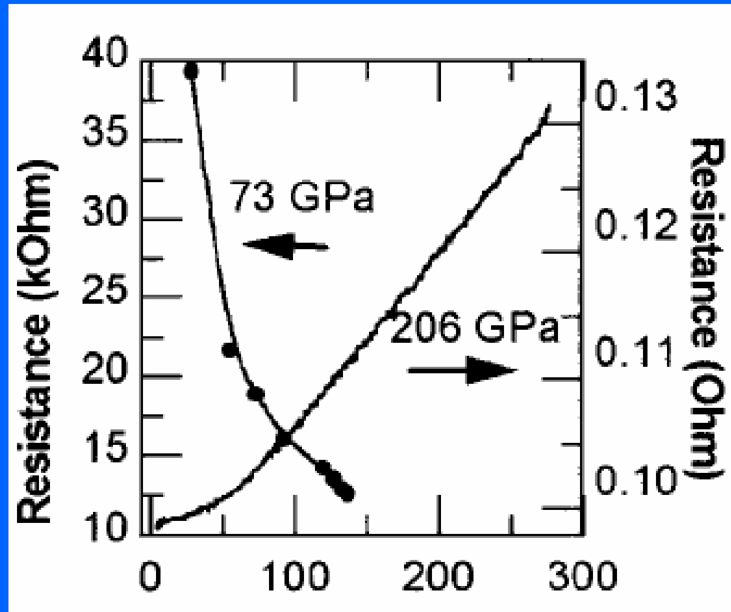

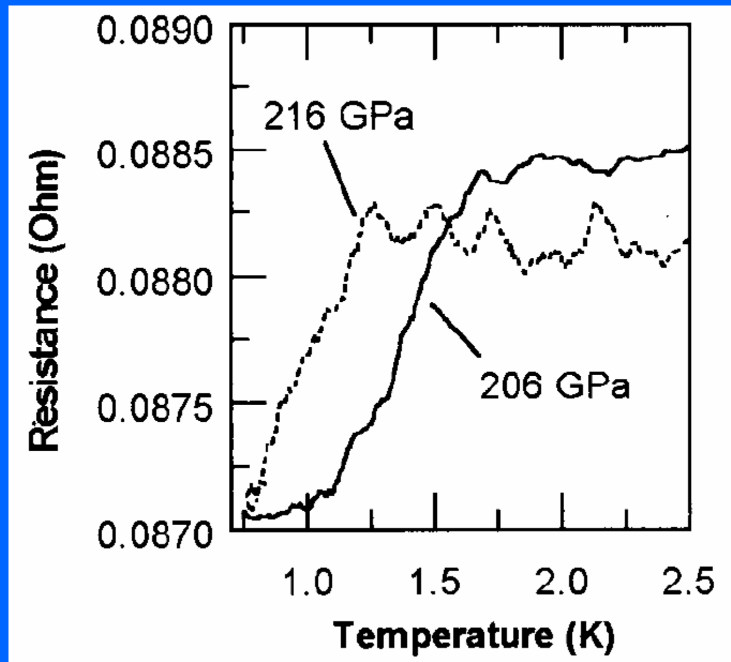

Superconductivity of lithium, (Shimizu et al, 2002)

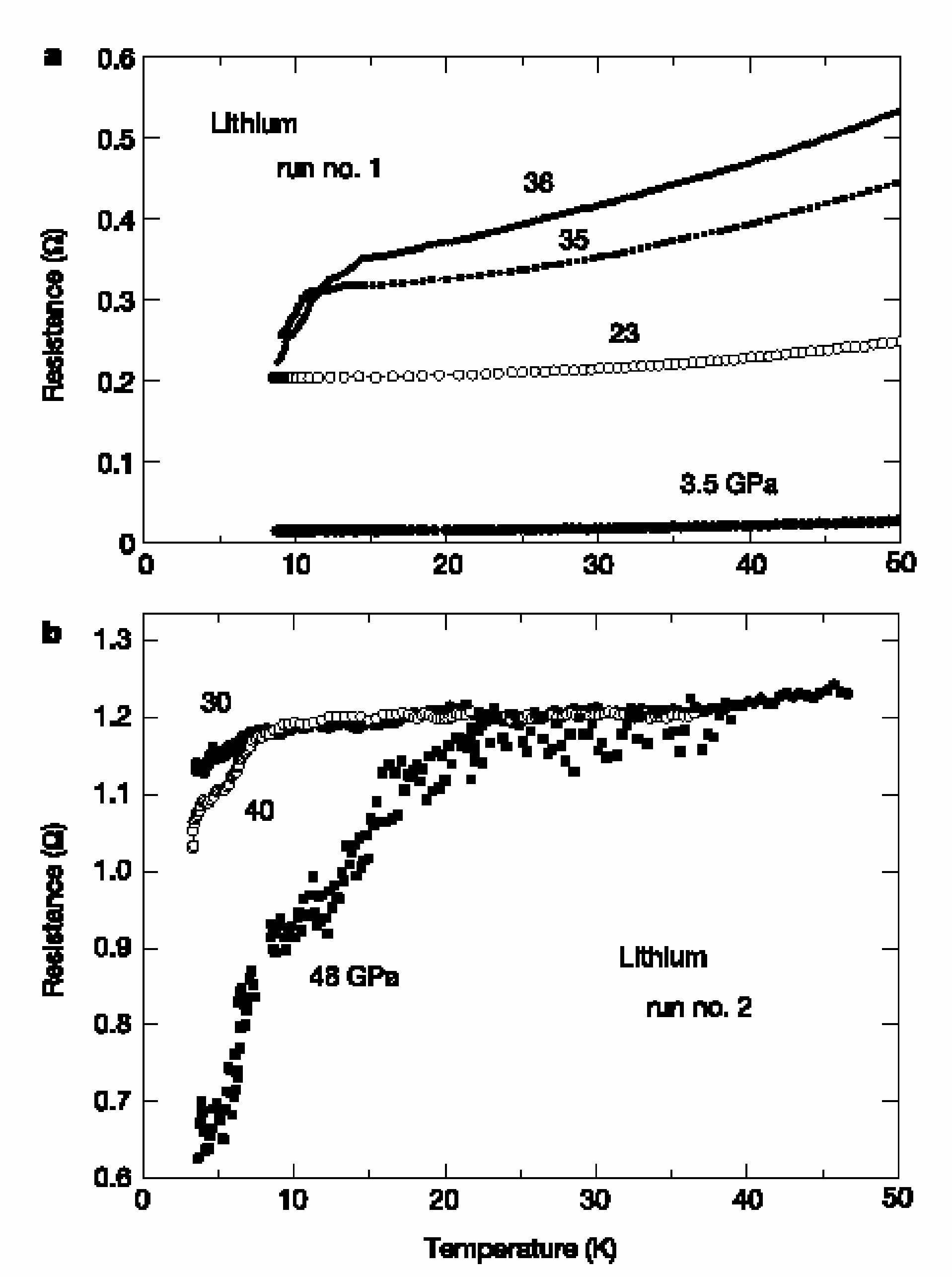

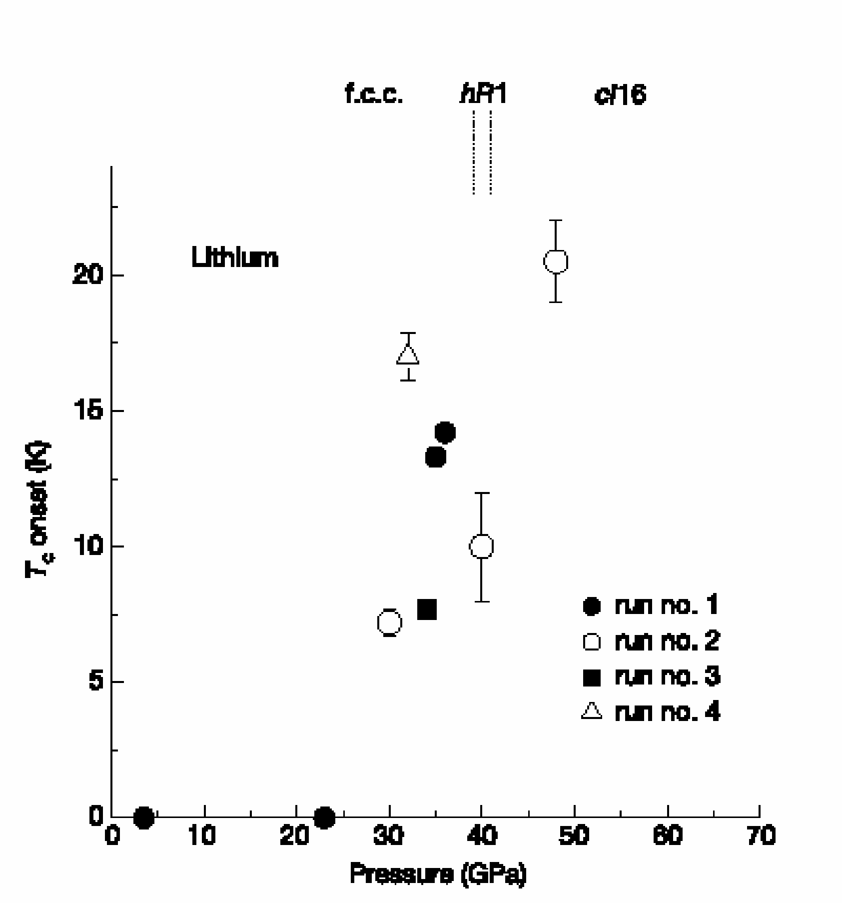

Superconductivity in lithium (Deemyad & Schilling, 2003)

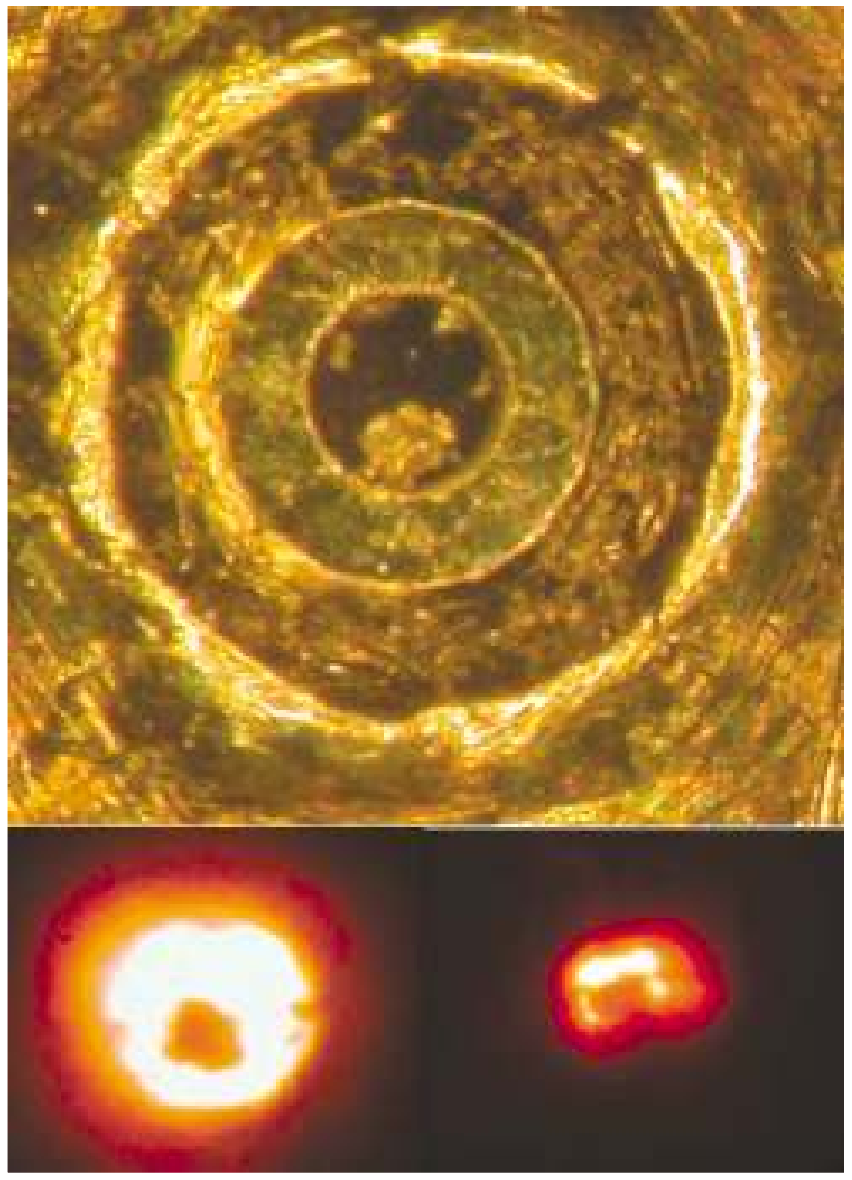

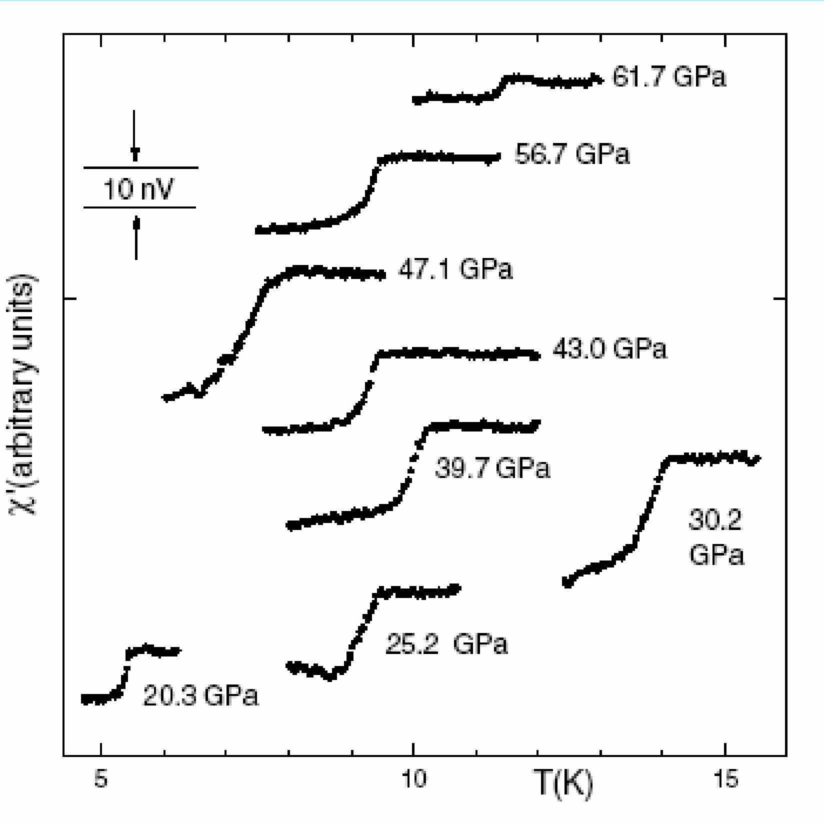

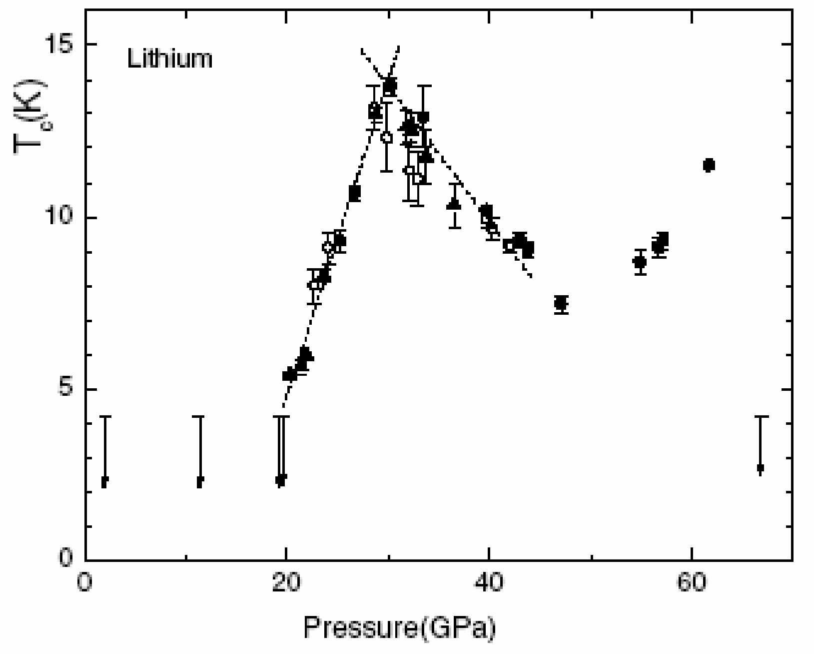

Superconductivity in Boron-doped Diamond (HPPI & LANL, 2003)

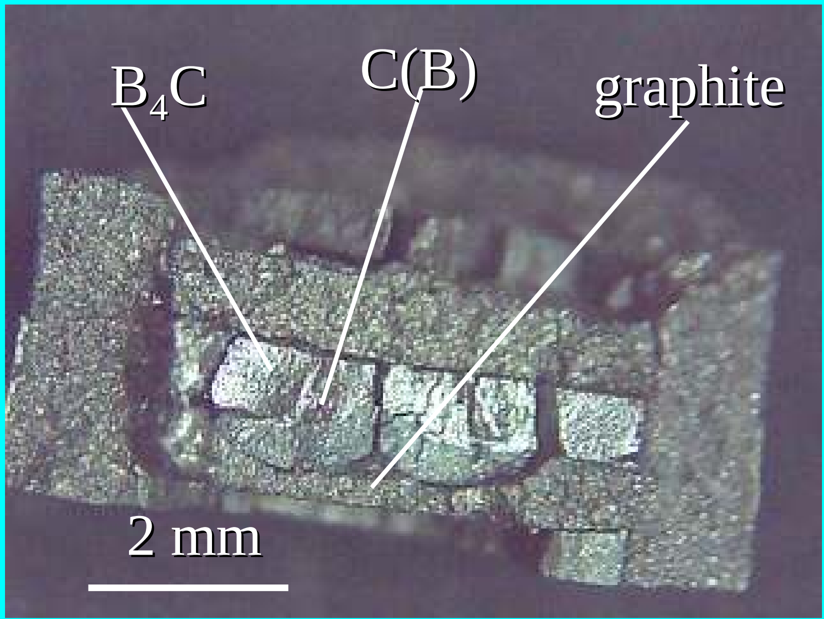

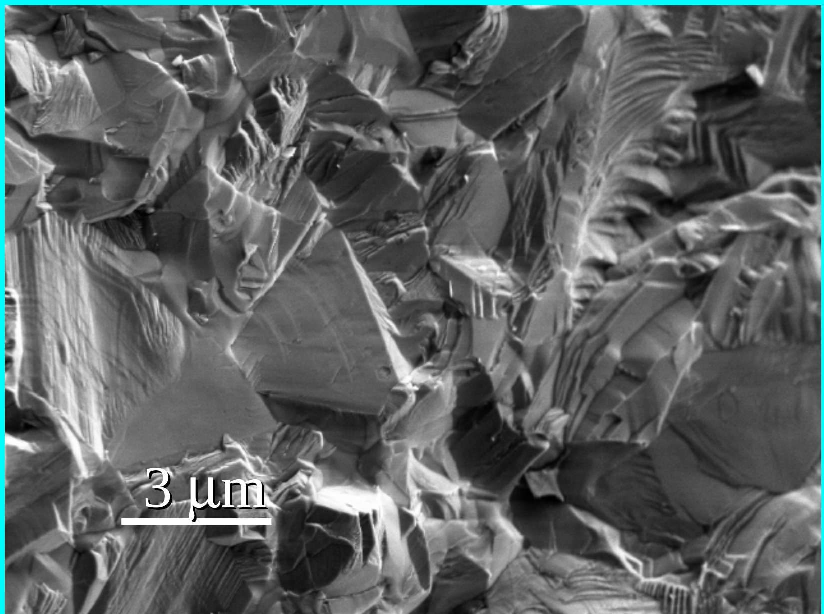

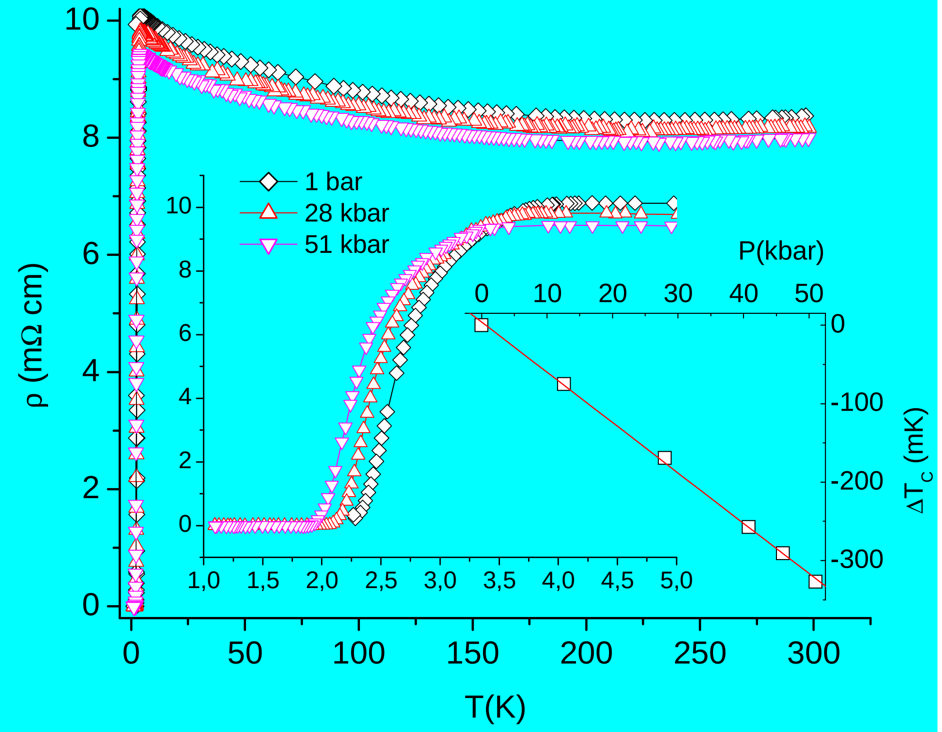

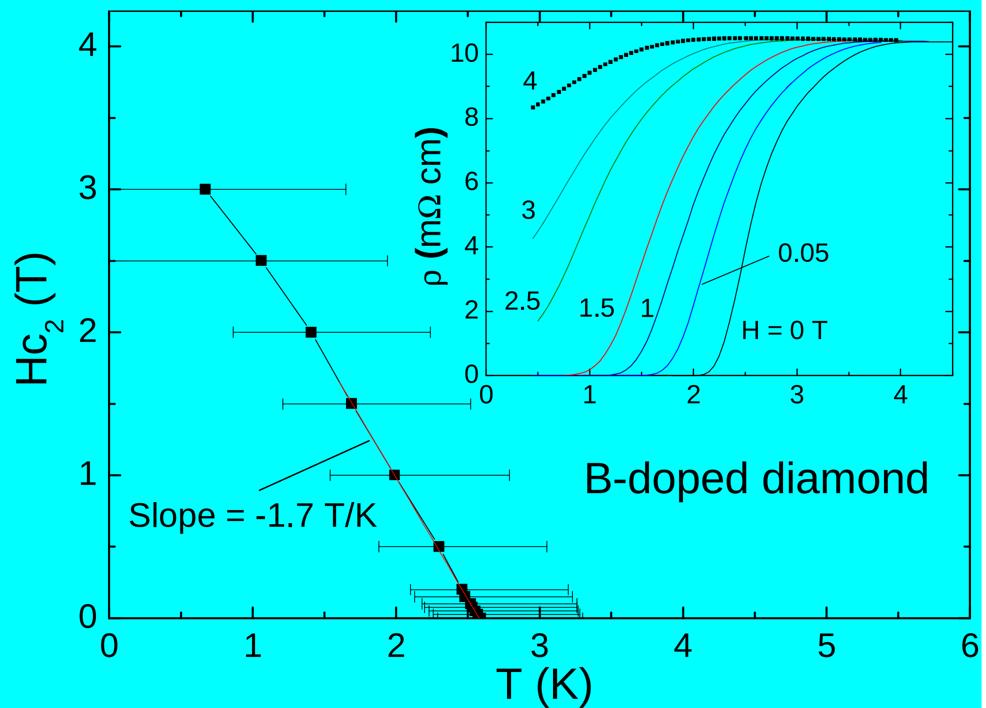

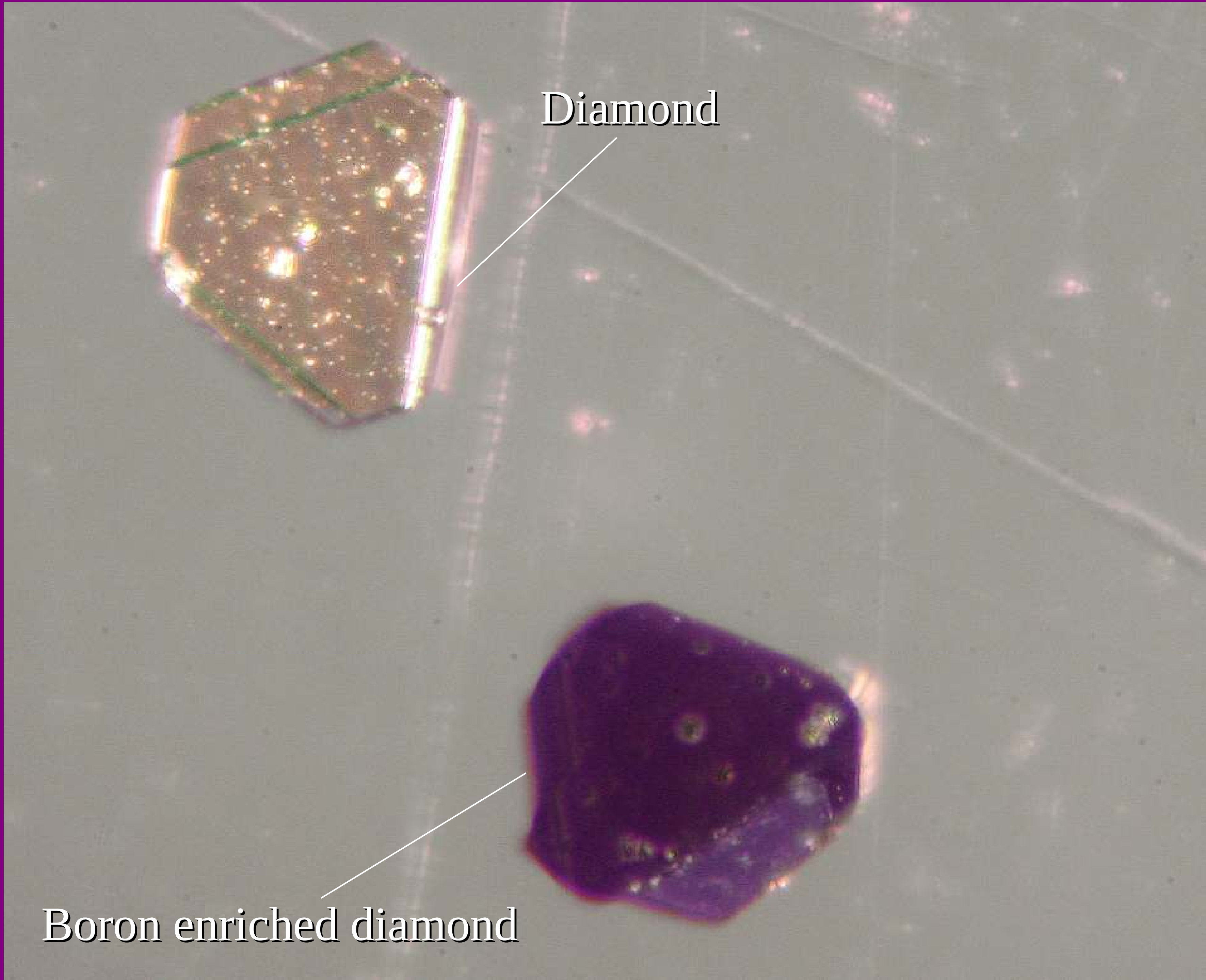
Diamond
Boron enriched diamond

Classical and quantum phase transitions (Coleman, 2001)

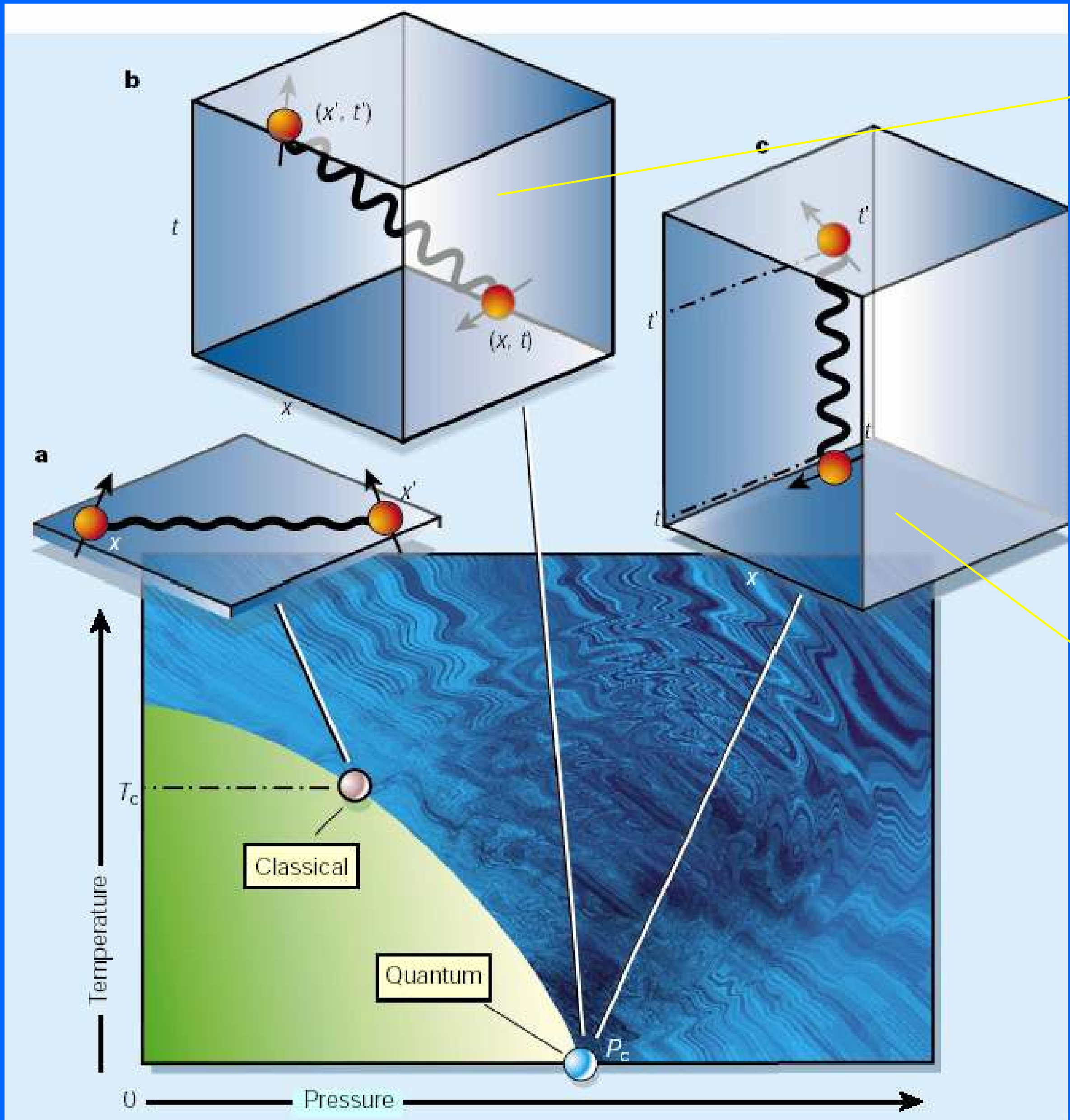

Hertz theory (Hertz, 1976)

Space and time electron-electron correlations in magnetic metals

Si et al. results for $CeCu_6$ (2001)

Quantum Critical Phenomena

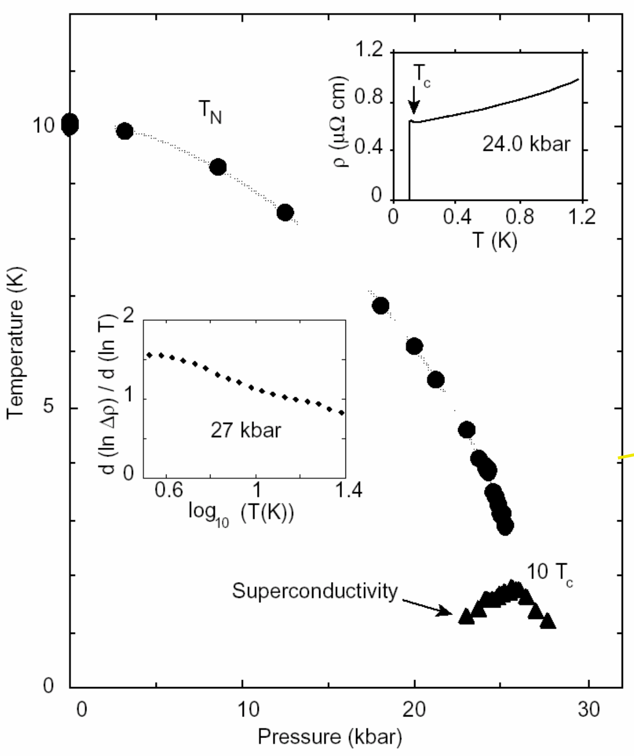

(Mathur, 1998)

$CeIn_3$, $CePd_2Si_2$

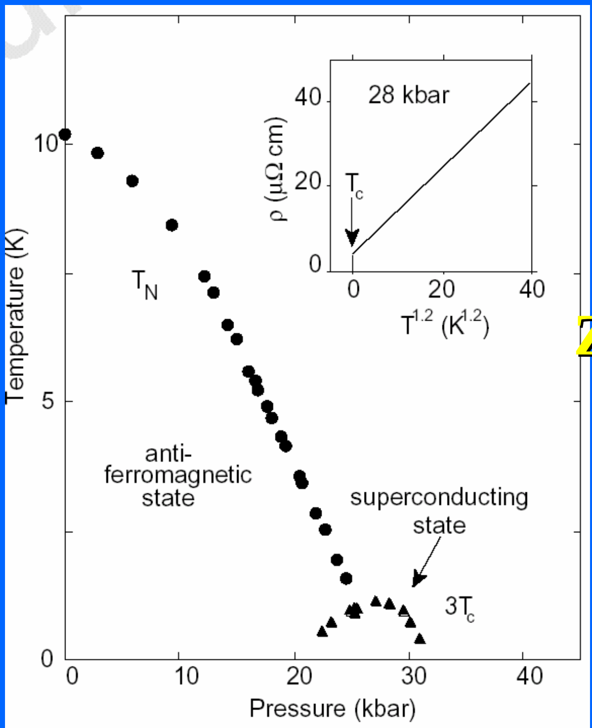

MnSi (Pfleiderer, 1997)

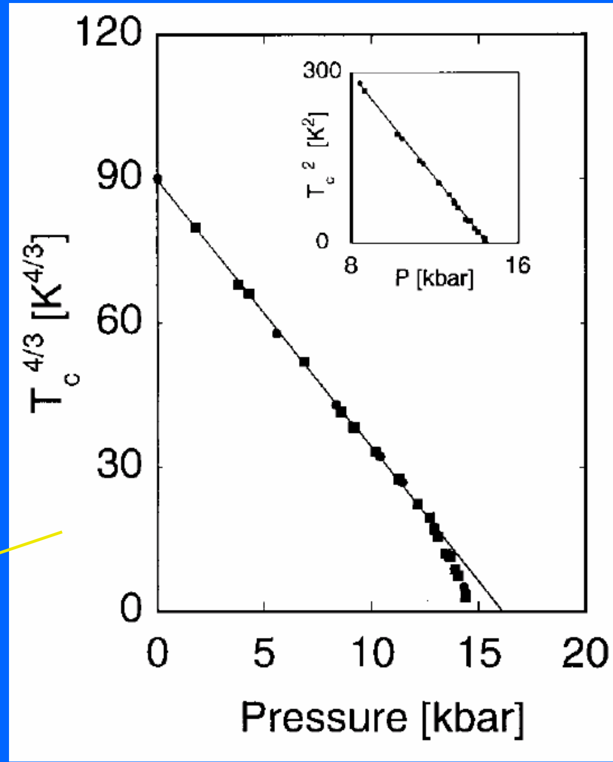

$ZrZn_2$ (Pfleiderer, 2001)

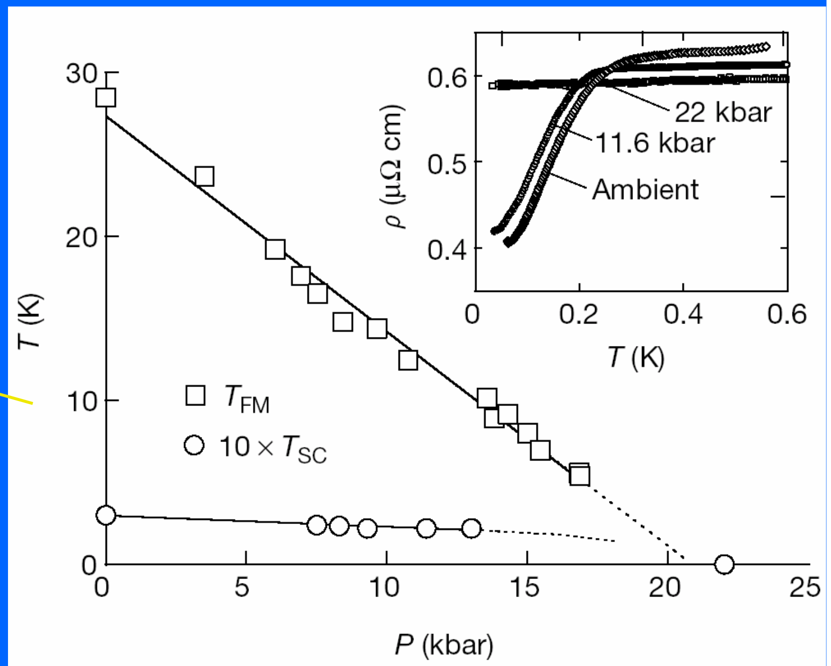

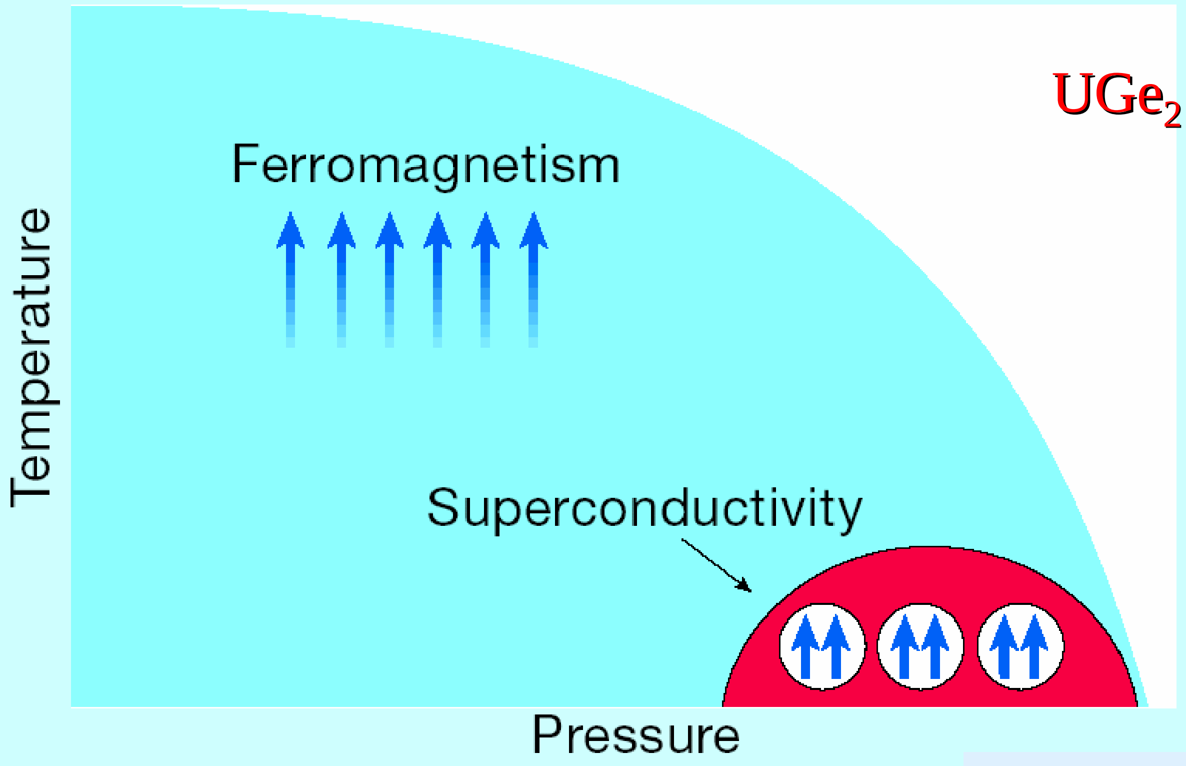

UGe$_2$ (Saxena, 2000)

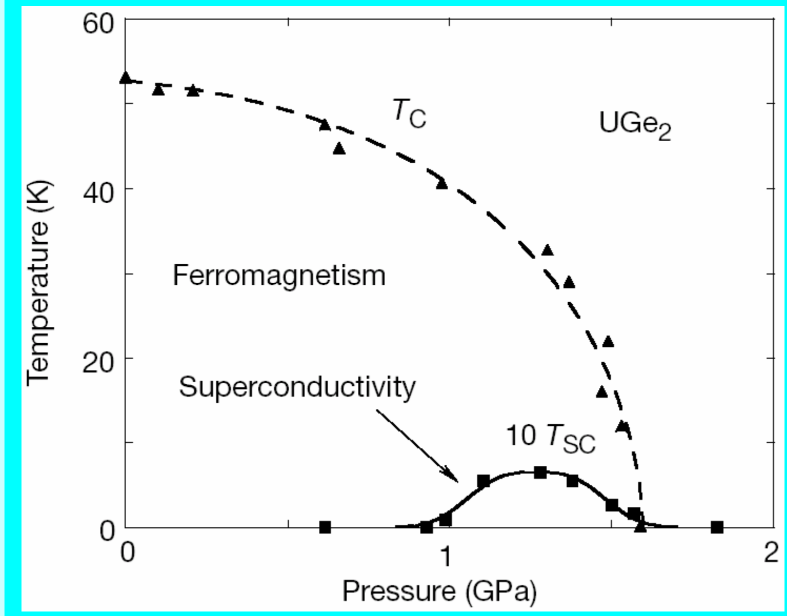

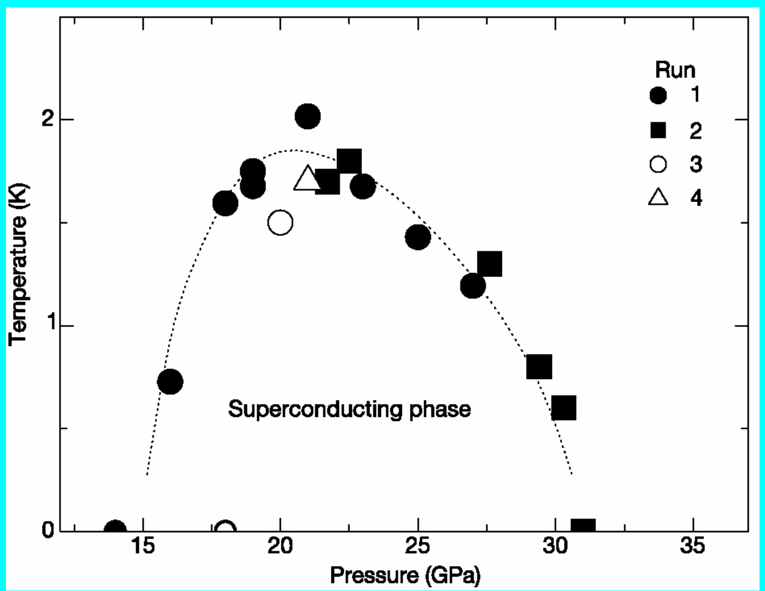

Fe (Shimizu, 2001)

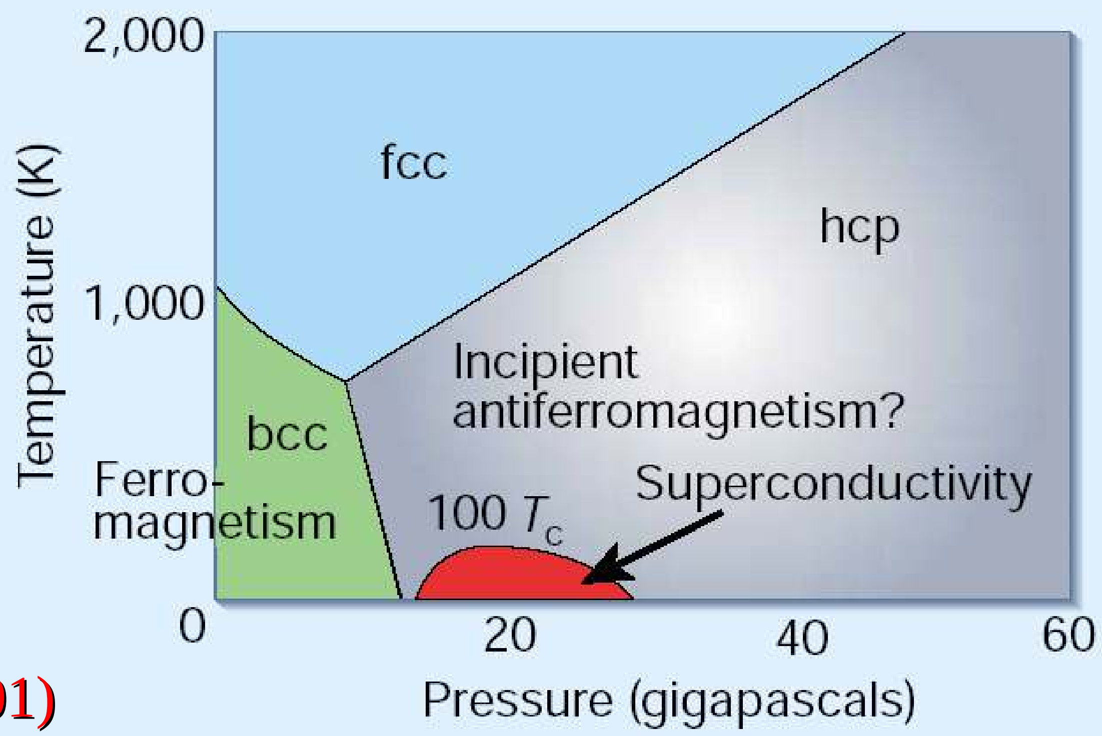

Inelastic neutron scattering in Fe

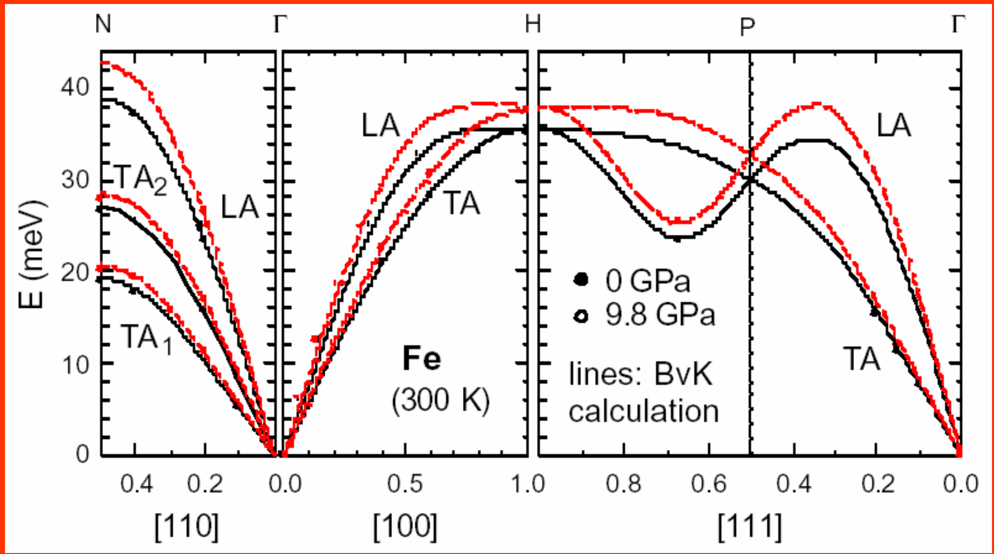

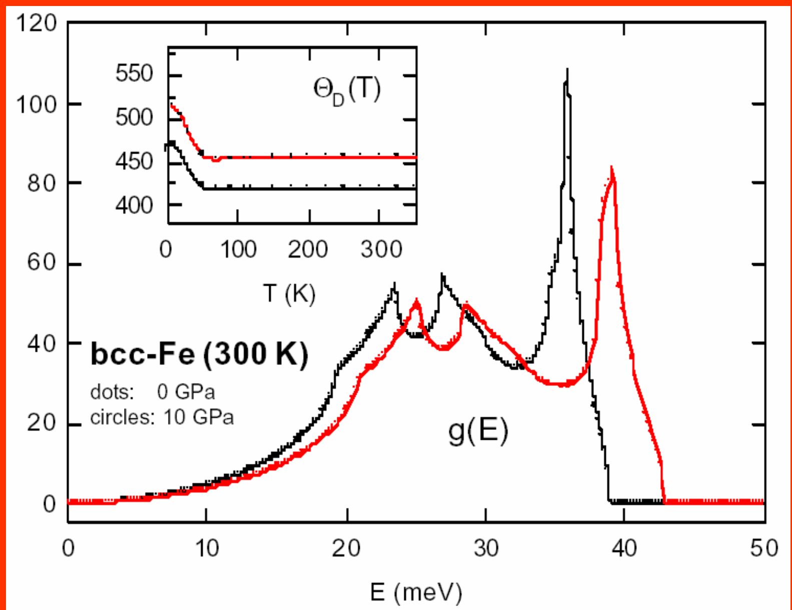

Klotz, Braden, 2000

Raman Scattering in Fe

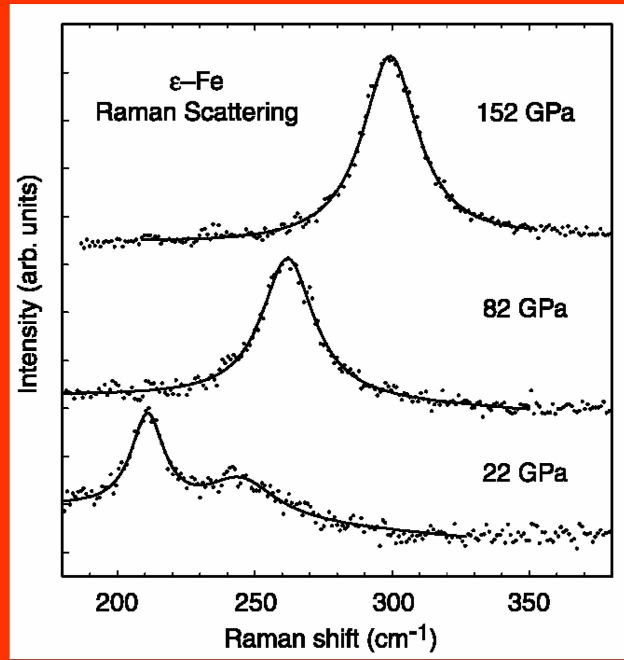

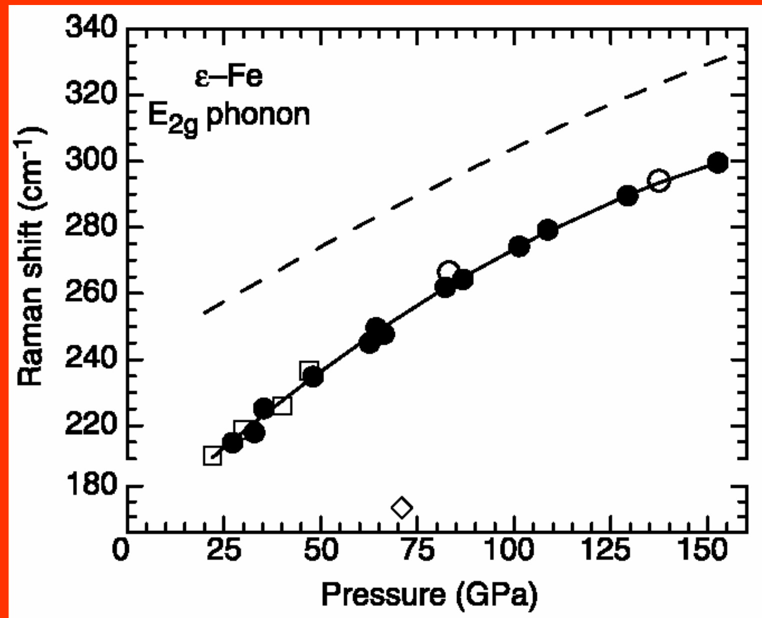

Merkel, Goncharov et al. 2000

Nuclear Inelastic Resonant X-ray Scattering in Fe

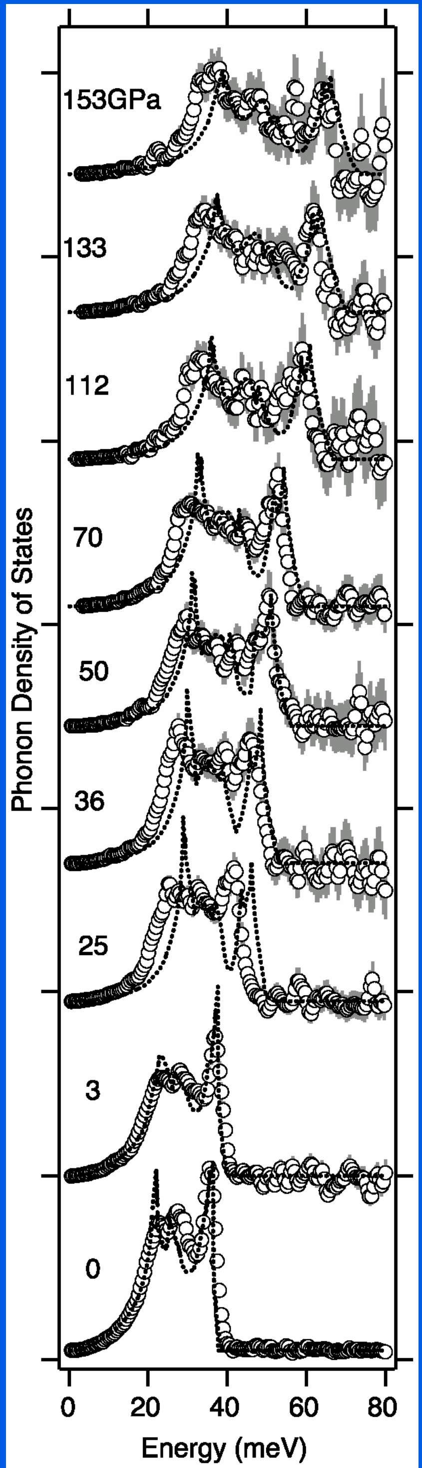

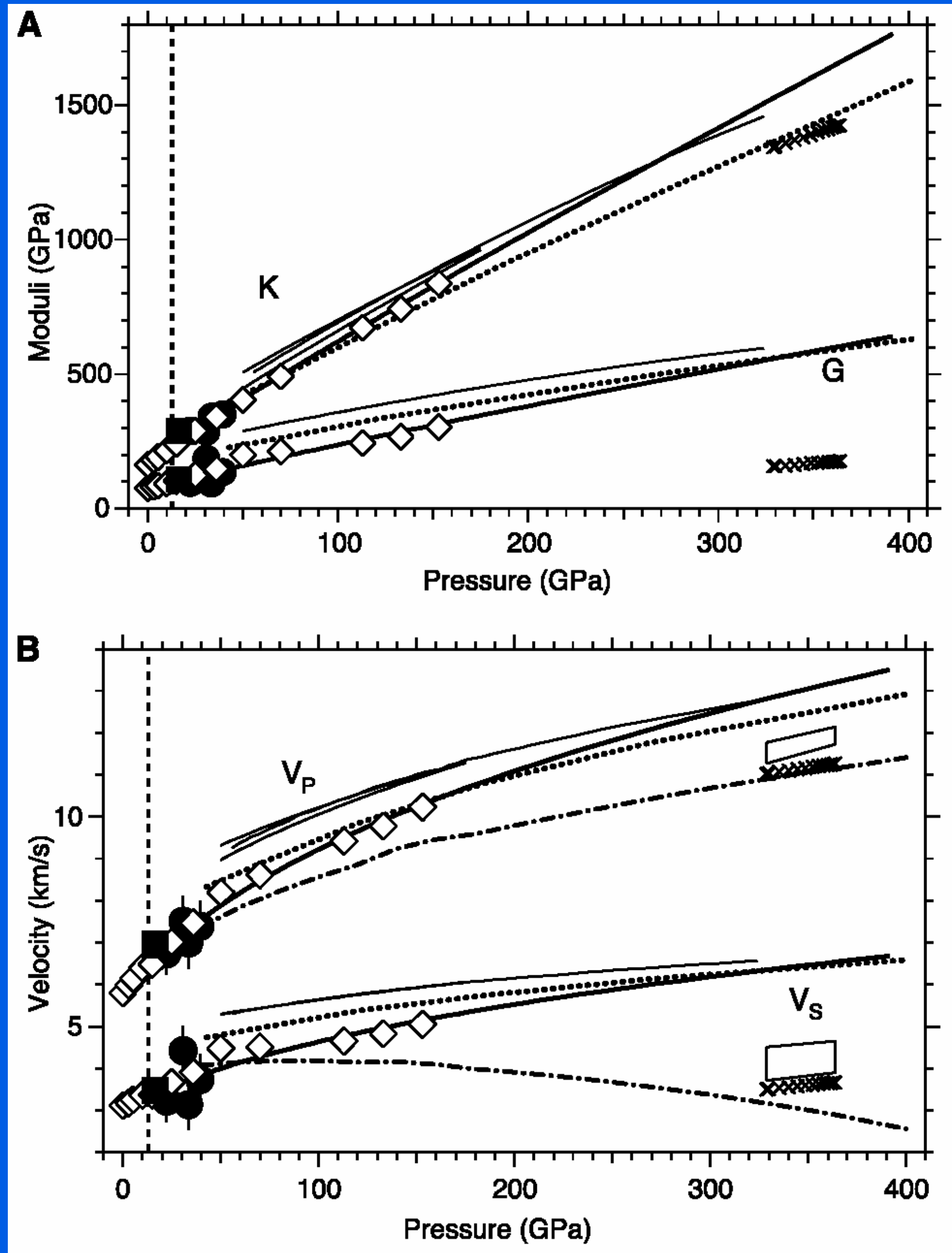

Mao, Xu, Struzhkin, 2001

Radial X-ray diffraction in Fe

(Mao, Shu, Shen, 1998)

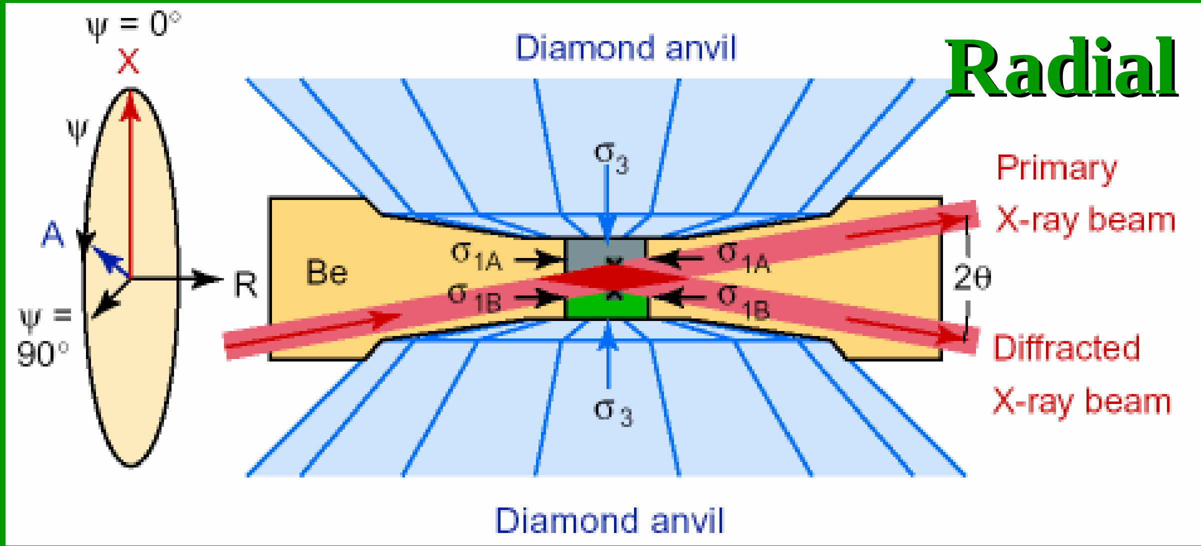

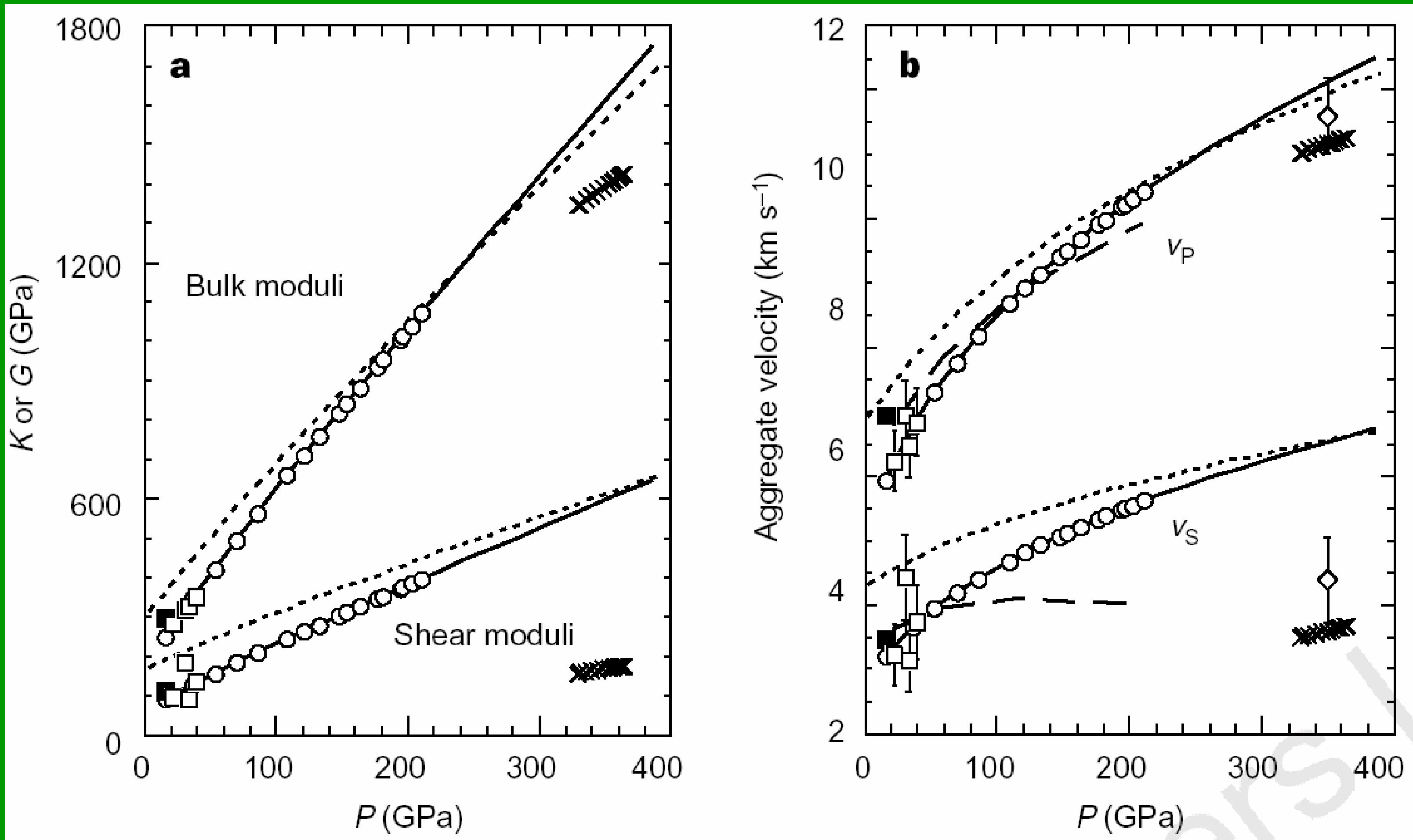

Институт физики высоких давлений РАН им. Л.Ф. Верещагина

(основан в 1958)

Административный корпус

Лабораторный корпус

корпус Большого пресса


НКМЗ
НКМЗ
НКМЗ

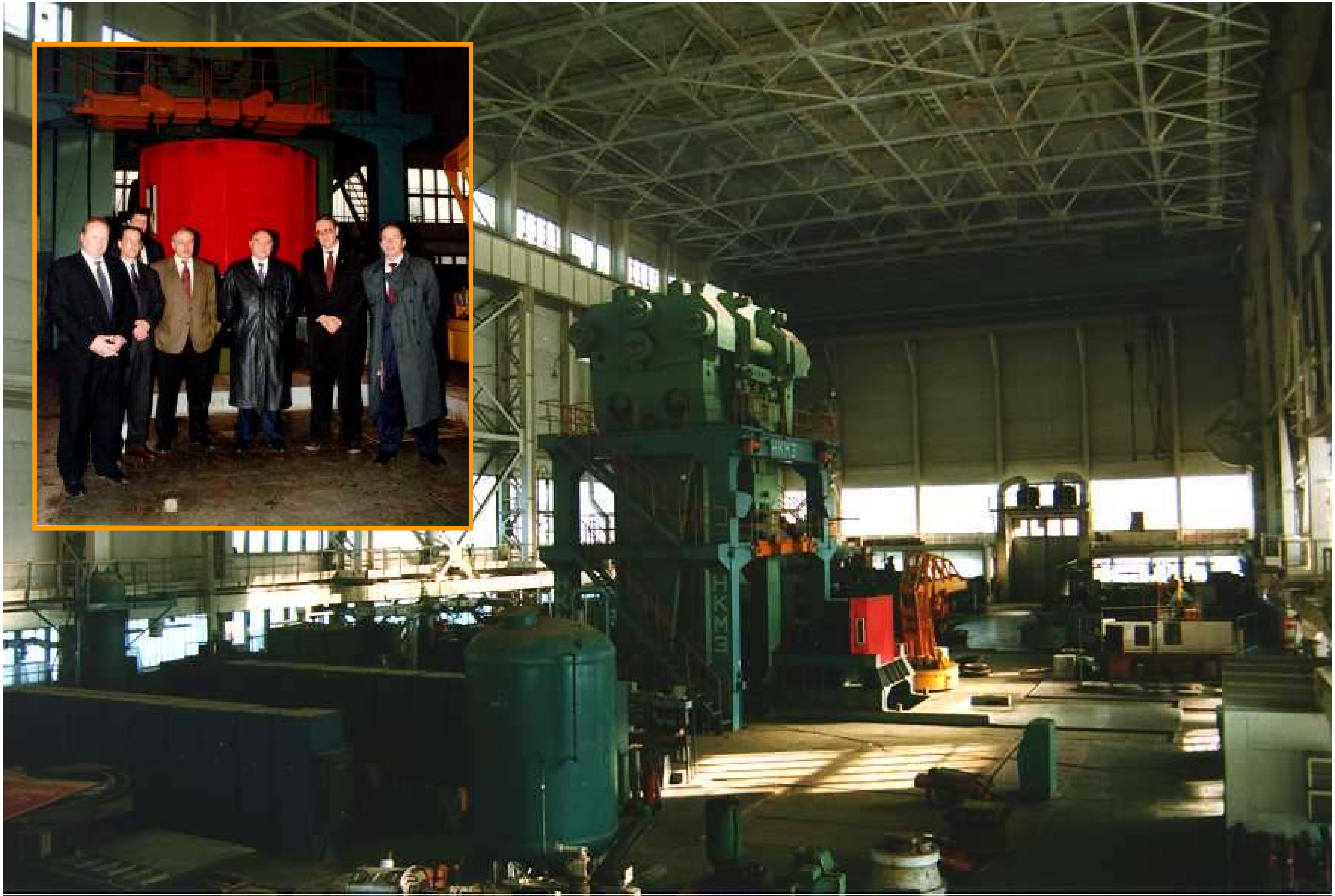
НКМЗ